UC San Diego
UC San Diego Electronic Theses and Dissertations

Title

Planar cell polarity pathway and axon guidance in the developing spinal cord

Permalink

Author

Shafer, Jeong Deok Beth

Publication Date

2010

Peer reviewed|Thesis/dissertation

UNIVERSITY OF CALIFORNIA, SAN DIEGO

Planar Cell Polarity Pathway and Axon Guidance
in the Developing Spinal Cord

A dissertation submitted in partial satisfaction of the requirements for the degree
Doctor of Philosophy

in

Biology

by

Jeong Deok Beth Shafer

Committee in charge:

Professor Yimin Zou, Chair
Professor Darwin Berg
Professor Shelley Halpain
Professor Gentry Patrick
Professor Charles Stevens

2010

The Dissertation of Jeong Deok Beth Shafer is approved, and it is acceptable in quality and form for publication on microfilm and electronically:

_____

_____

_____

_____

_____

Chair

University of California, San Diego

2010

DEDICATION

I dedicate my dissertation to my family and my significant other. To my parents, Michael Shafer and Evelind Schecter, for their unwavering encouragement, support and wisdom that has helped me to be strong throughout my entire graduate school career. To my siblings, Belle and Jeong Hwan, for their love and reminder of what is truly important in life. And to my life partner, my best friend and my editor, Michael Saxe, for his constant love, faith, and encouragement that keeps me looking forward.

TABLE OF CONTENTS

LIST OF ABBREVIATIONS

A   Anterior

A-P   Anterior-Posterior axis

ARF   ADP-Ribosylation Factor

bHLHs   Basic Helix Loop Helix proteins

BMPs   Bone Morphogenic family of Proteins

CamK Ca^{2+}/calmodulin-dependent protein Kinase

Celsr3   Cadherin, EGF LAG seven-pass G-type receptor 3

D   Dorsal

DCC   Deleted in Colorectal Cancer

Dgo   Diego

dI   Dorsal Interneurons

DIC   Differential Interference Contrast

DiI   1,1'-Dilinoleyl-3,3,3'3'-tetramethyllindocarbocyanine perchlorate

Dp   Dorsal Progenitors

DRG   Dorsal Root Ganglia

D-V   Dorsal-Ventral Axis

Dvl   Dishevelled

E   Embryonic

EGF   Epidermal Growth Factor

Ena/VASP   Enabled Vasodilator Stimulating Protein

Fmi   Flamingo

FP	Floor Plate
Fzd	Frizzled
GAPDH	Glyceraldehyde 3-phosphate dehydrogenase
GFP	Green Fluorescent Protein
GPCR	G Protein Coupled Receptor
GRKs	G Protein Coupled Receptor Kinases
GTPases	Guanosine Triphosphatases
HEK	Human Embryonic Kidney
Het	Heterozygous
JNK	c-JUN N-terminal Kinase
KO	Knockout
LIM	Lin-11, Islet-1, Mec-3 family
Lp	Loop-tail protein
LRP	LDL receptor-related proteins
MN	Motor Neurons
MZ	Mantle Zone
NSF	N-ethylmaleimide Sensitive Factor
p	progenitor
P	Posterior
PCP	Planar Cell Polarity
Phospho	Phosphorylated
PI3K	Phosphoinositide 3-Kinase
PKC	Protein Kinase C

Prkl	Prickle
RP	Roof Plate
Shh	Sonic Hedgehog
SNAREs	Soluble NSF Attachment protein Receptors
Stan	Starry night
Stbm	Strabismus
TAG-1	Axonal surface glycoprotein
TGFβ	Transforming Growth Factor β
TI-VAMP	Tetanus neurotoxin Insensitive VAMP
TM	Transmembrane
TransHet	Trans Heterozygotes
t-SNAREs	target-SNAREs
V	Ventral
VAMPs	Vesicle Associated Membrane Proteins
Vang	Van Gogh
Vangl	Van Gogh-like
v-SNAREs	vesicle-SNAREs
VZ	Ventricular Zone
Wnts	Wingless and INT genes

LIST OF FIGURES

ACKNOWLEDGEMENTS

I would like to thank my thesis advisor, Dr. Yimin Zou, for his guidance, support and mentorship for the past three years. Thank you for allowing me to continue my graduate studies in your laboratory, for your patience and for your continued effort to help me push this project into publication. I also thank the members of my dissertation committee, Drs. Darwin Berg, Shelley Halpain, Gentry Patrick and Charles Stevens for their invaluable advice and encouragement.

I would also like to thank my former mentors, Drs. Jane Dodd and Aaron Shatkin, for thorough training in research that prepared me for my graduate studies at UCSD. I also thank members of the Zou lab for their helpful discussions; in particular, Charles Lo, Liseth Parra and Delphine Delaunay. Their advice, support and friendship helped me to push through difficulties and made my time in the lab an enjoyable experience. I would also like to acknowledge the invaluable friendships that resulted form my graduate studies; thank you to Neal Padte, Sivan Harel, Jose Galan and Marin McDonald for your countless hours of support and advice.

The materials of Chapters 2-4 are currently under preparation for resubmission and will include Charles Lo and Delphine Delaunay and Yimin Zou as authors. "Planar cell polarity components, Vangl2 and Frizzled3, synergistically mediate Wnt attraction and anterior-posterior guidance of commissural axons." The dissertation author was the primary investigator and author of this material.

VITA

2010   **Ph.D.**, Biology
University of California San Diego, Division of Biological Sciences, La Jolla, CA

2006   **M.Phil.,** Cellular and Molecular Biophysics
Columbia University, College of Physicians and Surgeons, New York, NY

2005   **M.A.,** Cellular and Molecular Biophysics
Columbia University, College of Physicians and Surgeons, New York, NY

2002-2003   Laboratory Technician, Center for Advanced Biotechnology and Medicine, Piscataway, NJ

2002   **B.A.,** Rutgers University, New Brunswick, NJ
Molecular Biology and Biochemistry - Highest Honors

PUBLICATIONS

Shafer B., Lo CG., Delaunay D., and Zou Y. Wnt-mediated planar cell polarity components control anterior-posterior guidance of commissural axons. 2010-*Unpublished*

Wilson SI., Shafer B., Lee KJ., and Dodd J. 2008. A Molecular Program for Contralateral Trajectory: Rig-1 Control by LIM Homeodomain Transcription Factors. *Neuron.* 59(3): 413-24.

Wolf AM., Lyuksyutova AI., Fenstermaker AG., Shafer B., Lo CG., and Zou Y. 2008. Phosphatidylinositol-3-kinase-atypical protein kinase C signaling is required for Wnt attraction and anterior-posterior axon guidance. *J Neurosci.* 28(13): 3456-67.

Höök P., Mikami A., Shafer B., Chait BT., Rosenfeld SS., and Vallee RB. 2005. Long Range Allosteric Control of Cytoplasmic Dynein ATPase Activity by the Stalk and C-terminal Domain. *J Biol Chem.* 280(38): 33045-33054.

Shafer B., Chu C., and Shatkin AJ. 2005. Human mRNA cap methyltransferase: alternative nuclear localization signal motifs ensure nuclear localization required for viability. *Mol Cell Biol.* 25(7): 2644-9.

ABSTRACT OF THE DISSERTATION

Planar Cell Polarity Pathway and Axon Guidance
in the Developing Spinal Cord

by

Jeong Deok Beth Shafer

Doctor of Philosophy in Neurobiology
University of California, San Diego, 2010
Professor Yimin Zou, Chair

The ability of the mammalian central nervous system to interpret the environment accurately, integrate information efficiently, and generate appropriate responses depends on the precise wiring and organization of billions of neurons into functional networks. The establishment of neural circuits to enable the eventual flow of sensory information requires that axons navigate across vast (on a cellular scale) distances. For somatosensory neurons, guidance takes place during development when axons must grow to the brain via a series of intermediate targets, each step of which involves the detection and response to numerous extracellular cues. Therefore, to develop a comprehensive understanding of how neurons form appropriate connections

requires that axonal responses to these molecular guidance cues be clearly defined.

This dissertation presents studies of axon guidance in a model cellular system, the somatosensory commissural neurons of the spinal cord. I have characterized the role of Wnt-Frizzled signaling in these neurons, and found that the non-canonical Wnt-Fzd signaling, known as the Planar Cell Polarity (PCP) pathway, is fundamental to commissural axon guidance. Further, by analysis of animal models of PCP dysfunction, *Celsr3* null and *Vangl2* mutant mice, I show that PCP is required for anterior guidance of commissural axons toward the brain. Equally important, I describe the mechanism by which the PCP pathway mediates axon growth decisions through the use of primary spinal neuron and eukaryotic cell cultures and biochemical techniques. I present evidence to show that modifications of PCP surface receptors, Fzd3 and Vangl2, at the cell membrane are critical to PCP signaling and constitute a spatio-temporal response to Wnt molecules secreted from the ventral spinal cord. Together, these data reveal a novel role for the PCP pathway in axon guidance. It is hoped that the results of these studies will provide a more general model for the role of membrane receptor modifications in the establishment of neuronal circuitry.

CHAPTER 1: INTRODUCTION

1.1 Commissural neurons as a model system

The somatosensory system functions to transmit, integrate, and process sensory information from the body surface. The relay of information regarding touch, pain, pressure, temperature, and muscle position/proprioception (somatosensory modalities) requires integration of peripheral sensory information by commissural neurons in the spinal cord, which then transmit this information to the brain via their ascending projections. Commissural neurons of the somatosensory system provide a model system for studying the molecular mechanisms underlying axon guidance because they make a series of known guidance decisions. During development, axons from these neurons are faced with a series of distinct pathfinding choices as they initially project along the dorso-ventral axis towards the ventral midline, then cross to the contralateral side of the spinal cord, and eventually turn along the anterior-posterior axis to grow anteriorly towards the brain.

Commissural-somatosensory relay neurons derive from dorsal interneurons (dIs) of the embryonic spinal cord. During mouse embryonic days 9.5-13.5, neural progenitor cells dividing in the ventricular zone (VZ) of the spinal cord give rise to the eight known populations of dorsal spinal interneurons, distinguished by the expression of distinct molecular markers as well as the position at which they settle in the dorsal horn of the spinal cord. dI precursors

1

migrate out of the VZ toward the outer mantle (MZ), where they exit the cell cycle and begin to differentiate into commissural neurons (Figure1.1), (Helms and Johnson, 1998; Lee et al., 1998).
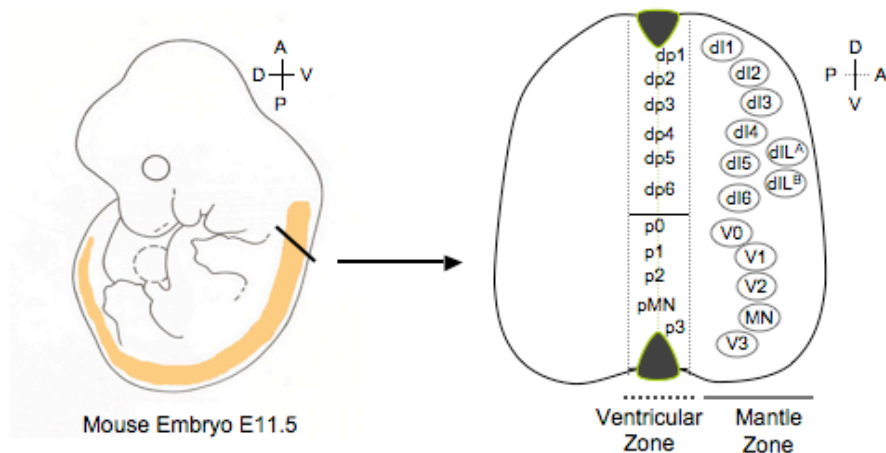
Figure 1.1 Mouse embryonic spinal cord
A schematic of a mouse embryonic day (E) 11.5 embryo is shown on the left. The cross hair shows the anterior (A), posterior (P), dorsal (D) and ventral (V) axis in the embryo.
On the right is a schematic of a transverse section of the spinal cord, which is also a magnified view of the black line segment on the left. This depicts the dorsal and ventral progenitor domains of the spinal cord. The oval-circles in the mantle zone are the molecularly-defined populations of spinal neurons. (dp, dorsal progenitor; p, progenitor; dI, dorsal interneurons; V, ventral interneurons; MN, motor neurons)

The progenitor domains of the embryonic spinal cord are specified early in development by the actions of basic helix-loop-helix (bHLH) transcription factors. These factors are regulated by TGFβ signals that emanate from the roof plate (RP) and Shh signals secreted from the floor plate (FP). In the dorsal spinal cord, the transduction of TGFβ signals (e.g. BMPs) leads to the activation of

proneural bHLH transcription factors, Pax7, Math1, Ngn1/2 and Mash1. Upon exit from the VZ and entry in the mantle zone (MZ), dorsal interneurons down-regulate bHLH genes and up-regulate the LIM homeodmain proteins Lhx2/9, Lhx1/5, Islet1/2 and Lim1/2 (Augsburger et al., 1999; Ben-Arie et al., 1996; Gowan et al., 2001; Helms and Johnson, 1998; Lee et al., 1998; Liem et al., 1997; Ma et al., 1999). At this stage in development, dI1-6 cells begin to differentiate into commissural neurons, send out axonal processes, and express commissural-neuron specific receptors TAG-1, DCC and RIG-1 (Dodd and Jessell, 1988; Dodd et al., 1988; Sabatier et al., 2004; Serafini et al., 1994; Wilson et al., 2008).

Upon exit from the VZ, commissural neurons first project their axons toward the ventral midline, then across the floor plate of the midline, and finally turn rostrally towards the brain, as illustrated in Figure 1.1. Graded extracellular cues instruct the commissural axon to navigate in this precise manner.
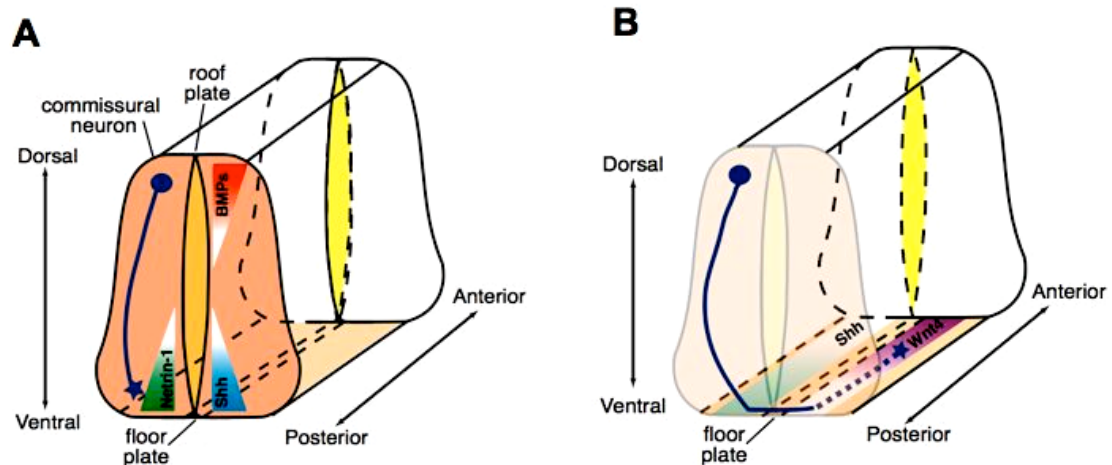
Figure 1.2 Schematic representation of axonal trajectory of commissural neuron
(A) Transverse section of mouse ~E10.5 (rat E12) spinal cord showing the ventral midline trajectory of commissural axon. Dorsal-ventral gradients of BMPs, Netrin, and Shh are shown in red, green, and blue, respectively.
(B) Transverse section of mouse ~E11.5 (rat E13) spinal cord depicting midline crossing and anterior turning of commissural axon. Anterior-posterior Wnt gradients in the floor plate are depicted in purple.

Early in dI neurogenesis, BMPs derived from the RP instruct precursors to differentiate into commissural neurons, and repel away from the RP (Augsburger et al., 1999; Butler and Dodd, 2003; Liem et al., 1997; Liem et al., 1995). Commissural axons express TGFβ family of receptors on their growth cones, which allow them to bind BMPs and repel. Commissural cell bodies migrate and settle in the deep dorsal horn of the spinal cord, but their axons continue to navigate toward intermediate targets. Axons are then attracted towards the ventral midline by floor plate (FP) derived cues, Netrin and Shh (Charron et al., 2003; Kennedy et al., 1994; Serafini et al., 1994) (Figure 1A), cross the midline of the spinal cord, and become responsive to Wnt derived FP cues (Figure 1B).

Wnt4 and Wnt7b are expressed by the FP in a rostro-caudal gradient and, after midline crossing, commissural axons follow this graded attraction rostrally towards the brain (Lyuksyutova et al., 2003; Zou, 2004).

1.2 Wnt-Fzd signaling and commissural axon guidance

Much work has been done to elucidate the mechanisms that underlie the ability of commissural axons to integrate extracellular cues along the body axis, and translate them into directional axon growth. It has been demonstrated that specific ligand-receptor signaling pathways facilitate each of these axon guidance decisions. Wnt proteins, which are known to serve as anterior-posterior guidance cues in the spinal cord are secreted by FP cells, attract commissural axons anteriorly toward the Wnt protein gradient. FP-derived diffusible Wnts are thought to bind the Frizzled3 (Fzd3) receptor, which is expressed on the commissural axon and commissural neurons that lack Fzd3 receptors have axons that become randomized and lose their anterior direction after midline crossing (Lyuksyutova et al., 2003). While, it has been established that Wnt-Frizzled signaling is required for anterior turning of commissural axons after they have crossed the midline of the spinal cord, little is known about the intracellular mechanism downstream of receptor binding.

There are four well-characterized signaling pathways downstream of Wnt-Frizzled binding: Canonical, Protein Kinase C (PKC)/ calcium, Phosphoinositide 3-kinase/ atypical PKC, and the Planar Cell Polarity (PCP) pathway (Figure 1.2).
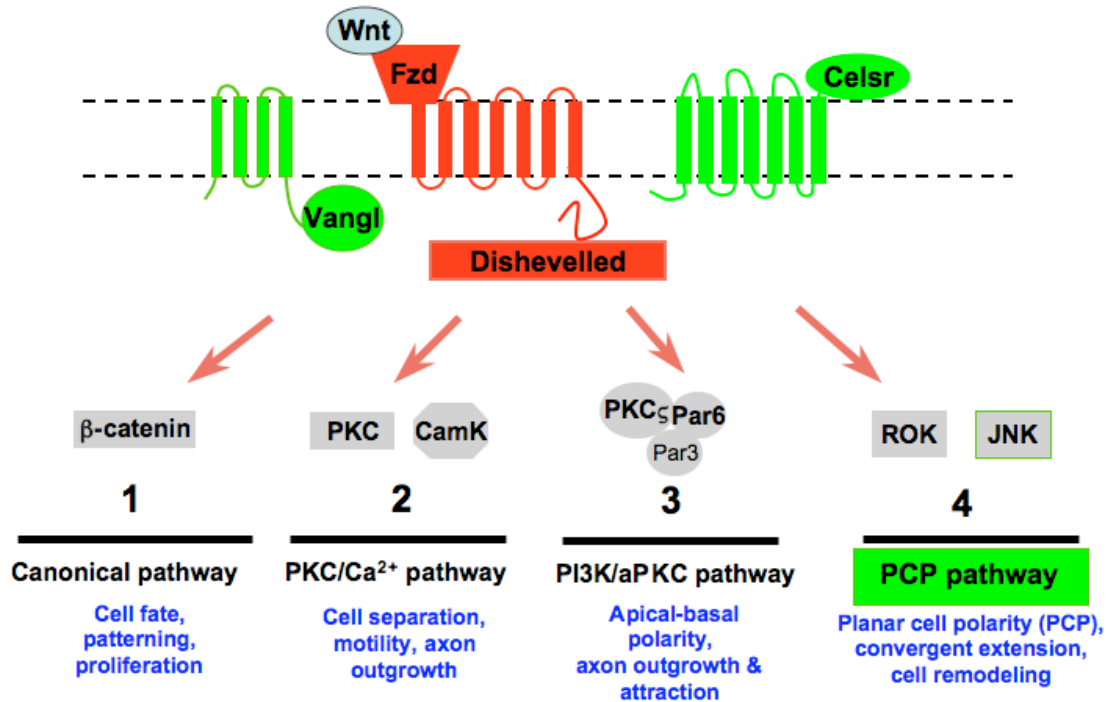
Figure 1.3 Wnt-Fzd3 signaling pathways
Upon binding of the Wnt ligand to the Fzd receptor several pathways can be activated. All pathways lead to the activation of central downstream signaling molecule Dishevelled (Dvl).   In grey are the molecules specific to each pathway, and in blue are the morphological events that each has been implicated in.   Membranous components specific to the PCP signaling pathway are in green.

The canonical pathway requires the Fzd co-receptor, LDL receptor-related proteins 5 or 6 (LRP5/6), and binding of Wnts leads to the eventual activation β-catenin dependent transcription.   Studies have shown that the canonical pathway is not required for anterior guidance of commissural axons since LRP5/6 null mice do not show misguided commissural axons. Similarly, the involvement of the PKC/Ca2+ pathway in commissural axon guidance has been ruled out, as PKC inhibitors had no effect on Wnt-dependent turning of commissural axons

(Lyuksyutova et al., 2003; Wolf et al., 2008). However, the binding of Wnt4 to Fzd3 appears to activate PI3Kinase gamma and PKCzeta-dependent signaling cascades that direct the commissural growth cone to turn anteriorly toward the brain (Lyuksyutova et al., 2003; Wolf et al., 2008). The work in this thesis investigates the fourth pathway and shows a requirement for the PCP pathway in Wnt-mediated commissural axon guidance.

1.3 Planar cell polarity pathway

Among the known signaling pathways that mediate Wnt functions, PCP pathway is an appealing candidate for Wnt-mediated axon guidance for several reasons. First, PCP signaling in other tissues results in a variety of developmental events involving cell-fate decisions, morphogenesis and organized cell movements. Second, studies have shown that the PCP pathway is highly conserved in regulating polarized cellular morphology in a number of processes, such as *Drosophila* wing hair cell polarity, directed cell movement during vertebrate gastrulation, and polarized organization of mammalian stereocilia of cochlear hair cells (Adler, 2002; Montcouquiol et al., 2006a; Qian et al., 2007; Seifert and Mlodzik, 2007). Furthermore, in *C. elegans*, Wnts are clearly an instructive signal during neuroblast division and activate PCP components to control spindle orientation (Hardin and King, 2008; Langenhan et al., 2009). However, the Wnt-PCP pathway has yet to be investigated in the context of axon guidance during development.

Much of what we know about the PCP signaling pathway and the resulting tissue morphogenesis derives from studies in *Drosophila,* where this pathway is responsible for directing parallel alignment of wing hairs, sensory bristles and ommatidia. Planar polarity of 700 polarized ommatidia can be seen in the fly eye, and it is known that the PCP pathway helps to determine the balance between R3 and R4 photoreceptor fate which later effects rotation and chirality of the ommatidia containing the eight photoreceptors (Jenny et al., 2003). Also during fly development, the wing epithelial cells initiate growth of a pre-hair containing F-actin and microtubules in the distal-most part of the cell, and at maturity planar polarity of fly wing hairs are observed pointing in a distal direction. Similarly, the sensory hair bristles on the thorax point uniformly in the posterior direction (Adler, 2002). However, defects in the PCP pathway lead to disruptions in these polarized processes (Lee and Adler, 2002) and the resulting disorganizations are termed PCP phenotypes.
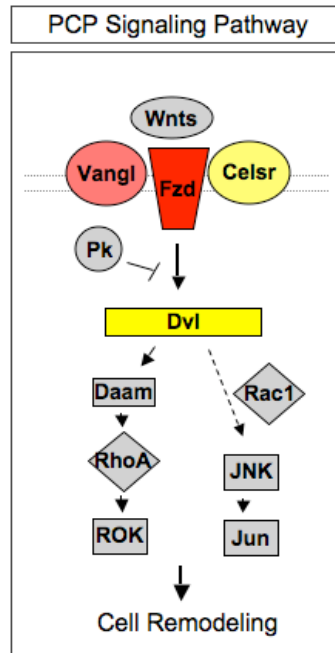
Figure 1.4 The PCP Signaling Pathway
The PCP pathway is activated by core PCP components which include a GPCR Frizzled (Fzd), Dishevelled (Dvl), Van Gogh or Strabismus (Vang/Stbm or Vangl), a Flamingo/starry night (Fmi/Stan or Celsr3), an ankyrin repeat protein Diego (Dgo) and a Lim domain protein Prickle (Prkl, Pk). These pathway components have been shown to activate Daam, RhoA and ROK, as well as Rac1, JNK and Jun during cell remodeling processes.

The mechanism by which planar polarity is established involves the activation of PCP signaling pathway and several conserved core components: the seven transmembrane GPCR Frizzled (Fzd), an intracellular Frizzled-binding protein Dishevelled (Dvl), a four-pass transmembrane protein Van Gogh or Strabismus (Vang/Stbm or Vangl), an atypical cadherin with 7-pass transmembrane domains Flamingo/starry night (Fmi/Stan or Celsr3), an ankyrin repeat protein Diego (Dgo) and a Lim domain protein Prickle (Prkl, Pk) are among the most prominent (Zallen, 2007), (Figure 1.4). In *drosophila* and

xenopus model systems, PCP components have been shown to activate RhoA and ROK to facilitate actin remodeling that is required for cell morphogenesis (Fanto et al., 2000; Habas et al., 2001; Strutt et al., 1997; Winter et al., 2001). Further, it is known that the PCP pathway leads to activation Jun N-terminal kinase and Jun by phosphorylation, and the modulation of Jun signaling affects PCP phenotypes (Boutros et al., 1998; Weber et al., 2000).

The PCP pathway has also been characterized in vertebrate convergent extension during neurulation. Neural tube closure occurs early in development when the neural plate bends and fuses to form a neural tube that will eventually give rise to the brain and spinal cord. Cells undergoing convergent extension drive this morphogenesis and PCP proteins have been shown to be involved in tissue movement during neural tube closure (Simons and Mlodzik, 2008). In addition, several mouse lines with altered PCP genes have neural tube defects including *Fzd3/6* null mice, *JNK1/2* null mice, Vangl2 mutants, and Dvl mutants (Sabapathy et al., 1999; Wang et al., 2006a; Wang et al., 2006b; Wang and Nathans, 2007).

The studies in this thesis will show a novel role of the PCP pathway in commissural axon guidance. Specifically, we show that this pathway is activated during Wnt-mediated anterior turning of commissural axons toward the brain. In chapter 2 we present studies of two genetic models of PCP dysfunction, *Celsr3* null mice and Vangl2 mutant mice (*Loop-tail)*. Our analysis revealed that commissural neurons in these mice project along the dorso-ventral axis, but fail

to find anterior direction along the anterior-posterior body axis, indicating a defect in Wnt-mediated anterior turning of commissural axons *in vivo*. In chapter 3 we show that the spinal cords express the core PCP components at a time and place that is consistent with a role in commissural axon anterior-posterior guidance. In addition, we found that expression of PCP components in dissociated spinal neurons display enhanced growth in the presence of Wnts.

Finally, in chapter 4, we directly explore the mechanism by which the PCP proteins mediate a Wnt-dependent response. Both Fzd3 and Vangl2 proteins were found to be modified by phosphorylation, which had differential effects on Wnt-mediated PCP signaling. We also describe a novel Wnt-mediated feedback loop in which Dvl1 affects PCP signaling and Fzd3 receptor levels at the membrane. Taken together, these data provide the first evidence that PCP components are required for the anterior trajectory of commissural axons during development, and provide novel insight into both the role of PCP function in axon guidance, and the variety of functions subserved by this conserved signaling pathway across different species and developmental timepoints.

CHAPTER 2: ANALSYSIS OF PCP MUTANTS

2.1 Dorsal-ventral and anterior-posterior guidance of commissural axons

During development commissural axons make a series of known changes in trajectory en route to the brain (Figure 2.1). They first project to the ventral midline of the spinal cord and express the cell surface receptor protein TAG-1. TAG-1 immuno-reactive axons are termed "pre-crossing" axons because after crossing the midline these axons down-regulate TAG-1 and up-regulate the cell surface glycoprotein L1 (Dodd et al., 1988). Immunostaining of a transverse section of the E11.5 mouse or E13 rat spinal cord shows the stereotyped trajectory of commissural axons along the dorsal-ventral axis of the spinal cord (Figure 2.1B). TAG-1 and L1 positive misprojections are indicative of dorsal-ventral commissural axon guidance defects (Matise et al., 1999). After midline crossing commissural axons turn anteriorly toward the Wnt spinal gradient and continue grow along the anterior-posterior axis. To visualize this event an open-book preparation of the spinal cord was injected with DiI at E11.5 (Figure 2.1A). This technique can used to demonstrate anterior-posterior (A-P) guidance defects, such as previously reported in commissural axons of Fzd3 knock embryos (Lyuksyutova et al., 2003). DiI labeling of wildtype spinal cords showed normal axons that turn rostrally after FP crossing (Figure 2.1C).
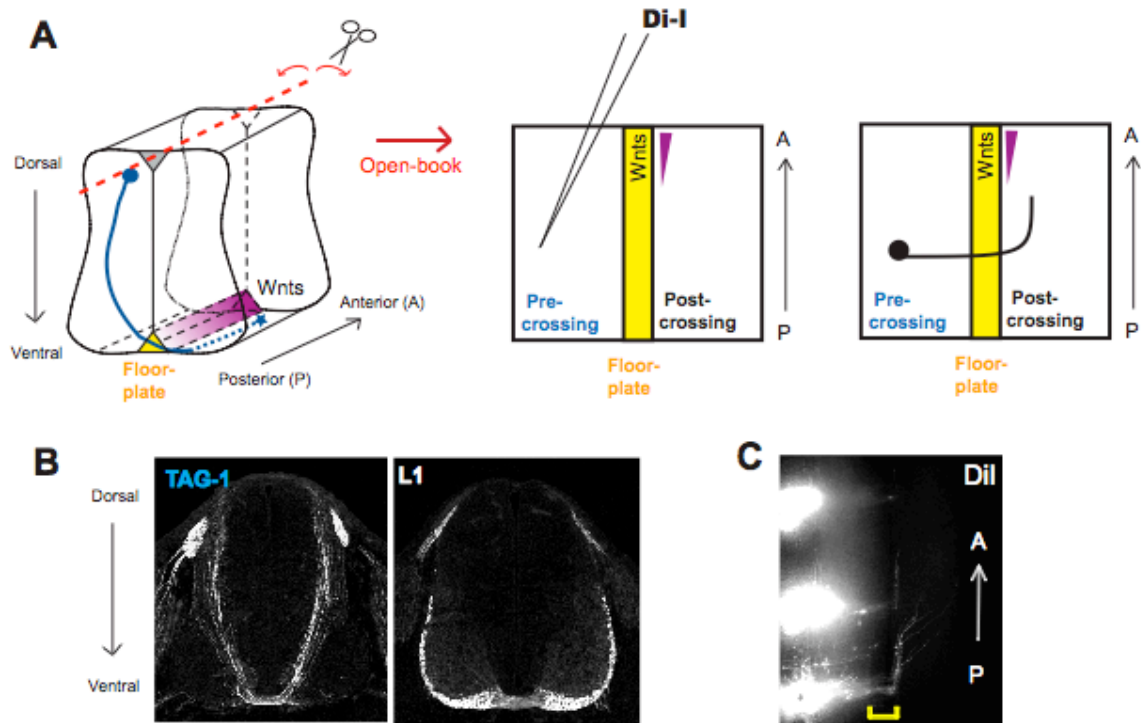
Figure 2.1 Methods to visualize guidance of commissural axons
(A) Schematic of the open-book assay. Spinal cords are dissected from E11.5 mouse embryos (or E13 rat embryos) and cut along the roofplate, then splayed out flat. Lipophillic dye injected into the commissural cell bodies will diffuse along the axon membrane and fill in the axonal projections.
(B) TAG-1 and L1 are classic markers used to visualize the dorso-ventral trajectory of commissural axons.
(C) An example of a DiI injected mouse spinal cord, the yellow bar depicts the location of the floor plate.

2.2 Vangl2 is required for anterior-posterior guidance of commissural axons *in vivo*

Previous work showed that Fzd3 is required for proper A-P guidance of post-crossing commissural axons (Lyuksyutova et al., 2003). Fzd3 is a known component in multiple Wnt signaling pathways, including PCP signaling. To address whether PCP signaling is required for A-P guidance of commissural

axons *in vivo*, we analyzed mouse mutants with a specific deficiency in PCP signaling.

A well-known PCP mutant mouse, the *loop-tail* mouse, has a point mutation of the *Vangl2* gene (S464N) that renders the protein ineffective and unstable. To confirm the loss of protein expression, we immunoblotted for Vangl2 protein in spinal lysates from wildtype, heterozygous and *Lp/Lp* embryos and found that protein levels were absent in the homozygotes (Figure 2.2).
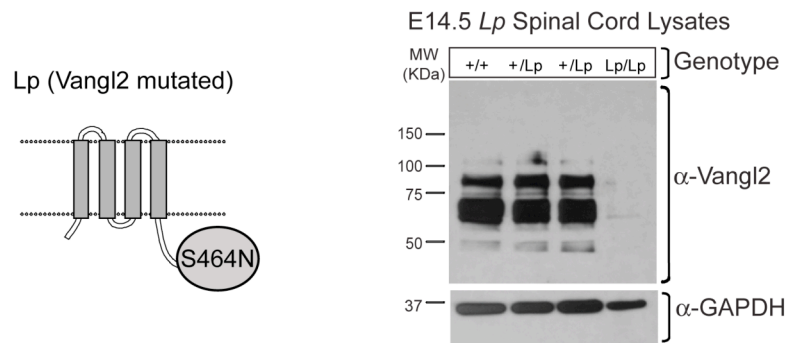
Figure 2.2 Vangl2 protein expression is diminished in the Lp mouse
On the left is a schematic showing the location of the Lp mutation in the Vangl2 protein, which renders it unstable. On the right is an immunoblot of E14.5 spinal lysates from wildtype, heterozygous and Lp embryos and Vangl2 immuno reactivity is absent in the Lp lysates.

However, because the *loop-tail* mouse displays an open neural tube (caused by secondary convergent extension defects), and because the roof plate is an essential source of morphogens, we examined the cell patterning and fate markers in Lp mutants. We found no discernable defects in specification of the neural tube at E11.5, and the spinal markers in *Lp/Lp* embryos were similar to both heterozygote and wildtype embryos. A schematic of the dorsal progenitor

domains and post-mitotic neurons in the developing spinal cord is shown in Figure 1.1 and Figure 2.3 (left panel). Pax7, which defines the spinal dorsal progenitor domains dp3, dp4, dp5, dp6 and part of the ventral progenitor domain p0, appeared normal in the *+/+, Lp/+*, and *Lp/Lp* embryos. Nkx2.2 immunoreactivity for pMN and p3 domains showed no defects in embryos of all three genotypes (Figure 2.3), and the post-mitotic dorsal interneuron (dI) markers Lhx1/5 for dI2, dI3, dI4 were unaffected by the open neural tube. Finally, the immunoreactivity for Iselet1 showing the dI3 and some motor neuron populations appeared normal (Figure 2.3).
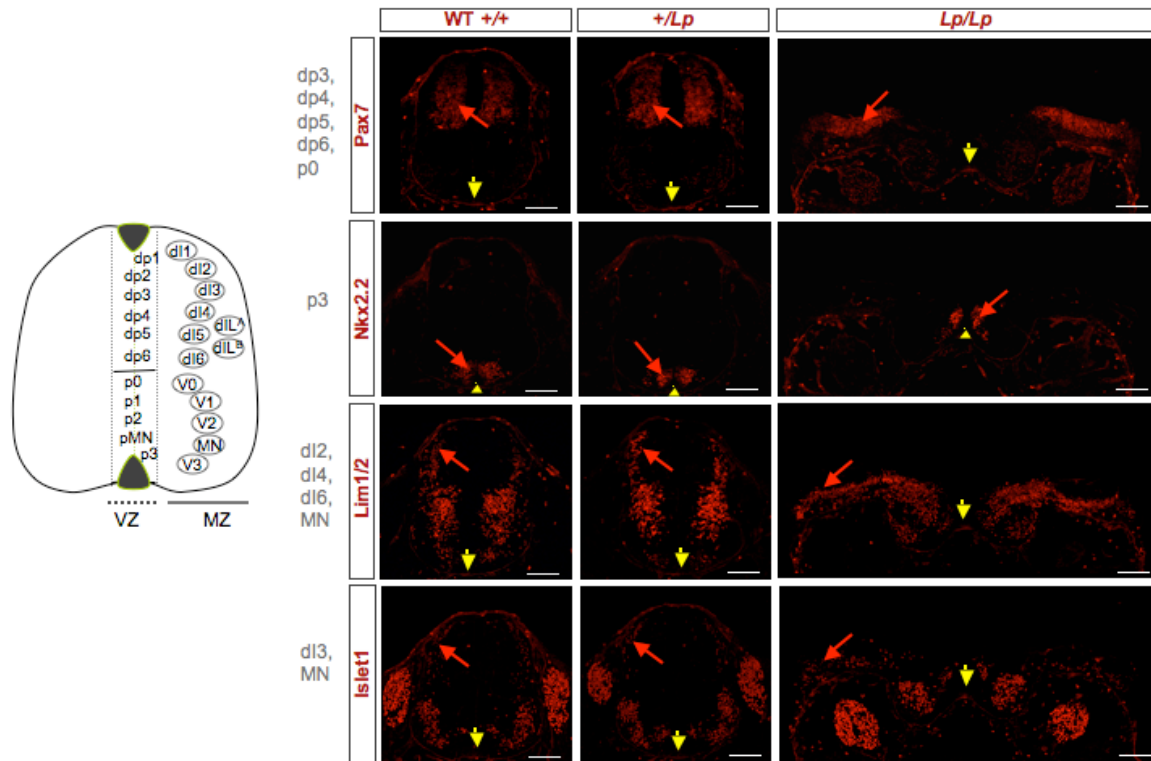
Figure 2.3   Progenitors and neurons appear normal in the *loop-tail (Lp)* embryos
At left is a schematic of a mouse transverse section depicting the neuronal progenitor domains and neuron types in the spinal cord at E11.5. (dI, dorsal interneurons; MN, motor neurons; dp, dorsal progenitor; p, progenitor)
Pax7 and Lhx1/5 expression is unchanged in the *Lp* spinal cords. Transverse sections of E11.5 *Vangl2+/+, Vanlg2+/Lp* and the open neural tube *Lp/Lp* embryos were immunostained with transcription factors expressed by either spinal progenitors or neurons. Pax7 expression by the progenitor domains dp3, dp4, dp5, dp6, p0 and p3 did not change in the wildtype, heterozygous or homozygous embryos. Similarly, Lhx1/5 expression by the post-mitotic neurons of dI2, dI4, dI6, dI3 and MN showed no gross differences.   *Vangl2+/+, Vanlg2+/Lp* and the open neural tube *Lp/Lp* embryo spinal sections immunostained with Nkx2.2 and Islet1 showed no gross defects in immunoreactivity. (Red arrow, cell bodies expressing indicates transcription factors; Yellow arrow, location of the floor plate; White bar, 100um scale)

We next examined the trajectory of commissural axons in transverse

sections using TAG-1 and L1 staining.   The diagram of dorso-ventral (D-V)

trajectory of commissural axons is shown in Figure 2.4A. We used TAG-1 immunoreactivity showed that commissural axons projected with no gross defects from the dorsal spinal cord to the ventral midline in the *+/+, Lp/+*, even in the open neural tube *Lp/Lp* embryos (Figure 2.4B-D). Furthermore, after crossing the axons grew within the ventral and lateral funiculis normally, as shown by L1 staining (Figure 2.4E-G). These results demonstrate that commissural neurons in the developing spinal cord of the Lp mouse project without defect in the dorso-ventral direction, but show severe anterior-posterior guidance defects.
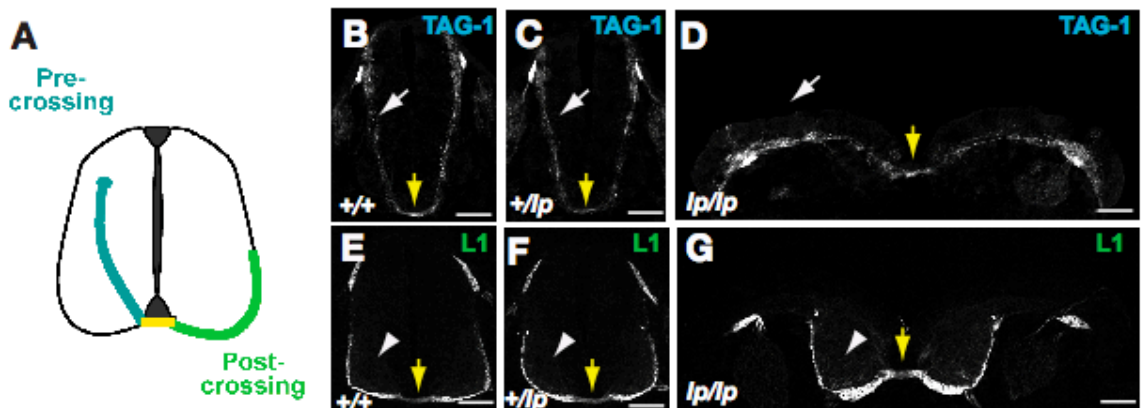
Figure 2.4 Dorsal-ventral commissural axonal projections in *Lp* litter
(A) Schematic of mouse E11.5 transverse section showing commissural axon trajectory. (B-G) The dorso-ventral trajectory of commissural axons occurs in Lp spinal cords. TAG-1 immunostaining of E11.5 *Vangl2+/+, Vanlg2+/Lp* and *Lp/Lp* embryos sections showed that commissural axons in all the embryos reach the midline (B-D). L1 immunostaining of E11.5 *Vangl2+/+, Vanlg2+/Lp* and *Lp/Lp* embryos sections showed normal post-crossing enrichment (E-G). (White arrow, pre-crossing commissural axons; Yellow arrow, location of the floor plate; White arrowhead, post-crossing commissural axons; White bar, 100um scale)

We then analyzed the post-crossing trajectory of commissural axons in the *Lp* mouse by open-book DiI injection at E11.5, the time when commissural axons are beginning their anterior turn (Figure 2.5A). Our analysis and quantification of DiI injections in the spinal open-book prep revealed that while all commissural axons crossed the midline, the post-crossing axons in the *Lp/Lp* embryos became randomized. The heterozygous and homozygous embryos both displayed clear anterior-posterior axon guidance defects, as compared to the wildtype littermates, which primarily turned anteriorly at E11.5 (shown in Figure 6P and quantified in Figure 2.5F). Of the 70 DiI injection sites in 11 *Lp/Lp* embryos, 94.6% (+/-SEM 2.92) of the labeled axons showed an aberrant trajectory (Figure 2.5E). About half of these axons projected anteriorly (up) and the other half posteriorly (down), suggesting that growth along the longitudinal axis was intact, but up or down directionality was lost. In the 15 heterozygous littermates analyzed, 68.2% (+/-SEM 5.14) of axons from the 96 injection sites showed aberrance, and only 1/3 of the axons turned in the anterior direction (Figure 2.5B and C).
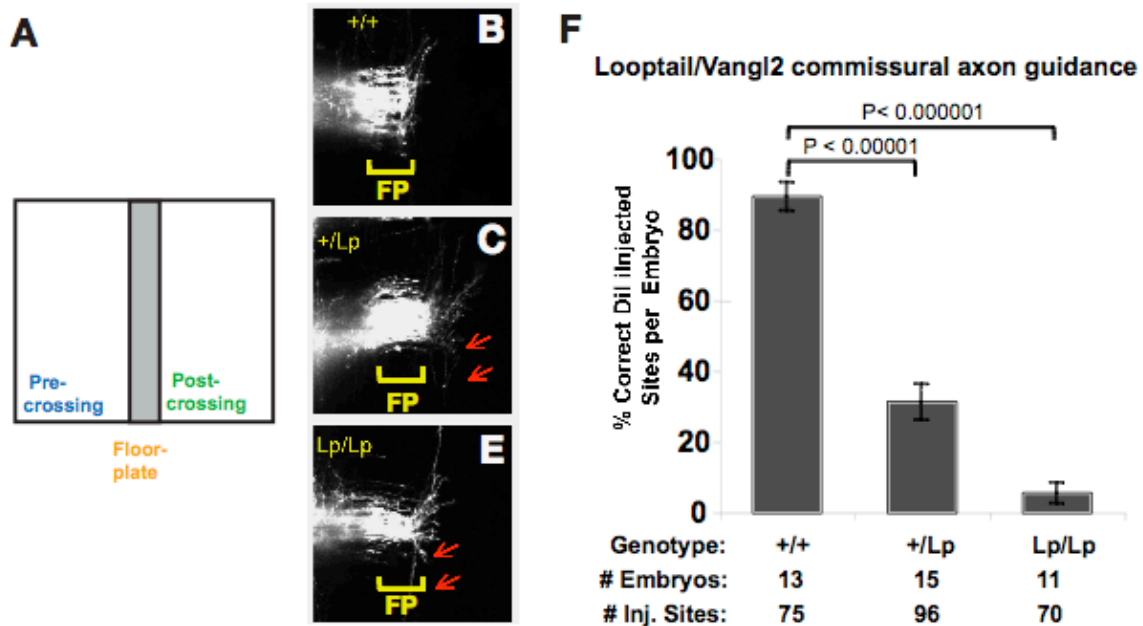
Figure 2.5 Anterior-posterior commissural axon guidance defects in the *Lp* embryos

(A) Schematic of DiI injected commissural axons in the open-book prep.

(B-E) *Vangl2+/Lp* and *Lp/Lp* embryos displayed aberrant A-P guidance. In these embryos only 31.1% and 5.41% of the DiI injection sites respectively showed correct commissural axon A-P guidance. Red arrows indicate axons projecting posteriorly. (F) Quantification of DiI injection sites in *Vangl2+/+, Vanlg2+/Lp* and *Lp/Lp* embryos. 89.2% (SEM+/-3.99%) of wildtype, 31.1% (SEM+/-5.16%) of heterozygous, and 5.14% (SEM+/-2.93%) of the Lp/Lp embryos showed correct DiI injection sites. Scale bars represent 100um.

2.3 Celsr3 is required for anterior-posterior guidance of commissural axons *in vivo*

To further demonstrate that the PCP signaling pathway is responsible for proper anterior-posterior guidance of commissural axons, we assessed whether the third transmembrane component of the PCP signaling pathway, Celsr3, was required. Similar to the analysis for the *loop-tail* mouse, we first verified that the Celsr3 null embryos did not have defects in cell specification or dorso-ventral

axon guidance. There were no observable differences in the Pax7 and Nkx2.2-positive spinal progenitor pools in the mutants, and expression of the post-mitotic markers Lhx1/5 and Islet1 were comparable to the Celsr3 wild type (Figure 2.6).
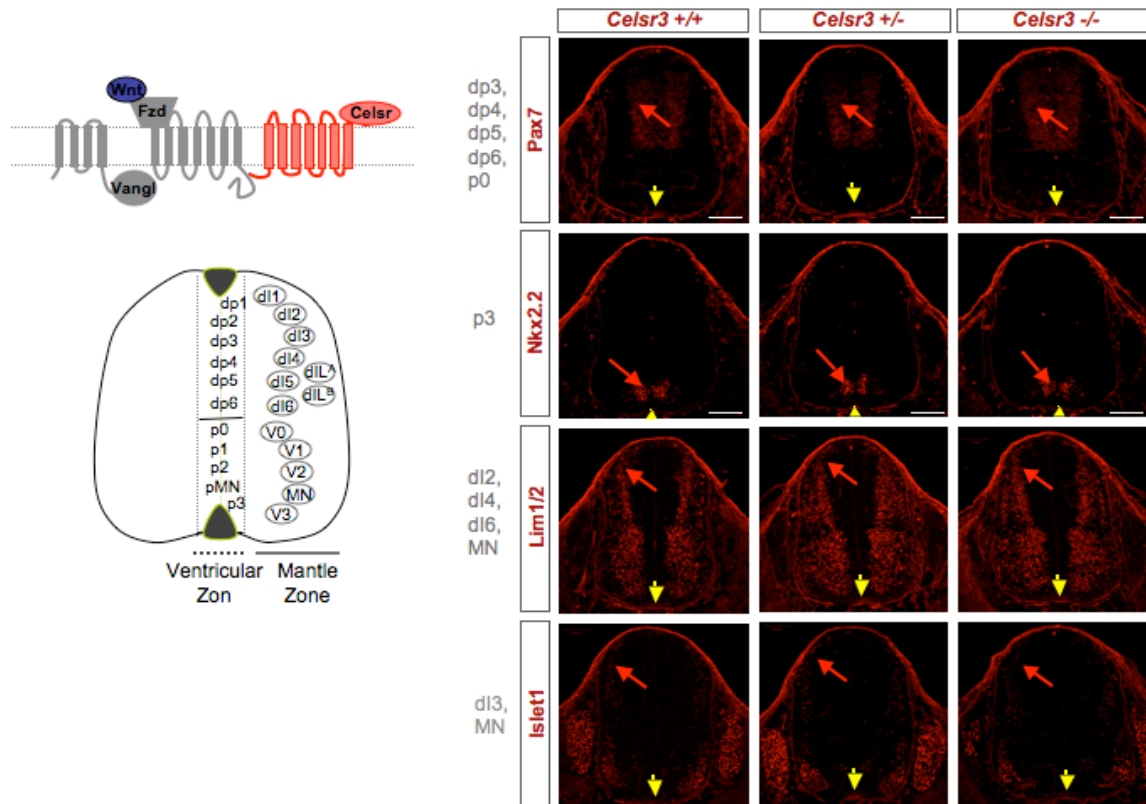
Figure 2.6 Progenitors and neurons are specified correctly in Celsr3 null embryos
On the left is a schematic of the PCP membranous components and a mouse transverse section depicting the neuronal progenitor domains and neuron types in the spinal cord at E11.5. Pax7 expression by the progenitor domains did not change in wildtype, heterozygous or homozygous *Celsr3* embryo spinal cords at E11.5.   Lhx1/5 expression remained unaltered in the Celsr3 wildtype, heterozygous and homozygous null embryos at E11.5.   NKx2.2 and Islet1 immunoreactivity in *Celsr3+/+, Celsr3+/-* and *Celsr3 -/-* embryos were similar. (Red arrow, cell bodies expressing indicated transcription factors; Yellow arrow, location of the floor plate).

TAG-1 and L1 immunoreactivity suggested normal dorso-ventral commissural axon trajectory, and no differences were observed in the homozygous Celsr3 null embryos as compared to the wildtype or heterozygotes (Figure 2.7). However, *Celsr3* null embryos at E11.5 showed severe defects in anterior-posterior commissural axon guidance, while the wildtype and heterozygous littermates remained normal.
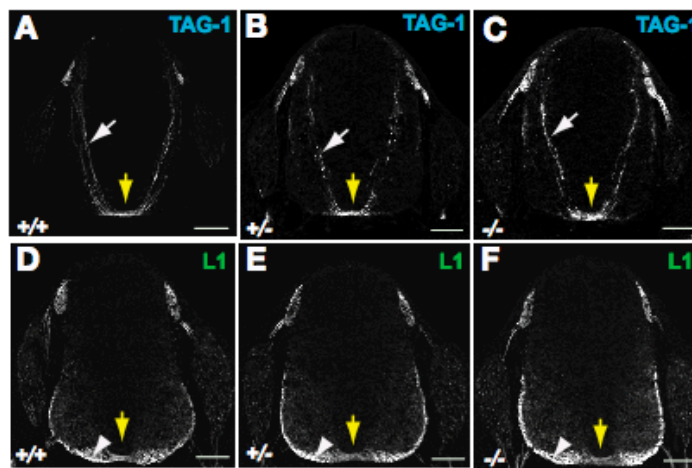
Figure 2.7 Dorso-ventral trajectories of commissural axons are normal in *Celsr3-/-* embryos
(A-C) TAG-1 immunostaining of E11.5 *Celsr3+/+, Celsr3+/-* and *Celsr3-/-* embryos sections showed that commissural axons in all the embryos reach the midline. (D-F) L1 immunostaining in E11.5 *Celsr3+/+, Celsr3+/-* and *Celsr3-/-* embryo sections (White arrow, pre-crossing commissural axons; Yellow arrow, location of the floor plate; White arrow head, post-crossing commissural axons; Scale bar represents 100um).

Examination of open-book DiI injections in *Celsr3 +/+* and *Celsr3+/-* embryos at E11.5 showed that axons turned in the correct anterior orientation, 90.0% (+/-SEM 10.0%) and 94.6% (+/-SEM 2.34%) of injection sites, respectively (Figure 2.8A). However, axons in the *Celsr3-/-* embryos that were randomized

such that only 6.00% (+/-SEM 3.88%) of DiI injection sites were classified as normal. In 50 injection sites and 7 embryos, 94% of axons displayed defects in anterior (up)-posterior (down) direction (Figure 2.8A and B).
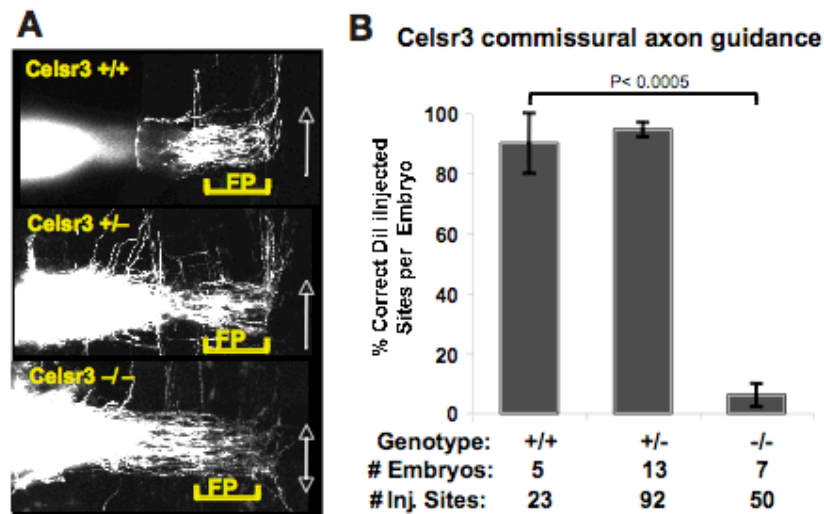
Figure 2.8 Celsr3 is required for A-P guidance of commissural axons
(A) Commissural axons in *Celsr3+/+ and Celsr3+/-* embryos showed normal anterior posterior guidance at E11.5, but *Celsr3-/-* embryos displayed randomized axons.
(B) The axonal trajectory in the *Celsr3+/+, Celsr3+/-* and *Celsr3 -/-* embryos were quantified, 90.0% (SEM+/-10.0%), 94.6% (SEM+/-2.34%), and 6.00% (SEM+/-3.88%) of the injection sites respectively displayed correct anterior trajectory.

2.4 Analysis of trans-heterozygotes to determine a genetic interaction

Taken together, we have shown a requirement for Vangl2 and Celsr3 in the anterior-posterior (A-P) guidance of commissural axons. The post-crossing A-P randomization phenotypes were similar to those of the Fzd3 null mice, which indicating that all three membranous components of the PCP pathway are required for proper C axon guidance. We next sought to determine if there was a

genetic interaction between the three PCP components, Fzd3, Vangl2 and Celsr3. To do so, we examined the A-P trajectory of the trans-heterozygotes of the following genotypes: *Fzd3+/-Celsr3+/-, Fzd3+/-Lp/+, and Celsr3+/-Lp/+.*

We first examined Fzd3 and Celsr3 trans-heterozygotes at E11.5 to determine if loss of one allele of Fzd3 or Celsr3 would be sufficient to cause aberrant commissural axon guidance. Our analysis of open-book DiI injections sites revealed no abnormal A-P randomization phenotype of the Fzd3+/-Cels3+/-, *Fzd3+/-* or Celsr3+/- embryos (Figure 2.9).
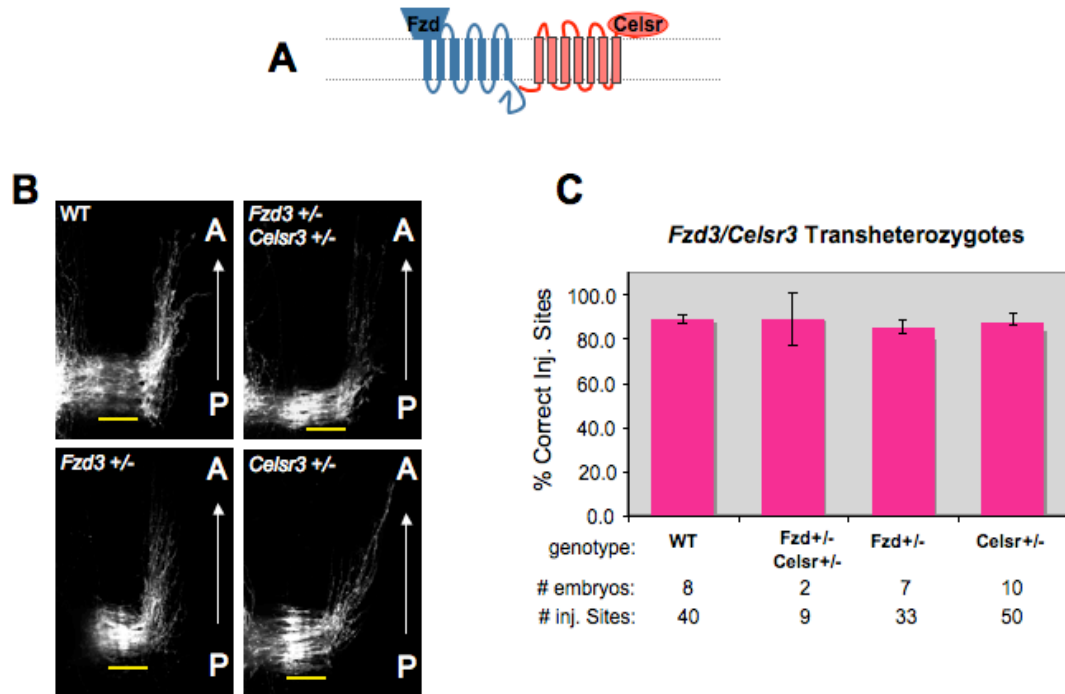
Figure 2.9 Fzd3+/- Celsr3+/- trans-heterozygotes have commissrual axons that turn anteriorly
(A) Schematic of the seven transmembrane (7TM) GPCR, Fzd3, and 7TM atypical cadherin, Celsr3. (B) Fzd3+/-*Celsr3+/+, Fzd3+/-,* and *Celsr3+/-* embryos showed normal anterior-posterior guidance (Yellow line; FP). (C) Quantification of the injection sites.

WT, *Fzd3+/-Celsr3+/-, Fzd3+/-* and *Celsr3+/-* embryos at E11.5 showed axons that turned in the correct anterior orientation, 88.8% (SEM+/-2.1), 88.9% (SEM+/-11.8) in 87.9% (SEM+/-3.00), and 86.0% (SEM+/-2.70) of the injection sites, respectively.

We next examined the Lp trans-heterozygotes. *Lp/+* hets already display A-P randomization, and 2/3 of the commissural population develops aberrant commissural axons after crossing. However, we asked if removal of either the Fzd3 or Celsr3 allele would exacerbate this phenotype. Neither the *Lp/+Fzd3+/-* nor the *Lp/+Celsr3+/-* displayed increased randomization after crossing and all phenocopied their *Lp/+* het littermates (Figure 2.10).
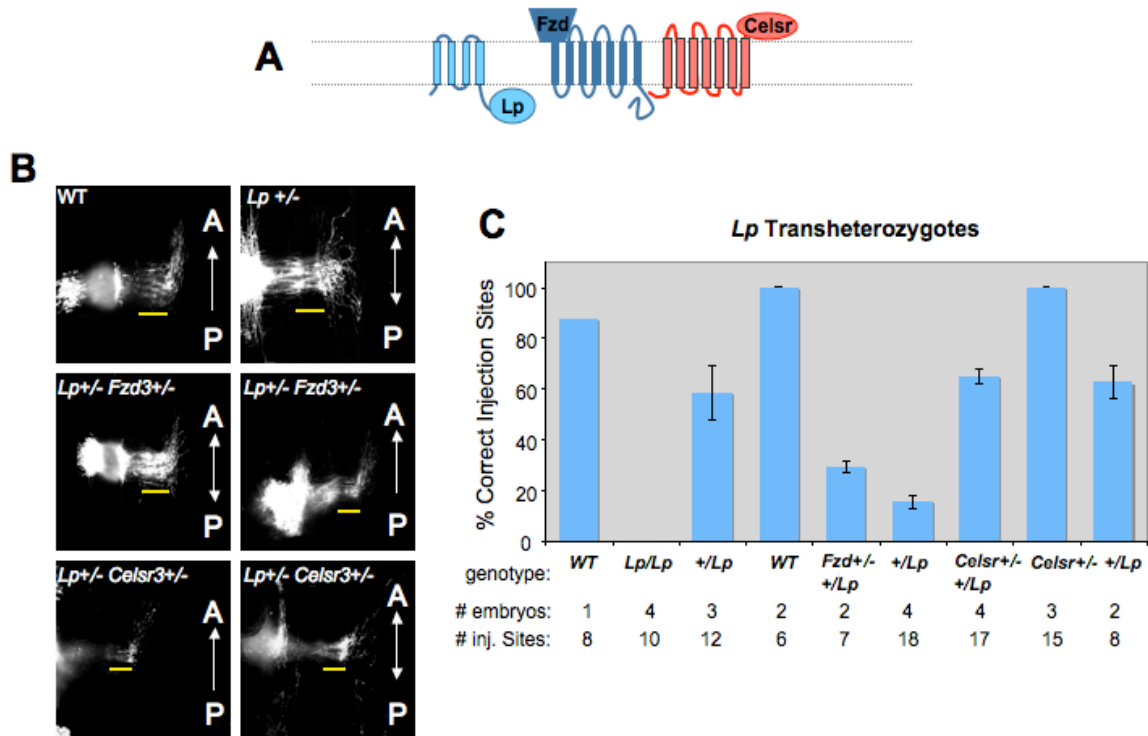
Figure 2.10   Lp/+ trans-heterozygotes show normal A-P guidance of commissural axons at E11.5
(A) Schematic of the four transmembrane Lp protein, 7TM-GPCR Fzd3, and atypical cadherin Celsr3. (B) DiI injections of the transhet embryos (Yellow, FP) (C) Quantification of the injection sites.

Examination of the embryonic trans-heterozygotic spinal cords revealed no difference in phenotype compared to the single heterozygotes. Although Celsr3 and Fzd3, and Fzd3 and Vangl2 have been shown to physically interact, it is possible that all three PCP components may be acting independently. At present we cannot rule out the possibility that these PCP components control different aspects of axonal guidance. For example, Celsr3, an atypical cadherin molecule that has been shown to self adhere and facilitate non-autonomous interactions between neighboring cells (Fanto and McNeill, 2004; Zallen, 2007), could

potentially be responsible for a non-autonomous mechanism of commissural axon guidance. In support of this model, we have consistently observed defasiculated axons after midline crossing in our analysis of Celsr3 null embryos, suggesting a possible role for Celsr3 in axon-axon fasciculation.

The analysis of the PCP mutant embryos demonstrated that Fzd3, Vangl2 and Celsr3 proteins are required for anterior-posterior guidance of commissural axons. However, Celsr3 null and Lp tail embryos have axons that traverse normally across the D-V plane of the spinal cord. It is known that Wnts are dispensable for the D-V trajectory of commissural axons but are critical for commissural axon anterior turning. Taken together, we can conclude the requirement for the Wnt-mediated PCP pathway in A-P guidance of commissural axons. The following chapters of this thesis explore the mechanistic details of how PCP components regulate Wnt-mediated axon guidance.

2.5 Acknowledgements

thank our collaborators, Fadel Tissir and Andre Gofinet, for the *Celsr3* mutant mice.

CHAPTER 3: PCP COMPONENTS IN THE SPINAL CORD, COMMISSURAL NEURONS AND THE WNT CONNECTION

3.1 Core PCP components are expressed in commissural neurons when their axons are making A-P guidance decisions

To test whether the Wnt-PCP pathway is involved in anterior-posterior guidance of commissural axons, we first analyzed the expression patterns of the core PCP components in the developing spinal cord using *in situ* hybridization (Figure 3.1). We found that all core PCP components (Figure 3.1C-J) are expressed in commissural neurons at mouse E11.5, a time when their axons are anteriorly turning. *Celsrs1, 2 and 3* are the three vertebrate homologues of *Flamingo*. *Celsr1* and *Celsr2* were expressed in the ventricular zone (data not shown) whereas *Celsr3* transcripts were found selectively in the post-mitotic mantle zone of the spinal cord (Figure 3.1C) and were particularly abundant in the areas encompassing commissural neuron cell bodies and regions expressing the Netrin-1 receptor *DCC* (Figure 3.1I), a marker for commissural neurons (Keino-Masu et al., 1996). As previously reported, *Frizzled3* mRNA was broadly expressed in the spinal cord, including the mantle zone where commissural neuron cell bodies reside (Figure 3.1D) (Lyuksyutova et al., 2003). Both *Vangl1* and *Vangl2* were also expressed broadly in the spinal cord (Figure 3.1E, F). *Prickle2* expression was observed in the commissural neurons as well as in the

ventral spinal cord (Figure 3.1H), whereas *Prickle1* was expressed primarily in the ventrolateral regions of the spinal cord (Fig 3.1G). The *Dishevelled* genes were widely expressed in the central nervous system, as previously reported (Tissir and Goffinet, 2006).
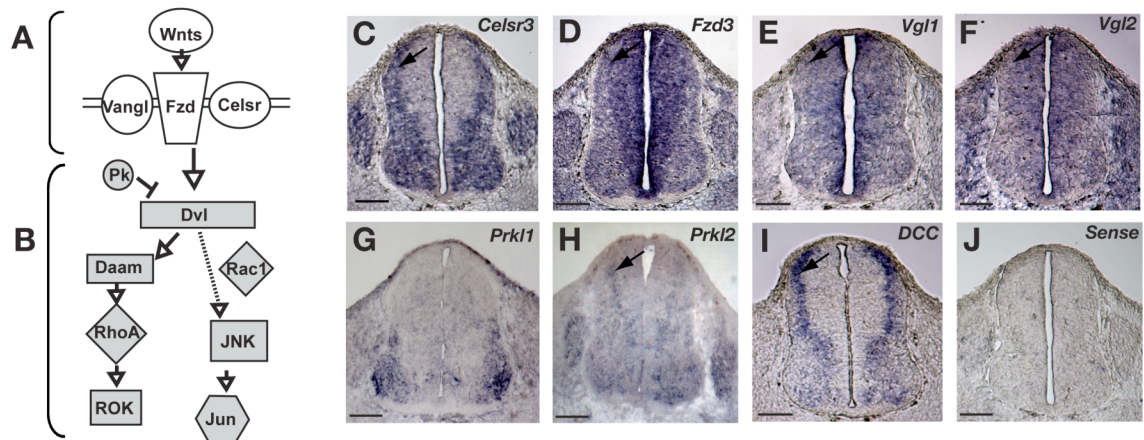
Figure 3.1 PCP signaling components are found in the developing spinal cord
(A-B) Schematic of the PCP pathway. The membrane components are depicted in (A) and the intracellular components activated by pathway are in (B)
(C-H) Expression of core PCP transcripts, *Celsr3, Fzd3, Vgl1, Vgl2, Prkl1* and *Prk2* in the E11.5 mouse spinal section. (I) Expression of the Netrin-1 receptor *DCC* at E11.5. Black arrow indicates commissural neuron cell body. (J) In situ hybridization of *Celsr3* sense control probe.

To characterize the expression patterns of the core PCP proteins in the spinal cord, we performed immunohistochemistry on mouse E11.5 spinal sections. Commissural axons have a pre-crossing and a post-crossing segment (green and red segments in Figure 1A, respectively) and a short crossing segment (yellow in Figure 1A). TAG-1 is expressed on the pre-crossing and

crossing segments in the spinal cord (Figure 3.2C) and L1 delineates post-crossing axons or growth cones (Figure 3.2D) (Zou et al., 2000). It has previously been shown that many proteins involved in directing commissural axons anteriorly after midline crossing are enriched in the post-crossing regions of the spinal cord. Accordingly, Celsr3 is broadly expressed in the spinal cord but enriched in the post-crossing segment (Figure 3.2B), along with Frizzled3 protein (Figure 3.2C).
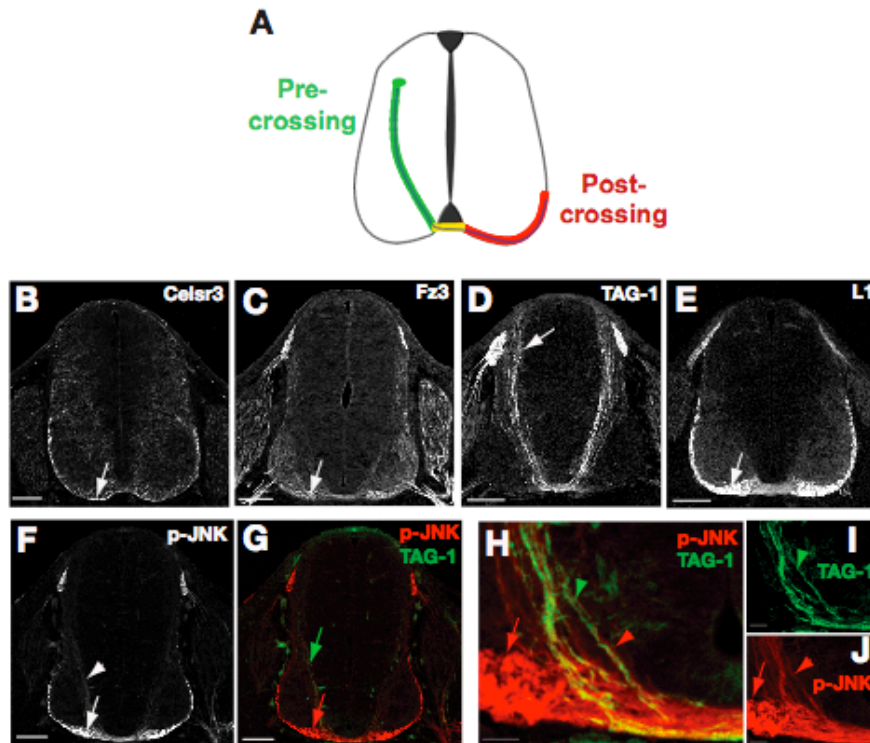
Figure 3.2 PCP components are expressed in commissural axons
(A) Dorsal-ventral schematic view of an E11.5 spinal cord section depicting the trajectory of the commissural axon (blue line). Green portion of the axon depicts pre-crossing the axons reaching the ventral midline, the yellow portion depicts the crossing segment, and the red portion depicts the axon after midline crossing (B-D) Celsr3 and Fzd3 receptor expression in the E11.5 mouse spinal cord. Note the up-regulation in the post-crossing region of the spinal cord as denoted by white arrow.   (D-E) Pre-crossing TAG-1 and post-crossing L1 receptor expression. White arrow denotes commissural axon fibers. (F) Phosphorylated-JNK (pJNK) staining in the spinal cord shows expression on commissural axons (short arrow) and enrichment in post-crossing commissural axons (long arrow).
(G-J)   Co-immunostaining in the mouse E11.5 spinal cord showing p-JNK positive axons (red, red arrow) co-express TAG-1 (green, green arrow). P-JNK enrichment in post crossing segment is shown by long red arrow. Short green and red arrowheads highlight colocalization.   (Black and white scale bars represent 100um and grey scale bars represent 20um.)

We tested the specificity of these antibodies by immunohistochemistry on E11.5

spinal sections, and by western blotting using samples from wildtype and

knockout embryos. The post-crossing staining of the antibodies is diminished in

Celsr3 and *Frizzled3* homozygous mutants (Figure 3.3A, B and C). Vangl2

protein has previously been shown to also be enriched in the post crossing axons

of the spinal cord (Torban et al., 2007).
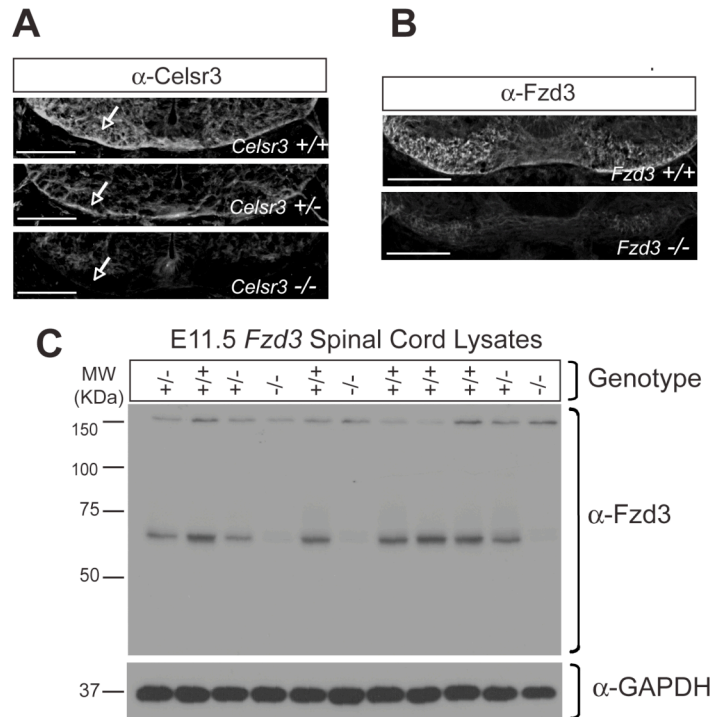
Figure 3.3 Specificity of Celsr3 and Fzd3 antibodies
(A) Post-crossing enrichment of the Celrs3 immunoreactivity is diminished in the *Celsr3-/-* embryos. E11.5 spinal sections of *Celsr3+/+, Celsr3+/-* and *Celsr3 -/-* embryos immunostained with the polyclonal antibody generated against the intracellular carboxyl terminal region of Celsr3 (amino acids 3099 to 3301). (B) Fzd3 immunoreactivity is reduced in the post-crossing spinal section of E11.5 *Fzd3-/-* embryos. (C) Fzd3 immunoreactivity in spinal lysates from E11.5 *Fzd3* embryos from heterozygous cross. Immunoreactivity is diminished in the heterozygous lysates and nearly absent from the homozygous lysates.

One downstream signaling component of the PCP pathway is Jun N-terminal Kinase (JNK), and PCP signaling activation is often measured by increased phosphorylation of JNK and/or Jun (Boutros et al., 1998). We found that the phosphorylated-JNK is present on commissural axons, as shown by co-immunoreactivity with TAG-1 (Figure 3.2F-J), and is enriched in the post-crossing segment of the E11.5 spinal cord (Figure 3.2F) in a similar manner to Vangl2, Celsr3 and Frizzled3 protein expression. Therefore, PCP components are expressed in the developing spinal cord in the right spatio-temporal pattern necessary to regulate anterior-posterior guidance of commissural axons.

To test whether PCP signaling components are present in axonal growth cones, we analyzed their distribution in dissociated commissural neuron cultures. We cultured dissociated commissural-specific neurons using a previously established method ((Augsburger et al., 1999)). We found that Celsr3, Fzd3, Vangl2 and Dvl are all present in dorsal commissural neurons and their growth cones after 24 hours of culture (Figure 3.4A-D). In addition, we noticed that Fzd3 and Vangl2 were often co-localized in subdomains of the growth cone plasma membrane or on the tips of growing neurites (Figure 3.4E-H).
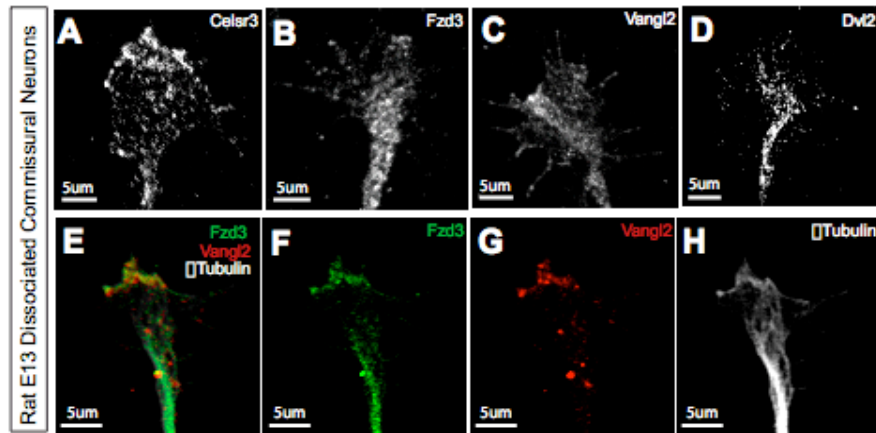
Figure 3.4 Dissociated commissural growth cones express PCP proteins
(A-E) Endogenous expression of Celsr3, Fzd3, Vangl2 and Dvl2 in pre-crossing commissural neurons. All components display punctate and membranous localization in the commissural growth cone. (E-H) Endogenous Fzd3 and Vangl2 co-localization in the commissural growth cone

3.2 Vangl2 and Frizzled3 synergistically mediate Wnt-stimulated outgrowth of commissural axons

To directly test the function of PCP components in Wnt-mediated outgrowth of commissural axons, we electroporated DNA constructs to express ectopic EGFP or mCherry fusion proteins of PCP components in dissociated commissural neurons. To do so we first establish an electroporated commissural culture system. The spinal cord of E11.5 mouse or E13 rat contains a ventricle into which plasmid DNA can be introduced (Figure 3.5A). After injecting DNA intro the ventricle and electroporating the spinal cord, an open-book preparation was performed, and then the commissural progenitor domains were dissociated as previously described ((Augsburger et al., 1999), Figure 3.5B). The

electroporated and dissociated neurons were TAG-1 immuno-reactive, confirming their commissural identity (Figure 3.5C).
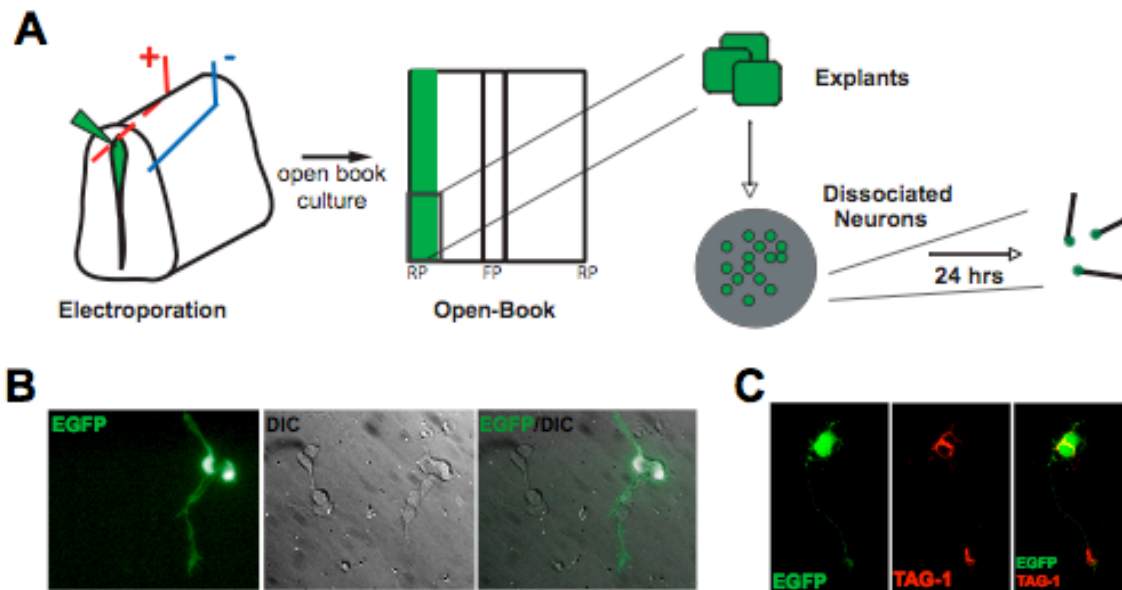
Figure 3.5   Establishing the electroporated-dissociated commissural neuron culture system
(A) Schematic of method used. (B) Commissural neurons electroplated with EGFP grow neurites within 24 hours of plating on Poly D Lysine-laminin coated coverslips. (C) Electroporated neurons are TAG-1 positive, which confirms their commissural identity.

Using this method we examined the effects of over-expression of PCP components on commissural neuron axonal growth.

Fzd3 and Vangl2 over-expression in pre-crossing neurons did not affect the growth of commissural axons compared to controls (Figure 3.6B, C), and an average axon length of 55 um was observed (Figure 3.6I).   Similarly, co-expression of both Fzd3 and Vangl2 showed no effect on axon length (Figure

3.6D and I). However, when we cultured the commissural neurons on Wnt5a-coated coverslips, we found that the electroporated over-expression of PCP components significantly enhanced axon length after 24 hours (Figure 3.6F and G). Neurons expressing Fzd3 or Vangl2 showed an increase in average axon length in the presence of Wnt5a (77.1um +/-SEM 3.1um and 77.0um +/-SEM 3.8um respectively, Figure 2.6I). Moreover, neurons that co-expressed Fzd3 and Vangl2 in the presence of Wnt5a displayed a synergistic increase in axon length, with an average length of 125uM after 24 hours of culture (Figure 3.6H and I).
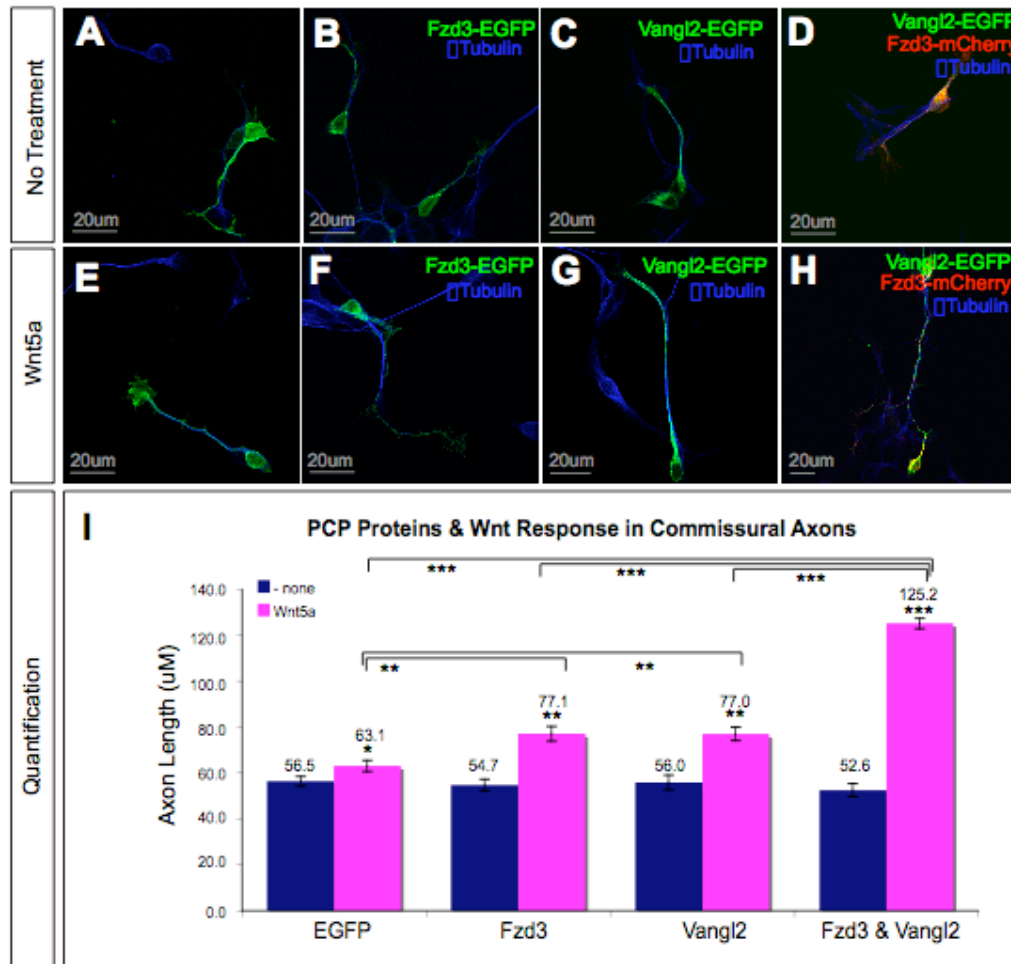
Figure 3.6   Over-expression of PCP components in pre-crossing commissural axons shows enhanced growth on Wnts
(A-D) Commissural neurons cultured for 24 hrs after electroporation with either EGFP, Fzd3-EGFP, Vang2-EGFP or both Fzd3-mCherry and Vangl2-EGFP. Axon length is quantified in (I), blue bars.   (E-H)   Commissural neurons electroporated with EGFP, Fzd3-EGFP, Vang2-EGFP or co-electroporated with Fzd3-mCherry and Vangl2-EGFP and grown on Wnt5a coated coverslips for 24 hrs.   The increased axon lengths are quantified in (I), purple bars.   (Q) Quantification of commissural axons depicted in (I-P).   * Denotes P value of <0.005, ** P value of <0.00005, *** P value of <0.000005.

Control neurons expressing EGFP exhibited a much smaller, but still

significant increase in axon growth in response to Wnt5a, with an average length

of 63.1um +/-SEM 2.2um (Figure 2I, 2M, 2Q and S3D). We attribute this increase to the endogenous levels of PCP components in pre-crossing axons (Figure 2A-H). As a result, our data suggest that these PCP components mediate Wnt5a stimulated axon outgrowth, and since Fzd3 and Vangl2 synergistically mediate this Wnt5a-dependent response both of these components may function in a PCP-like fashion in neuronal growth cones.

3.3 Dvl1 promotes the outgrowth of commissural axons in the absence of Wnts

Although the over-expression of the PCP surface molecules Fzd3-EGFP and Vangl2-EGFP alone, or Vangl2-EGFP and Fzd3-mCherry in combination, in the absence of Wnts had little effect on axon outgrowth as compared to the controls (Figure 3.6), the over-expression of the immediate downstream PCP intracellular component, Dvl1-EGFP, enhanced commissural axon outgrowth within 24 hours (Figure 3.7A and B). In addition, the presence of Wnt5a did not further enhance this increase this axon growth (data not shown). This is consistent with a previous report that Dvl1 increases the growth of cortical axons (Zhang et al., 2007b).
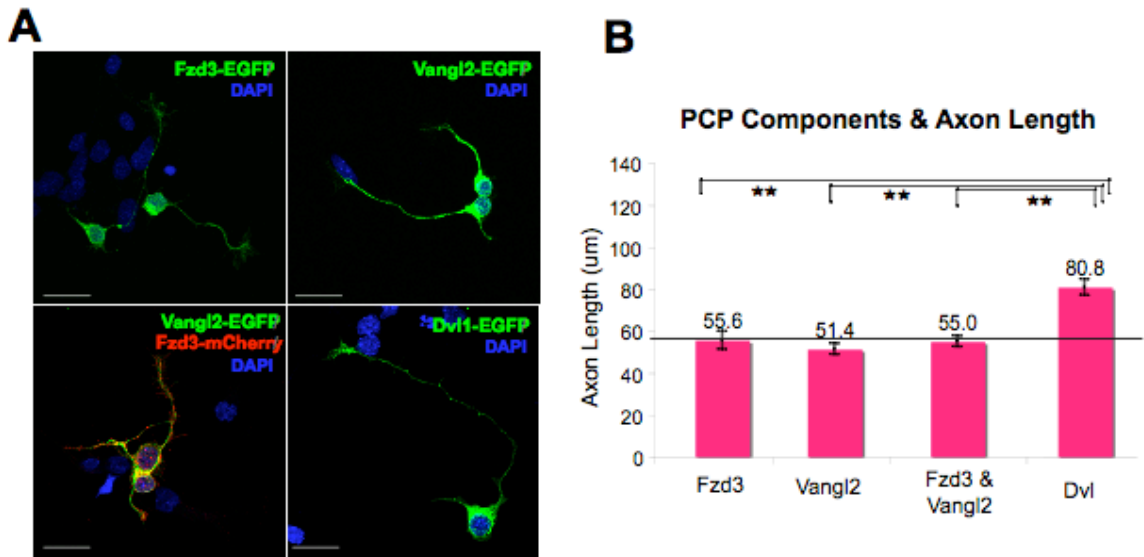
Figure 3.7 Dvl1-EGFP promotes axon elongation in the absence of Wnts
(A) Dvl1-EGFP promoted axon elongation in the absence of Wnts.
(B) Increase in length was similar to neurons grown on Wnt5a overexpressing PCP membrane components.

In addition, over-expression of Dvl proteins has been shown to enhance PCP signaling (Boutros et al., 1998; Li et al., 1999; Yao et al., 2004). Notably, the increase in axon length achieved by over-expression of Dvl1 in the absence of Wnts is of a similar magnitude to that observed with Fzd3 or Vangl2 in the presence of Wnts (Figure 2Q), suggesting that Dvl may be a downstream effector of Frizzled3 and Vangl2.

3.3 Acknowledgements

We thank Jeremy Nathans for the Frizzled3 antibody and *Frizzled3* mutant mice, and Anthony Wynshaw-Boris for the Dvl1 constructs. We also thank Anna Lyuksyutova, Leslie King and Jean Lu for the *in situ* probes used in Figure 3.1.

The materials of this chapter are under preparation for resubmission and will include Charles Lo and Delphine Delaunay and Yimin Zou as authors.

CHAPTER 4: MODIFCATION OF PCP COMPONENTS AT THE PLASMA MEMBRANE EFFECTS PCP SIGNALING

4.1 Dvl1 can be recruited to the cytoplasmic membrane of the growth cone by Fzd3

It is known that Fzd3 and Vangl2 can both bind to Dvl (Wong et al., 2003); (Torban et al., 2004a). Because Fzd3 is a cell surface Wnt-binding receptor it may recruit or stabilize Dvl at the growth cone plasma membrane. To test whether Fzd3 affects Dvl1 localization we co-expressed both Fzd3-mCherry and Dvl1-EGFP in dissociated commissural neurons. Dvl1-EGFP expression alone in commissural neurons resulted in a punctate vesicular pattern along the neurite and in the growth cone (Figure 4.1B and E-H). However, upon co-expression with Fzd3-mCherry, the punctate aggregates completely dispersed and appeared to localize to the membrane of the commissural axon and growth cone (Figure 4.1C and J-L). This finding is similar to previous studies in other cellular contexts where Dvl was found recruited to the membrane by Fzds in the drosophila epithelia (Axelrod et al., 1998). Whereas Fzd3 normally localizes both to the plasma membrane and internal membrane compartments in the commissural growth cone, where it is thought to associate with both microtubules and the actin cytoskeleton (Figure 4.2). Then again, when co-expressed with Dvl1-EGFP, Fzd3-mCherry was found solely localized to the plasma membrane (Figure 4.1C and K).
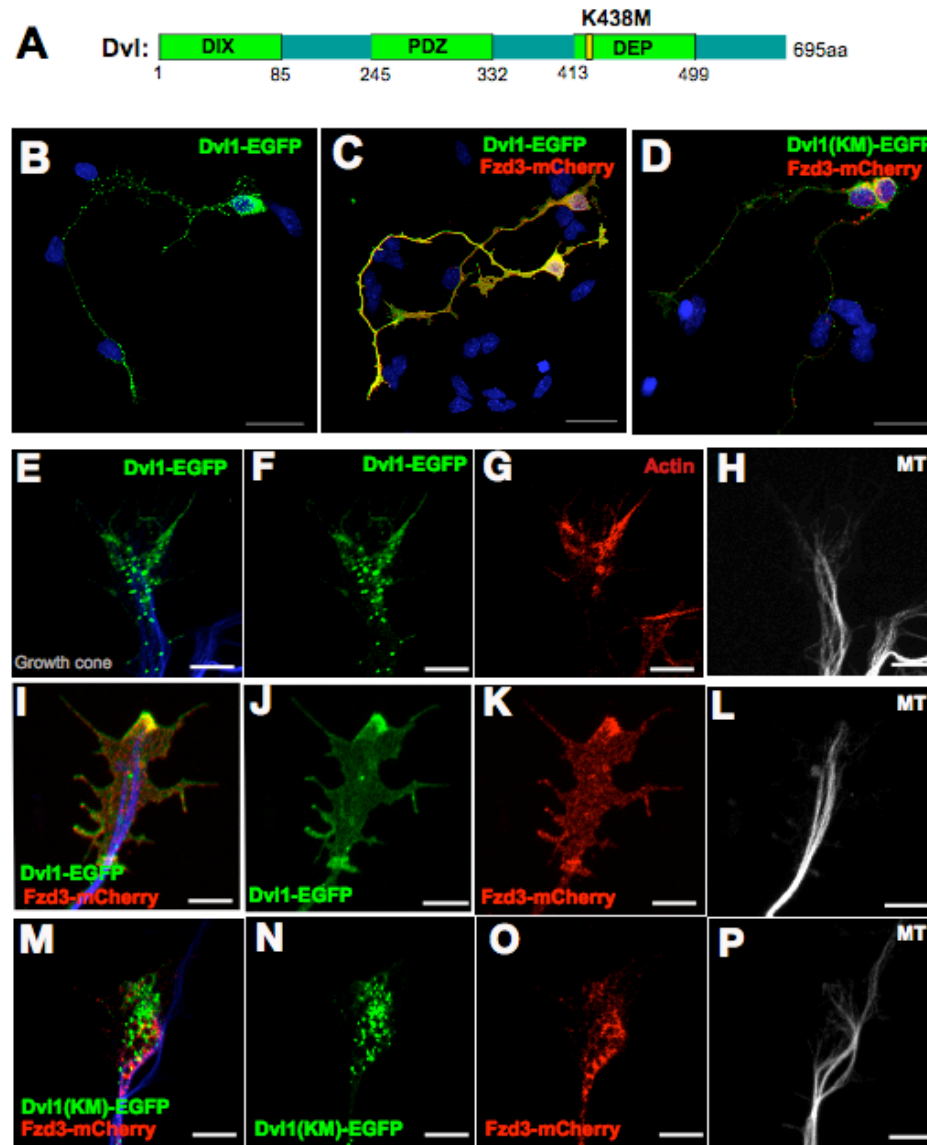
Figure 4.1 Fzd3 recruits Dvl1 to the plasma membrane of commissural axons

(A) Schematic of all three characterized domains in Dvl1 including the location of a K438M mutation that renders the protein PCP signaling defective. (B) Dvl1-EGFP showed punctate expression pattern in commissural neurons. (C) Dvl1-EGFP became membranous when co-expressed with Fzd3-mCherry.   (D) However, Dvl1 DEP domain mutant, Dvl1(KM)-EGFP, with Fzd3-mCherry did not result in translocation to the membrane. (E-H) The commissural growth cone expressing Dvl1-EGFP (I-L) both Dv1-EGFP and Fzd3-mCherry or (M-P) Dv1(KM)-EGFP and Fzd3-mCherry. (MT denotes microtubules outlined by α-tubulin staining within the growth cones.) Grey scale bars represent 20um and white scale bars represent 5um.

Here, we showed that co-expression of Fzd3 and Dvl1 caused both proteins to localize to the plasma membrane of commissural neurons rather than intracellular vesicles. It is of interest to note that excess membrane protrusions were observed along the neurites of neurons co-electroporated with both Fzd3-mCherry and Dvl1-EGFP. This suggests an interaction between Frizzled3-Dvl1 that may enhance axon outgrowth by regulating membrane insertion to the growth cone (Figure 4.2).
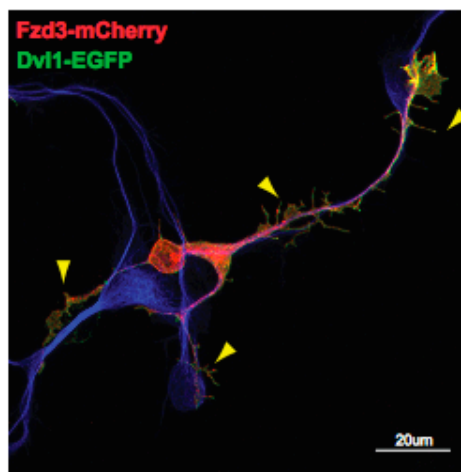
Figure 4.2 Fzd3-mCherry and Dvl1-EGFP co-expression in dissociated commissural neurons
Excess membranous protrusions (yellow arrowhead) resulted from Fzd3-mCherry and Dvl1-EGFP co-electroporation in rat E13 commissural neurons

Fzds and Dvls are known to be required in several other Wnt signaling pathways. Dvl proteins have three domains: an N-terminal DIX domain that is required for canonical signaling, a PDZ domain that is responsible for binding proteins like Fzds, and a C-terminal DEP domain that is necessary for PCP

phenotypes (Figure 4.1A) (Park et al., 2005);(Wang et al., 2006a). A single amino acid mutation of Lysine 438 to a Methionine within the DEP domain has been shown to be essential for PCP signaling activation (Boutros et al., 1998); (Moriguchi et al., 1999). To test whether the translocation of Dvl1 upon over-expression of Fzd3 is indeed dependent on PCP signaling, we expressed the Dvl1(KM) DEP mutant in commissural neurons and asked whether the mutant Dvl1 could still be targeted to plasma membrane. Our results showed that Dvl1(KM)-EGFP cannot be recruited to the plasma membrane by Fzd3-mCherry in commissural neurons (Figure 4.1D and M-P), and did not cause excess membrane protrusions as observed with the wildtype Dvl1-EGFP. Therefore, our data is consistent with a model that predicts endogenous Fzd3 and Dvl1 may interact in axonal growth cones in a PCP-like fashion, perhaps by stabilizing each other at the plasma membrane and promoting growth cone membrane protrusion towards the source of Wnts.

4.2 Dvl1 provides inhibitory feedback to Frizzled3-PCP signaling after activation by Wnt5a

The localization of Fzd3 and Dvl1 to the growth cone plasma membrane appears to be essential to promoting further membrane growth. Following our observation that Fzd3 and Vangl2 synergistically mediate Wnt5a attraction, we next asked what specific effects Vangl2 might have on Fzd3 at the plasma membrane. Co-expression of Fzd3-mCherry and Dvl1-EGFP in HEK293T cells resulted in the same excess membrane outgrowth and translocation of both

molecules to the membrane (Figure 4.3) as we observed in the growth cones of commissural neurons, suggesting a common function in both cell types.
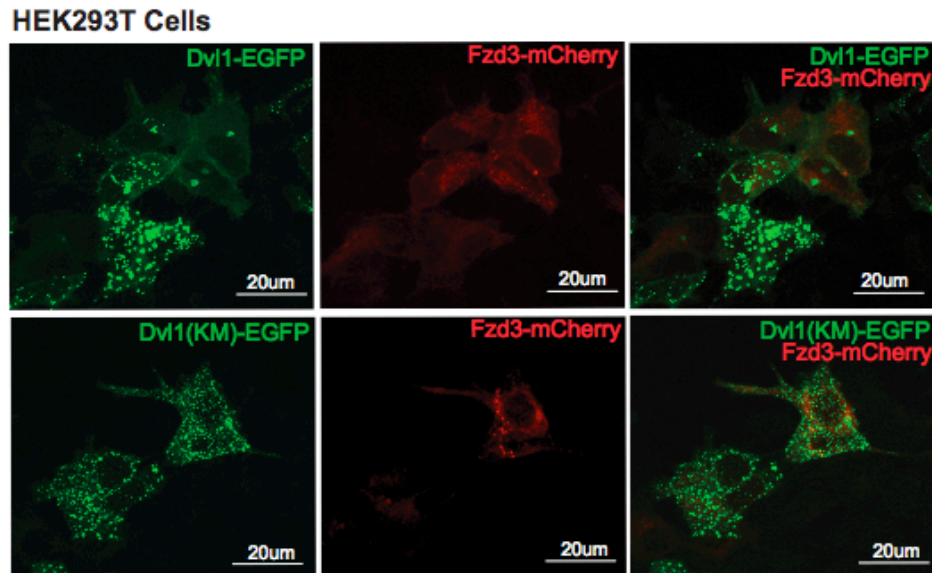
Figure 4.3 Fzd3-mCherry and Dvl1-EGFP co-expression in HEK293T cells
Dvl1-EGFP and Fzd3-mCherry when over-expressed in HEK293T cells translocate to the membrane. However, Dvl1(KM)-EGFP fails to localize to the membrane upon over expression of Fzd3-mCherry.

Therefore, to understand the biochemical effect how Fzd3 and Dvl1 components effect modification PCP components and signaling we decided to continue our studies in this heterologous cell line, as these cells are easier to prepare.

We transfected Fzd3-mCherry alone or Fzd3-mCherry with Dvl1-EGFP in HEK293T cells and added Wnt5a proteins for 15min or 30min. After Wnt5a treatment, we surface biotinylated the cells and immunoprecipitated (IP) the surface molecules with strepavidin-conjugated beads to obtain membrane-localized proteins. These surface fractions were then analyzed on immunoblots. To verify that only the surface-biotinylated proteins were isolated, we performed

a no-biotin membrane label control and found that Fzd3-mCherry was absent, suggesting the immunoprecipitation was specific to surface biotin-labeled proteins (lane 1 in Figure 4.4B and 4.5B). Two different bands for Fzd3 were observed, one for phosphorylated Fzd3 and one for non-phosphorylated Fzd3 (Figure 4.4B, lanes 2-4). However, co-transfection of Fzd3-mCherry with Dvl1-EGFP resulted in only the phosphorylated upper band (Figure 4.4B, lanes 5-7). It should be noted that this effect was found only in the membrane fraction, and the total cell fraction did not yield a difference in Fzd3 banding pattern between the single (Fzd3-mCherry) and double (Fzd3-mCherry and Dvl1-EGFP) transfected cell lysates.
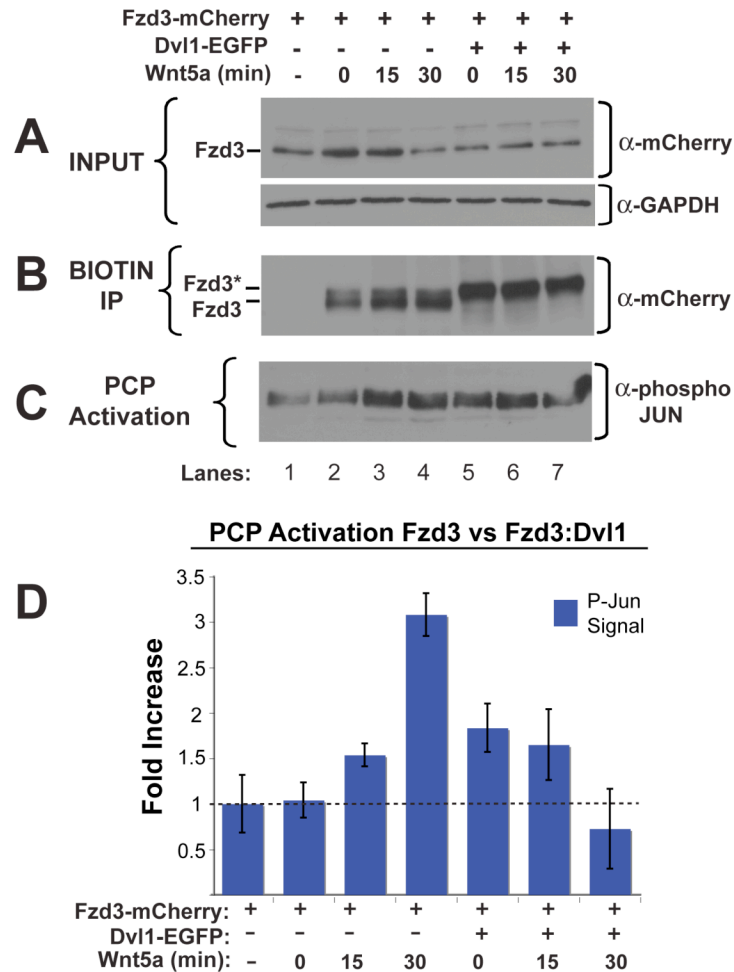
Figure 4.4 **Wnt5a modulates phospho-Jun in cells expressing Fzd3, but PCP signaling is down-regulated in a Dvl1 and Wnt5a-dependent manner**
(A) There was no difference in Fzd3-mCherry modification in total cell lysate when Fzd3-mCherry (lanes1-4) or both Fzd3-mCherry and Dvl1-EGFP (lanes5-7) were transfected into HEK293T cells and treated with Wnt5a as shown by immunoblot (IB) with anti-mCherry. The input lysates were also subject to anti-GAPDH IB to determine relative loading. (B) Fzd3-mCherry was phosphorylated at the membrane upon over-expression with Dvl1-EGFP. Inputs from (A) were surface biotinylated and immunoprecipitated (IP) with strepavidin beads and IB with ant-mCherry (lysates from Lane 1 were not surface biotinylated and therefore did not IP with the membrane fraction). (C) Phospho-Jun was activated in a Wnt5a-dependent manner in HEK293T cells expressing Fzd3 mCherry, but down-regulated in HEK293T cells expressing both Dvl1-EGFP and Fzd3-mCherry. Transfected cells were treated with either vehicle for 30 minutes (lanes 1,2 and 5), Wnt5a for 15 minutes (lanes 3 and 6), or Wnt5a for 30 minutes (lanes 4 and 7), and lysates were collected and subject to anti-phospho-Jun IB. (D) Quantification of relative phospho-Jun signal as measured by gel densitometry analysis with Image J.

To address how PCP signaling is affected by Fzd3 and Dvl interactions, we used a classic readout for PCP signaling, the phosphorylation of Jun (Boutros et al., 1998; Li et al., 1999; Yao et al., 2004). We found that the addition of Wnt5a at 15 and 30-minute time points resulted in a three fold increase in phospho-Jun levels in our over expressing cells (Figure 4.4C lanes 3 and 4, and Figure 4.4D). No differences in total Jun levels were observed (data not shown). In the absence of Wnts, the co-expression of Dvl1-EGFP and Fzd3-mCherry increased PCP signaling (Figure 4.4C, lane 5) and we observed a two fold increase in phospho-Jun compared to Fzd3-mCherry (Figure 4.4D, and 4.4C lanes 5 and 2 respectively). This activation by Dvls has been well documented (Boutros et al., 1998; Li et al., 1999; Yao et al., 2004). The increase in PCP signaling activity in the absence of Wnts may explain the Wnt-independent activation of PCP observed in the *Drosophila* model system (Fanto and McNeill, 2004; Saburi and McNeill, 2005). However, in the presence of Wnts, we observed Jun phosphorylation to dramatically decrease within 30 minutes, such that phospho-Jun levels now were comparable to baseline levels of Fzd3-mCherry alone without Wnts (Figure 4.4C lane 7, quantified in Figure 4.4D). We also observed a decrease in the surface levels of phospho-Fzd3 (Figure 4.4B lanes 5-7). To test whether Frizzled3 phosphorylation requires PCP signaling, we co-transfected Fzd3-mCherry with Dvl1(KM)-EGFP (Figure 4.5A, lane 6) and

found that the Dvl1 DEP domain mutant failed to give rise to phosphorylated Fzd3 at the membrane (Figure 4.5B).
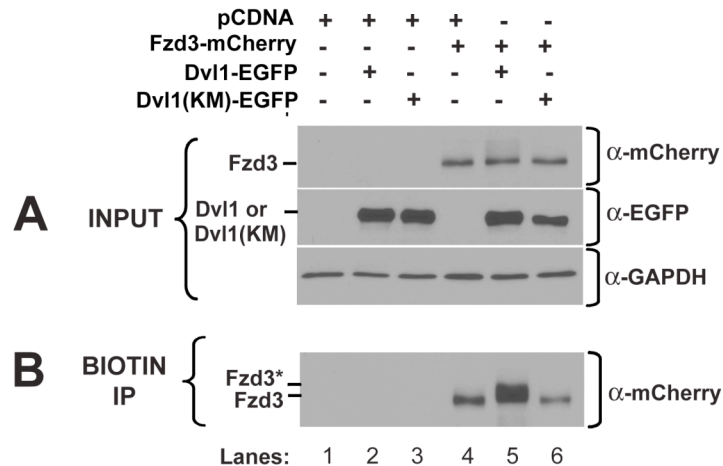
Figure 4.5 Fzd3 phospho-modification is specific to the PCP signaling pathway
(A-B) Dvl1 DEP domain mutant did not promote phosphorylation of Fzd3-mCherry at the membrane. Lysates from HEK 293T cells transfected with the indicated combinations were IB for anti-mCherry, anti-EGFP and anti-GAPDH. The surface biotinylated fractions were subject to IP, and anti-mCherry IB.

Phosphorylation of Fzds has been shown previously in *Xenopus* oocytes and *Drosophila* eye (Djiane et al., 2005; Yanfeng et al., 2006). Here, we show for the first time, by analyzing cell surface Frizzled3 protein, a novel Dvl1-mediated negative feedback loop that shuts down Wnt-Frizzled PCP signaling upon its activation.

4.3 Vangl2 antagonizes Dvl1 and its inhibitory feedback on PCP signaling

We have shown that Vangl2 and Fzd3 over-expression can synergistically promote commissural axon length (Chapter 3). To further delineate the role of Vangl2, we triple transfected Fzd3-mCherry, Dvl1-EGFP and 3xFlag-Vangl2 and treated the cells with Wnt5a for 15 or 30 minutes (Figure 4.6A, lanes 1-3). After isolating the membrane proteins, we found that co-expression of Vangl2 with Fzd3-mCherry and Dvl1-EGFP resulted in a re-appearance of the non-phosphorylated Fzd3 band at the membrane (Figure 4.6B, lanes 1-3). 3xFlag-Vangl2 either prevented complete Dvl1-EGFP-dependent phosphorylation of Fzd3-mCherry at the membrane or promoted the dephosphorylation of membrane bound Fzd3-mCherry that initially resulted from Dvl1-EGFP over-expression. We then assayed the effects on PCP signaling when Wnt5a was added and found that the presence of Vangl2 consistently attenuated the decrease of phospho-Jun levels, a negative feedback effect mediated by Dvl1 (Figure 4.6C, lanes 1-3). After normalizing phospho-Jun levels to input and time zero, the rate of decrease in phospho-Jun levels was plotted as a function of time in the presence of Wnt5a. We found that Wnt5a-induced decrease of Jun phosphorylation was recovered in the presence of Vangl2 expression (Figure 4.6D). Therefore, we hypothesize that Vangl2 can prolong PCP signaling through an antagonistic effect on the Dvl feedback loop.

The *Loop-tail* mouse, a classic PCP mutant, has a single amino acid substitution of the Vangl2 protein (S464N) that renders the protein unstable and nonfunctional (Kibar et al., 2001a; Kibar et al., 2001b; Montcouquiol et al., 2006b; Torban et al., 2004b). We triple transfected HEK293T cells with 3xFlag-Lp, Fzd3-

mCherry and Dvl1-EGFP, and then treated with Wnt5a, and did not observe the non-phosphorylated band of Fzd3-mCherry, suggesting that the mutant Vangl2 protein Lp cannot antagonize the phosphorylation of Fzd3 induced by Dvl over-expression (Figure 4.6B, lane 4-6). To examine how Lp affected PCP signaling, we again analyzed Jun phosphorylation following Wnt5a-stimulation. We found that Lp accelerated the down-regulation of phospho-Jun triggered by Wnt5a (Figure 4.6C, lanes 4-6), such that the signal was eliminated after 30 minutes in the presence of Wnt5a (Figure 4.6C, lane 6).
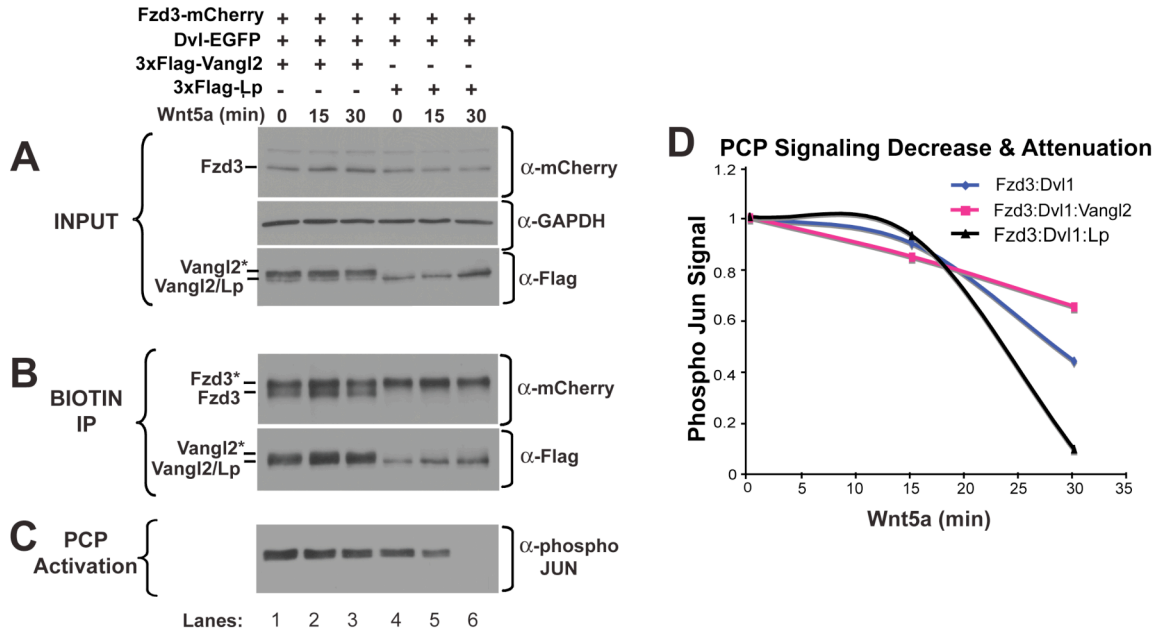
Figure 4.6 Vangl2 antagonizes the effects of Dvl1
(A) 3XFlag-Vangl2 was phosphorylated and Lp mutation S464N in Vangl2 lacks this modification. Triple transfection of the indicated PCP constructs were lysed and IB for anti-mCherry, and anti-GAPDH and anti-Flag. (B) Vangl2 promoted dephosphorylation of Fzd3, while Lp mutant fails to do so. HEK293T cells were transfected with the indicated three constructs, surface biotinylated, followed by IP and IB for anti-mCherry. Transfections including Vangl2 resulted in both non-phosphorylated and phosphorylated Fzd3-mCherry bands while triple transfections with Lp (3xFlag-Lp; Dvl1-EGFP; Fzd3-mCherry) resulted in only the phospho-Fzd3-mCherry band. Anti-Flag IB blot showed that both 3xFlag-Vangl2 and 3x-Flag-Lp bound to the membrane. (C) Vangl2 prolonged the phospho Jun signal. HEK293T cells were transfected with the indicated constructs and treated with Wnt5a. In the presence of 3xFlag-Vangl2, the Dvl1-EGFP-dependent decrease of phospho-Jun with Wnt5a stimulation was attenuated. However, 3xFlag-Lp was unable to prolong the phospho Jun signal. Rather, Lp promoted phospho-Jun signal decay in a Wnt5a dependent manner. (D) Quantification and plotting of phospho-Jun signal after normalizing time zero to the value of 1.

To test whether the inhibition of Fzd3 phosphorylation by Vangl2 at the plasma membrane depends on its interaction with Dvl1, we co-transfected 3xFlag-Vangl2 and Fzd3-mCherry in the absence of Dvl1-EGFP (Figure 4.7B, lane 1-3). Over-expression of 3xFlag-Vangl2 resulted in the presence of only the

lower, non-phosphorylated Fzd3 band at the membrane (Figure 4.7B, lanes 1-3).

With Fzd3-mCherry alone, we observed both phosphorylated and non-phosphorylated forms of Fzd3 at the cell surface (Figure 4.4B, lanes 1-4) indicating that Vangl2 can inhibit Fzd3 phosphorylation in the absence of Dvl.
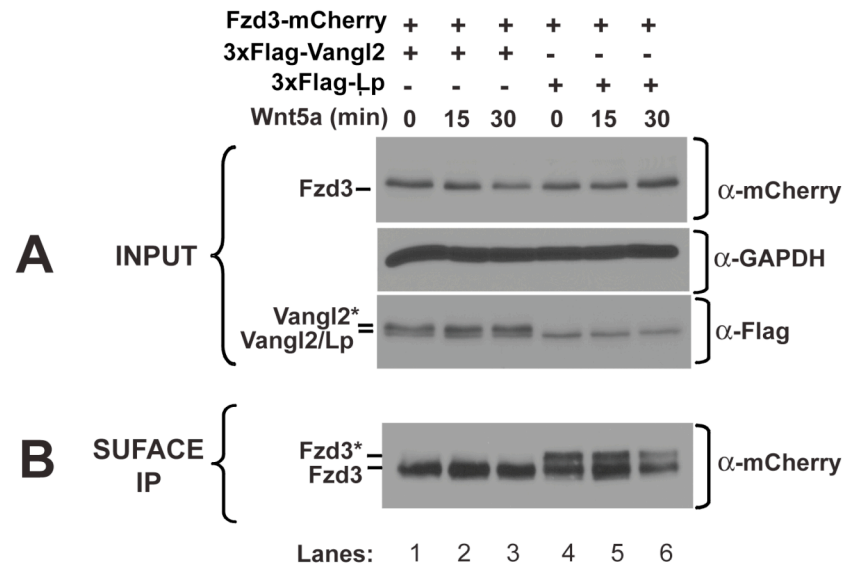
Figure 4.7   Vangl2 promotes the dephosphorylated form of Fzd3 at the membrane
(A) Vangl2 is phosphorylated in the absence of Dvl. In the absence of Dvl1-EGFP in the transfection Vangl2 still displayed a phospho band. (B) Vangl2 kept Fzd3 in a dephosphorylated state at the membrane.   HEK293T cells were transfected with the indicated plasmids and subjected to surface phosphorylation and strepavidin IP. Anti-mCherry IB revealed that Fzd3-Cherry in the presence of Vangl2 only exists in a non-phospho form (lanes 1-3). However, when co transfected with only 3xFlag-Lp, both forms of Fzd3-mCherry was observed, similar to Fzd3-mCherry single transfection.

We also analyzed the membrane preparation from the 3xFlag-Lp and Fzd3-mCherry co-transfection and found that both forms of Fzd3-mCherry were present, similar to what was observed with the Fzd3-mCherry alone (Figure 4.4B,

lanes 4-6).   Therefore, the *loop-tail* mutation appears to render Vangl2 non-functional, as Lp does not prevent the phosphorylation of Fzd3. Additionally, the Lp mutation affects the phosphorylation state of Vangl2 itself.   In the 3xFlag-Vangl2 inputs we observed two distinct bands with the anti-Flag immunoblot (Figure 4.7A, lanes 1-3); however, the upper band was not present following 3xFlag-Lp transfection (Figure 4.7A, lanes 4-6).   Phosphorylation of Vangl2 was not affected by the presence of Dvl, as the input from triple transfections with Dvl1-EGFP, Fzd3-mCherry and Vangl2 or Lp demonstrated identical anti-Flag band patterns as the transfections lacking Dvl1 (Figure 4.6A and 4.7A, α-Flag immunoblot).   Furthermore, both forms of Vangl2 appeared to localize to the plasma membrane, as shown by the surface IP and anti-Flag immunoblot (Figure 4.6B).

From the biochemical studies of PCP components in the heterologous HEK293T cells we found that Dvl1 and Vangl2 regulates the phosphorylation of Fzd3 at the cell membrane.   In addition, phosphorylation of Fzd3 and Wnt5a addition appear to effect the levels of phospho Jun and PCP signaling.

4.4   JUN/JNK signaling is required for the anterior-posterior guidance of axons

To determine if inhibition of Jun signaling is important to axon guidance in vivo, we returned to our classic spinal open-book assay.   Phospho-Jun is a classic readout of JNK activity (Boutros et al., 1998; Jaeschke et al., 2006), and we found that phospho-JNK was up-regulated in post-crossing regions of the

commissural axons *in vivo* (Chapter 3, Figure 3.2). Due to the high levels of redundancy and their importance for many processes in early development, analyzing knockout mice of JNK gene families to test whether JNK activity is required for anterior-posterior (A-P) guidance of commissural axons was technically not feasible. Therefore, to understand the effect of Jun/JNK signaling *in vivo,* we applied JNK inhibitors JNKI-1 and SP600125 in the spinal "open-book" explant assay at a time when commissural axons are making their anterior turning decision, rat E13 (Figure 4.8). These inhibitors block all three specific JNKs (Jun N-terminal Kinases 1-3) that are found in vertebrates.
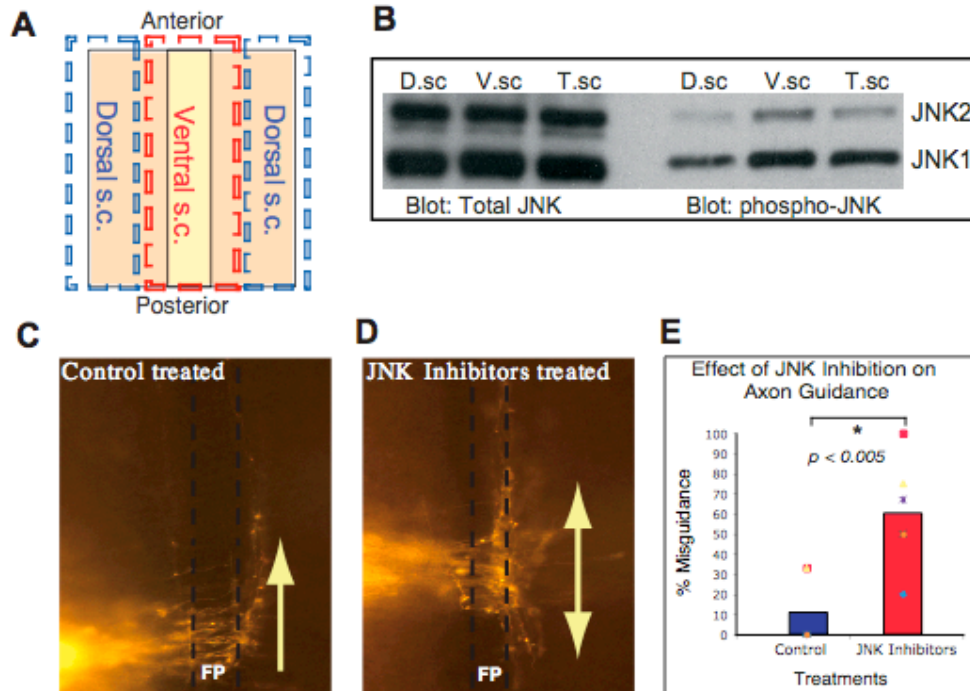
(Lo & Shafer, unpublished)

Figure 4.8 Activated phospho-JNK is enriched in post-crossing rat E13 spinal cords, and required for anterior-posterior guidance of commissural axons

(A) Schematic of E13 rat spinal cord open-book and regions used for western blot analysis (s.c., spinal cord) (B) Western blot analysis of dorsal spinal cord (D.sc) enriched with pre-crossing axons, ventral spinal cord (V. sc) enriched with crossing and post-crossing axons, and total spinal cord (T.sc) using anti-JNK (left) and anti-phosphorylated-JNK (right) antibodies (C-E) Functional inhibition of JNK and its effects on commissural axon guidance. E13 rat open-book spinal cords were incubated *in vitro* for 5-6 hours, then treated with control diluents or a combination of JNK inhibitors (JNKI-1 and SP600125) for 18 hours. Focal DiI injection of control (C) and of JNK inhibitor treated spinal cords. (E) Quantification revealed JNK inhibitor-treated spinal cords resulted in 54.2% (SEM +/-6.39%) misguidance, compared to only 9.00% (SEM+/-5.57%) with control.

We first took lysates from the E13 rat spinal cord to confirm an up-regulation of JNK in the ventral spinal cord enriched in post-crossing axon fibers. Both activated JNK1 and JNK2 were indeed up-regulated in the ventral spinal

cord (V.sc) as compared to the dorsal spinal cord (D.sc), (phospho-JNK blot, Figure 4.8B). Furthermore, inhibiting JNK activity lead to A-P randomization and misguidance of commissural axons. Approximately 9.00% (+/-SEM 5.57%) of control axons showed randomized behavior compared to 54.2% (+/-SEM 6.39) of JNK-inhibited axons (Figure S4D and E). Therefore, the downstream effector of PCP signaling, phospho-JNK, is required for the A-P guidance of commissural axons.

Previous studies in *Drosophila, Xenopus* and mice have demonstrated the importance of JNK/Jun signaling in PCP phenotypes (Boutros et al., 1998; Fanto et al., 2000; Li et al., 1999; Strutt et al., 1997; Weber et al., 2000; Yao et al., 2004). Studies of drosophila photoreceptor cell specification in the ommatidia showed that modulation of JNK signaling by reduction or over-expression, rather than its complete removal, leads to PCP phenotypes. Our data support a similar regulation since reducing JNK signaling with inhibitors caused commissural axon guidance defects, whereas this process was unaffected in *JNK1/2* knock out mice (data not shown). Although to definitively make this claim requires an analysis of the triple *JNK1/2/3* knock out mice it is clear that modification of PCP receptors by phosphorylation influence JNK signaling, and maintaining a spatio-temporal balance in JNK signaling appears to be necessary for commissural axon guidance.

4.5 Acknowledgements

CHAPTER 5: CONCLUSIONS, MODELS AND FUTURE DIRECTIONS

A mounting body of evidence supports a conserved function for Wnt-family proteins in vertebrate and invertebrate axon guidance (Zou, 2004). We studied Wnt-directed navigation of spinal commissural neurons and asked how this extracellular signal is propagated within the growth cone to initiate turning, and ultimately help establish proper somatosensory function. Our results indicate a novel and essential role for the planar cell polarity (PCP) pathway, which controls tissue polarity along the plane of epithelia and directed movement of cells during convergent extension, in anterior-posterior guidance of spinal cord commissural axons. Chapters 2 and 3 presented evidence that the core components of PCP signaling are present in commissural axons in a spatio-temporal pattern that is consistent with anterior turning of the growth cone, and that the two central PCP components (Vangl2 and Celsr3) are required for A-P guidance *in vivo*. Moreover, we directly show that Wnt proteins promote the growth of commissural axons through a mechanism involving PCP components at the growth cone tip.

In chapter 3 we used dissociated commissural neuron cultures to show that Vangl2 and Fzd3 act synergistically to promote Wnt-mediated growth of axons (Figure 5.1C). We later demonstrate in chapter 4 that Vangl2 and Dvl1 have opposing functions in regulating the phosphorylation state of Fzd3 and the PCP signaling molecule c-Jun. In *Drosophila* wing epithelial cells Dvl is normally

found distally while Vangl2 is found proximally (Simons and Mlodzik, 2008), but the precise nature of their interaction remains unclear. Our data reveal that these proteins have opposing roles in Fzd3 phosphorylation and PCP signaling, as measured by JNK activation. This information will help to provide new insights regarding the general mechanism of PCP signaling in different morphogenic process and species.

Our study introduces a novel inhibitory feedback loop that regulates PCP signaling and axon growth, and is mediated by Dvl. First, we show that Fzd3 can recruit Dvl1 to the plasma membrane of commissural axon growth cones, and that overexpressing Dvl1 can promote commissural axon outgrowth independent of Fzd3, suggesting that Dvl1 is downstream of Fzd3 in this functional pathway (Figure 5.1B and D).
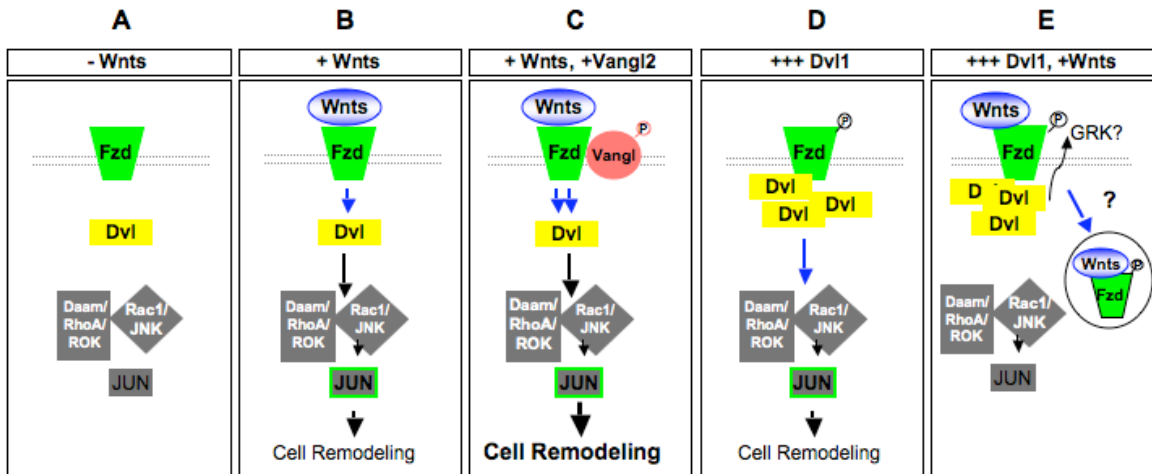
Figure 5.1 Schematic of conditions and effect on PCP signaling pathway
(A) In the absence of Wnts there is no effect on cell remodeling as measured by axonal growth (B) However in the presence of Wnts and PCP membraneous components we observed increased commissural axon growth. (C) In the presence of Wnts and both Fzd3 and Vangl2, we observed a synergistic increase of axon growth. (D) Dvl1 over-expression in the absence of Wnts activated PCP signaling and axon outgrowth. (E) In the presence of both Wnts and excess Dvl, Fzd-PCP signaling is inactivated, we propose through internalization of Fzd complex.

We found through the use of biotinylation that Dvl1 is required for the cell surface presentation of Fzd3. Remarkably, Dvl1 initially promotes the movement of Fzd3 to the membrane but then down-regulates Fzd3 surface levels following Wnt activation (Figure 5.1E), a function that requires the PCP domain (DEP domain of Dvl). We report in chapter 4, also for the first time, that Vangl2 can antagonize the effect of Dvl on Fzd3 and, as a consequence, may prolong the Wnt response and prevent feedback inhibition of PCP signaling by Dvl. In the *loop-tail* mouse, this function of Vangl2 is impaired, resulting in early inactivation of PCP signaling and randomization of commissural axon after midline crossing (Figure 5.2).
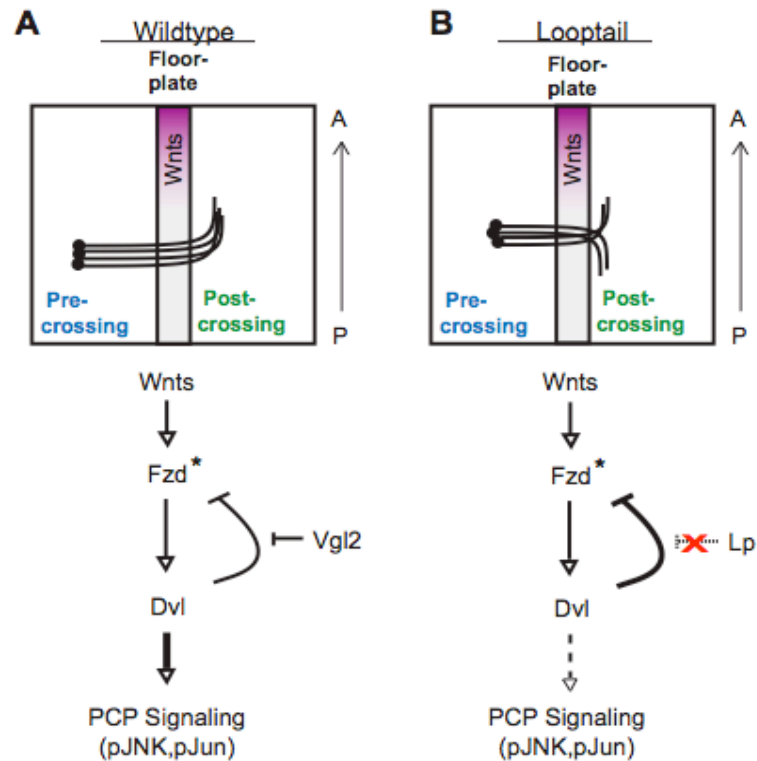
Figure 5.2 Wnt-PCP signaling in growth cone guidance
(A) Wildtype commissural axons up-regulate PCP components after midline crossing and activate PCP signaling in a Wnt dependent manner. Vangl2 assists in prolonging PCP signaling by antagonizing the Dvl1-dependent inactivation of phosphorylated Fzd3 at the plasma membrane. (B) In the *loop-tail* mouse Vangl2 protein is mutated such that the resulting Lp protein is unable to inhibit Dv1. Therefore, in the presence of Wnts, Dvl inactivates PCP signaling and axons lose their ability to grow in a directional manner, toward the Wnt gradient.

This Vangl2-dependent increase of PCP signaling may be the mechanism by which Vangl2 and Fzd3 increase Wnt5a-mediated axon attraction.

Our proposed model, in which Vangl2 and Dvl1 antagonize each other to regulate Fzd3 function, will rely on evidence to support that Fzd3 phosphorylation may lead to inactivation of PCP signaling. Indeed, preliminary evidence has

shown that *Xenopus* Fzd3 can be phosphorylated on Serine 576 (Yanfeng et al., 2006). Phosphorylation of Fzd3 was not required for its activity measured when by neural crest induction, but instead appeared to reduce signaling, since the unphosphorylatable form of Fzd3 leads to more neural crest induction. Our model proposes the involvement of a kinase in the phosphorylation of Fzd3. Indeed, mammalian G-protein couple receptors (GPCR) are phosphorylated by GPCR-associated protein kinases (GRKs), which are involved in signal attenuation, internalization or turn over of receptor or new signaling events (Pitcher et al., 1998).

We have shown that in the presence of Vangl2, Fzd3 at the cell membrane remains unphosphorylated (chapter 4). To determine how unphosphorylated Fzd3 affects PCP signaling we can analyze the level of phospho-Jun in the presence of Vangl2, as an indicator of PCP activity, using the transfection and treatment conditions described in Figure 4.7. We can predict elevated PCP signaling (shown as an increase phospho-Jun) because the presence of Vangl2 should prevent the phosphorylation of Fzd3 and thereby prevent Wnt-dependent inactivation of PCP signaling. Furthermore, because Lp protein is unable to promote Fzd3 dephosphorylation, applying the same experimental conditions with Lp instead of Vangl2 should not produce a decrease in PCP signaling.

A more direct readout would be to first identify and mutate the phosphorylation site on Fzd3, and then characterize the mutant in PCP signaling. There are 41 putative serine and threonine phosphorylation sites on the c-

terminus of the vertebrate Fzd3 protein (Yanfeng et al., 2006). To accurately determine the exact phosphorylation site observed on our western blots the Fzd3 phosphorylated band can be excised from the nitrocellulose membrane and analyzed by mass spectrophotometry. This is a common method that has been used successfully to identify other phosphorylation sites, including those present on GPCRs (Wu et al., 2003; Wu and Yates, 2003; Wu et al., 2008). Once identified, site-directed mutagenesis could be employed to mutate the modification site to an alanine residue.

While Fzd3 phospho-defective mutant could directly analyze the effect on PCP signaling and axon outgrowth there are notable caveats to this experiment. For example, alternative phospho-modification sites have been observed in the *Xenopus* Fzd3 protein after one site is mutated (Yanfeng et al., 2006). Therefore, (to obtain a Fzd3-phospho-defective product) multiple residues in the Fzd3 may have to be identified and mutated. If made, we can test its effect on Wnt5a-dependent neurite outgrowth with the prediction that prolonging PCP signaling should promote commissural axon length.

Another critical experiment for defining the potential importance of phospho-modification of PCP receptors involves validating this phenomenon *in vivo*, as we have only definitively observed Fzd3 and Vangl2 phosphorylation *in vitro*. To do so we can obtain spinal cell lysates from E11.5 mouse embryos and probe for endogenous proteins with Fzd3 and Vangl2 antibodies. Preliminary studies to validate Fzd3 and Vangl2 antibodies in wildtype and knockout lysates showed the appearance of a potentially slower migrating phospho-band.

Because we do not yet have phospho specific antibodies, we could validate that these are actual phospho modifications rather than ubiquitination, glycosylation or some other moiety that causes band shifts on a western blot, by treating the spinal lysates with a protein phosphatase to see if the removal of phosphates will abolish the putative phospho bands.

Frizzled receptors have been shown to internalize via an interaction between Dvl, β-arrestin2 and the clathrin adaptor AP-2 during PCP signaling (Chen et al., 2003; Yu et al., 2007). Fzd3 phosphorylation may regulate its endocytosis, and an asymmetric Wnt signaling event across a growth cone could conceivably be amplified by Frizzled3 endocytosis. In addition, other signaling components in the PCP complex, such as Prickle, are direct targets of ubiquitin-mediated degradation, which may either be or facilitate the downstream effectors of asymmetric Frizzled3 function (Narimatsu et al., 2009). Nevertheless, a primary feature of this models that we have yet to establish is whether phosphorylation of Fzd3 is required for its Wnt mediated endocytosis or if internalization of Fzd3 from the membrane could be the mechanism through which we observe a Dvl-dependent shutdown of PCP signaling.

To address these questions, we first need to establish that phosphorylated Fzd3 is removed from the plasma membrane in a Wnt dependent manner (Figure 5.1E). This could be accomplished by can cotransfecting Fzd3 and Dvl1 into HEK cells to obtain only phosphorylated from of Fzd3 at the plasma membrane. We can then apply Wnt5a for several time points from 15min to 1 hour, and

complete a membrane-IP to determine if membrane bound Fzd3 is decreased. We can further observe this by immunofluorescence, although the membrane IP and detection with western blotting is a more sensitive method. Next, to confirm that it is only phospho Fzd3 that is internalized in a Wnt dependent manner, we can repeat this experiment with Fzd3 transfection alone. While preliminary data suggests that only phospho Fzd3 is internalized in a Wnt5a dependent manner (data not shown), this experiment must be replicated and quantified to be certain. In addition, to establish that internalization results in loss of PCP signaling, we repeat these experimental conditions to test phospho-Jun levels.

β-arrestins have already be shown to bind preferentially to phosphorylated GPCRs and help to mediate their removal from the plasma membrane. For example, the phosphorylation of Fzd-like receptor smoothened has been shown to be required for its β-arrestin2-mediated internalization (Chen et al., 2004; Wilbanks et al., 2004), and phosphorylation of Fzd3 may similarly be required for its β-arrestin and AP2 mediated endocytosis.

The work in this thesis has provided new mechanistic insights relevant to both axon guidance and growth cone biology, as well as the role of the PCP signaling pathway in neuronal development and somatosensory circuit formation. We have discovered a novel feedback loop in PCP signaling by which growth cones may convert an extracellular Wnt gradient in the spinal cord into an intracellular signaling gradient using the PCP components Dvl and Vangl2, and

phospho modification of PCP receptors. In addition to transducing the signal generated by Wnt-Fzd binding, Dvl participates in a feedback loop in a temporal and/or concentration-dependent manner, which can be opposed by Vangl2 at the cell membrane.

To fully appreciate how interactions between PCP components may regulate commissural axon guidance decisions requires further investigation, as specific features of this novel pathway are still unknown. However, our results suggest two different ways in which Dvl and Vangl2 may interact to initiate turning of commissural axons anteriorly once they've crossed the midline. First, Dvl may asymmetrically down-regulate the PCP signaling strength on the side of growth cone that binds more Wnt proteins (nearest the Wnt source), while Vangl2 may act generally to ensure that PCP signaling is not completely shut down. Alternatively, Dvl could serve to inhibit PCP signaling (time/concentration-dependent) while asymmetric activation and localization of Vangl2 in the growth cone tip signal a critical node for establishing polarization, and initiates turning via downstream events such as RhoA and phospho-JNK activation (known effectors of structural/cytoskeletal elements). It is therefore critical to determine if asymmetric activation of Vangl2 can be observed, and if so, how it is regulated.

In addition to the scenarios described above, it is also possible that Wnt receptors other than Fzd, or alternative pathways that are activated by Wnt-Fzd signaling, may be responsible for regulating PCP activity. Finally, direct activity of Fzd itself (by asymmetric localization) has not been ruled out. At present, determining precisely how PCP activity introduces asymmetric signaling across

growth cones, and participates in turning events at the growth cone tip, awaits progress in both the delineation of additional Wnt/PCP signal transduction pathways, and advances in imaging techniques to visualize the localization and dynamic activity of PCP components within the growth cone.

APPENDIX A: MEMBRANE DYNAMICS IN AXON GUIDANCE

It is known that commissural neurons of the somatosensory system provide an excellent model system for studying the molecular mechanisms underlying axon guidance because they make a series of known pathfinding decisions. As described in Chapter 1 these neurons reside in the deep dorsal horn of the spinal cord, but project their axons first towards the ventral midline, then across to the contralateral side of the spinal cord, and finally anteriorly toward the brain. Interestingly, previous studies have demonstrated preferential addition of membrane to the tips of growth cones during axon growth (Bray, 1970; Pfenninger and Johnson, 1983). However, it is unknown whether the membrane of the growth cone contributes to the response of the commissural axon during turning and subsequent axon extension.

Although there are many studies focused on the intracellular signaling mechanisms that cause axon growth, attraction and repulsion, no studies have been dedicated to studying the response of the commissural membrane during these processes. Nevertheless, much is known about membrane fusion events during synaptic transmission and synaptogenesis, and we can borrow both tools and knowledge from these fields in order to study commissural membrane behavior. We can also use the SNARE (soluble N-ethylmaleimide-sensitive

factor attachment protein receptors) model of membrane fusion to study membranous vesicle delivery in commissural axon turning.

We have begun to examine the role of such membrane dynamics in commissural axon guidance by characterizing the movement of vesicles both in the presence and absence of attractive cues. Previous studies in our lab have demonstrated that Wnt proteins serve as anterior-posterior guidance cues in the spinal cord, attracting commissural axons anteriorly toward the Wnt protein gradient. Further, we have shown in Appendix B that membraneous vesicles VAMP2 and VAMP7 colocalize with the Wnt receptor Fzd3. However, it is unknown how the membrane of the commissural growth cone responds to Wnts, and whether this is a cause or is a consequence of anterior turning.

Synaptobrevn/VAMP2 and VAMP7/TI-VAMP (tetanus neurotoxin insensitive VAMP) are presynaptic proteins that can be used as markers of membranous vesicles (Bark and Wilson, 1994; Martinez-Arca et al., 2000a). VAMP2 is a four transmembrane vesicle protein used to faithfully label presynaptic terminals (Gandhi and Stevens, 2003; Matteoli et al., 2004; Schweizer and Ryan, 2006). Synaptobrevin/VAMP2 is also a vesicular SNARE that interacts with membrane-localized target SNAREs such as SNAP25 and Syntaxin1. VAMP2 containing vesicles are targeted to the plasma membrane for neurotransmitter secretion (Gerst, 1999). VAMP2 knockout studies show a 10 fold loss in spontaneous membrane fusion events in hippocampal neurons; however, these results also show that this v-SNARE is not absolutely required for synaptic fusion, possibly because of redundancy by other VAMPS (Schoch et al.,

2001).   VAMP2 was also shown not to be required for neurite outgrowth. Treatments with tetanus neurotoxin or botulinum toxin B inhibit VAMP2 and neurotransmitter release, but do not effect neurite outgrowth (Osen-Sand et al., 1996).   However, unlike VAMP2, VAMP7 is a tetanus neurotoxin-insensitive VAMP (TI-VAMP) that is involved in neurite outgrowth in hippocampal and PC12 cells (Coco et al., 1999; Martinez-Arca et al., 2000b). VAMP7 has an additional N-terminal region of 120 amino acids, which is analogous to the extensions found on syntaxins, the membrane-localized t-SNAREs (Fernandez et al., 1998). VAMP7's unique properties, especially its role implicated in neuritogenesis, make it a promising marker to study the dynamics of the commissural membrane.

These VAMP proteins have been characterized during synaptogensis or in post-natal neurons. To determine if they are present earlier in development, more specifically during commissural axon anterior turning, rat E13, we immunostained dissociated rat commissural neurons for endogenous VAMP2 and VAMP7 (Figure A1).
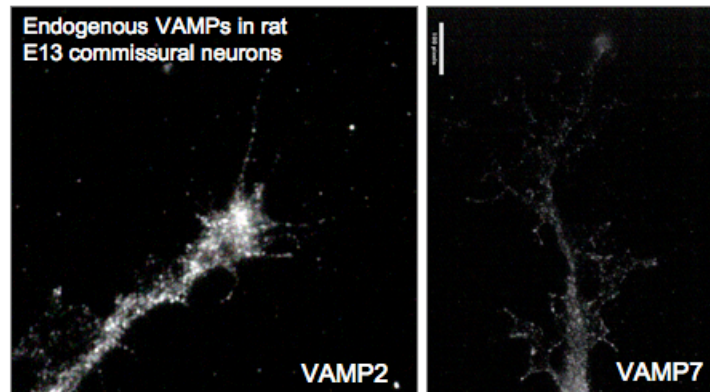
Figure A1 Endogenous VAMP2 and VAMP7
The growth cones of commissural axon express VAMP2 and VAMP7 in their classic punctate and vesicular pattern. White bar represents 5um

To determine if there is a correlation between membrane localization and axon turning, these candidate markers of membranous vesicles were imaged in commissural axons.   The fluorescent fusion proteins, VAMP2-EGFP and VAMP7-mCherry was made and tracked in dissociated commissural neuron using time-lapse microscopy. From our initial observations, VAMP2 and VAMP7 appear to have distinct localization patterns within the growth cone. VAMP7 vesicles appear to preferentially move in a out of a single filopodium, while VAMP2 vesicles appear to distributed ubiquitously (Figure A2).
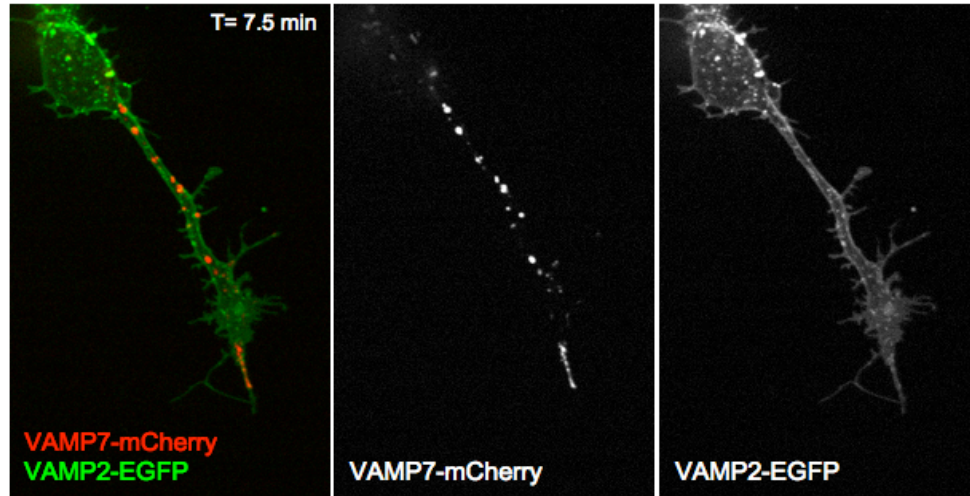
Figure A2 VAMP7 and VAMP2 fusion proteins in commissural neurites
After 24 hrs commissural axons are just extending out their neuritic process.
VAMP7-mCherry vesicles appear to localize to a specific stable filopodium during
this process. VAMP2-EGFP appears to move ubiquitously throughout the cell.

VAMP7 and VAMP2 could have different roles in specifying membrane
addition. For example VAMP7 may specify the direction of growth or turning by
moving in and peripheral domain of growth cone, while VAMP2 is responsible for
bulk membrane movement across the central domain of the growth cone.
Nevertheless, when we imaged the above neurons for 30 minutes we observed a
slow but distinct expansion in the membrane around the single filopodium (Figure
A3).
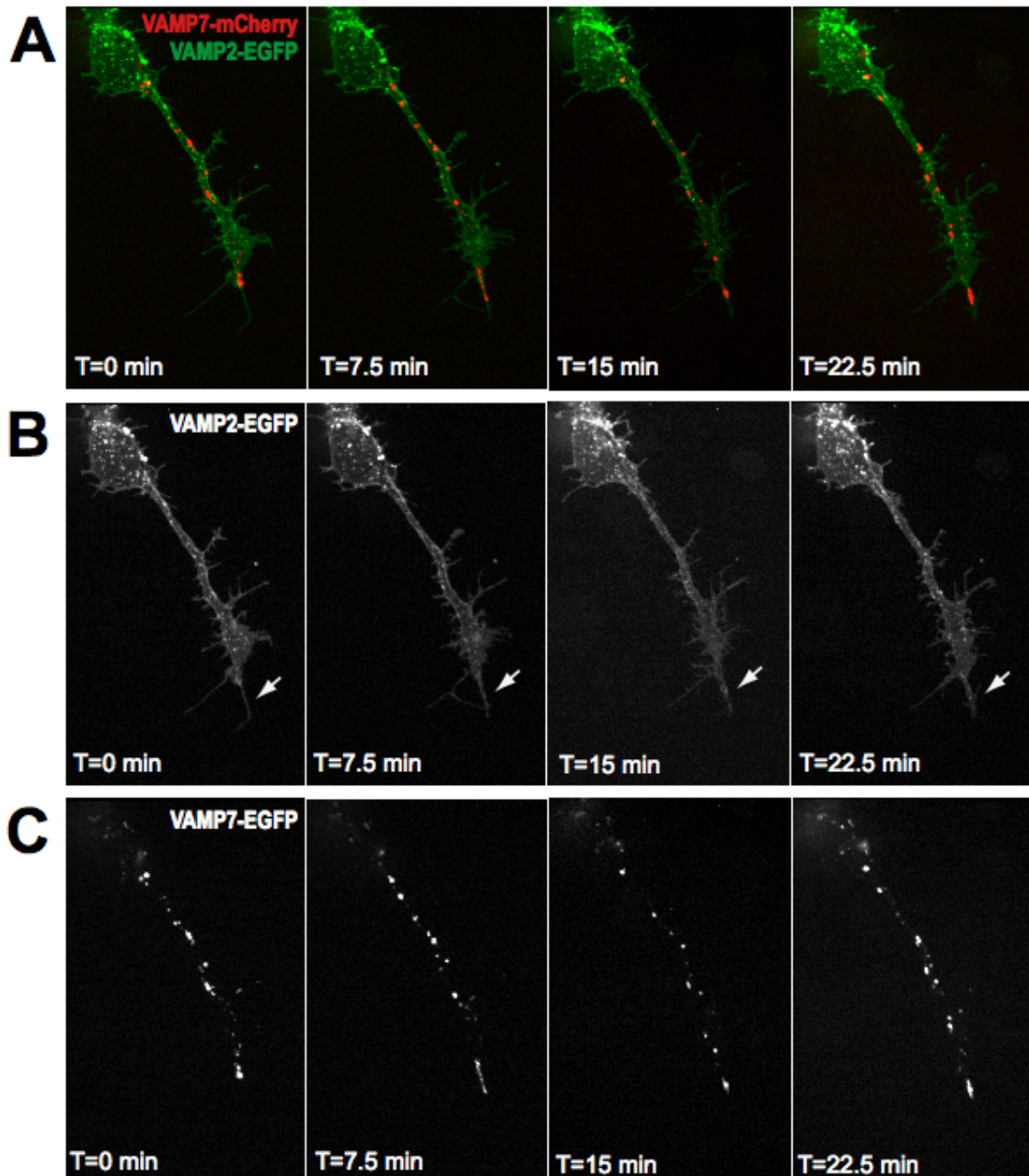
Figure A3 Time-lapse image sequence of commissural axon expressing VAMP7-mCherry and VAMP2-EGFP

Images were collected every 15 seconds for 30 minutes. (A) Depicts 4 frames from the time-lapse image sequence of this commissural neurite expressing both fusion proteins (B) VAMP2-EGFP distribution outlines the neuron as well as the filopodium that appears to have membrane added to it in the 30 minute time period. (White arrow denotes the growing filopodium) (C) VAMP7-mCherry distribution appears to be more linear toward the expanding filopodium. This filopodium appears also to be stable during 30 minutes of imaging.

It is know that F-actin filaments dominate the filopodial structures in the peripheral domain of the growth cone, whereas microtubules consisting of alpha/beta tubulin dimers are present in the growth cone's central domain, and enriched in the axon shaft (Dent and Gertler, 2003; Gordon-Weeks, 2004). Moreover, asymmetric actin delivery, and synthesis has been implicated in orchestrating the turning response of the growth cone (Leung et al., 2006; Yao et al., 2006). Therefore, VAMP7 movement in and out of single filopodium in the peripheral domain of the growth cone (Figure A3) may be coupled with the already existing asymmetric actin.

However, drug treatments of neurons in culture have shown that microtubules are required for insertion of vesicles into the plasma membrane. After focal application of nocodazole, a drug that promotes microtubule disassembly, labeled somatic vesicles normally en route to the distal axon were no longer detected at the axon tip. Different drugs that effect microtubule stability, taxol and vinblastine, prevented insertion of new membrane into the distal axon, showing that the dynamic instability of microtubules was required (Zakharenko and Popov, 1998, 2000). By contrast, treatment with cytochalasin, a drug that inhibits actin polymerization, had no apparent effect on the delivery of vesicles to the growth cone, or their addition into the plasma membrane (Zakharenko and Popov, 1998, 2000). Nevertheless, it was shown that vesicles are localized to actin rich filopodial structures, and that the presence and movement of VAMP2 labeled vesicles in these actin-rich protrusions was shown to be dependent on

both actin and microtubule filaments (Sabo and McAllister, 2003). Thus, the importance of cytoskeletal networks for the movement of membrane has been established; however, precisely which cytoskeletal tracks these vesicles are tethered to, and how they are transported during growth cone turning has yet to be elucidated.

There is recent evidence to suggest that stable filopodia are necessary for neurite outgrowth. F-actin and microtubules found in filopodia are also fundamental for axon growth and guidance (Dent and Gertler, 2003). Furthermore, Ena/VASP proteins regulate actin by preventing actin filament capping and mice that lack these proteins lack major axon tracts and also have cortical neurons that are unable to form neurites in culture (Dent et al., 2007). The study of these Ena/VASP mutant mice revealed that the lack of neurites were due to the absence of stable filopodia. This study also showed that filopodia are necessary but are not sufficient to promote neuritogenesis, rather neurite formation also requires stable microtubule extension into the filopodium. Interestingly, our observation of VAMP7 vesicles into a single filopodia appears to follow these requirements for neuritogenesis. We know theses vesicles are trafficked on microtubules (Sabo & McAllister, 2003) and during our imaging session we observed the expansion of the filopodia into a larger neurite.

A stable filopodia also appears to be a requirement for VAMP7 delivery into the filopodium. We imaged a non-stable filopodia and noticed that once the VAMP7-mCherry vesicles exit the filopodium, the filopodium retracts. We also saw the vesicles redistribute within the growth cone followed by a shift in the

membrane, which argues that VAMP7 could control the direction of growth cone movement in axon outgrowth. (Figure A4)
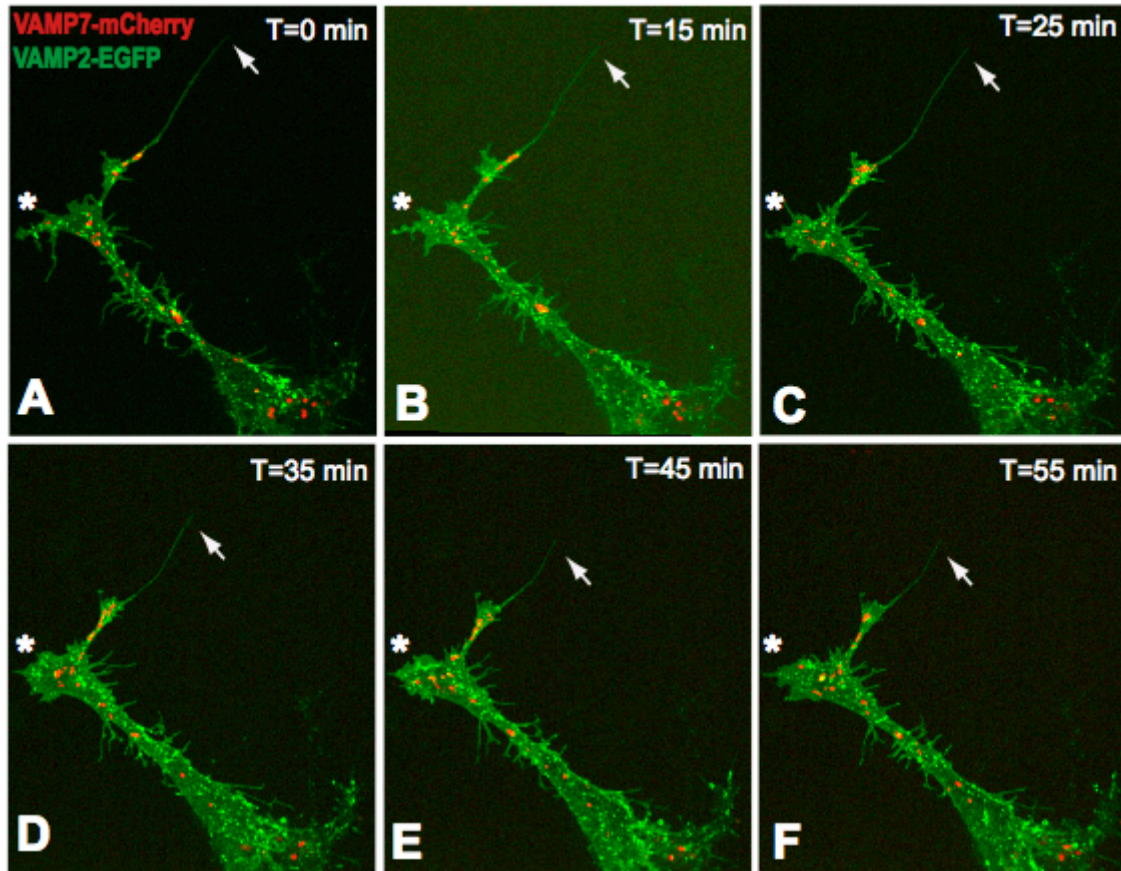
Figure A4 VAMP2-EGFP and VAMP7-mCherry in a non-stable filopodia
(A-B) VAMP7-mcherry vesicles are seen protruding into the filopodium, while VAMP2-EGFP vesicles show ubiquitous movement. White arrow denotes the filopodium (C) VAM7 vesicles are also seen exploring into the central domain of growth cone, more notably the areas marked by an asterisk. (D-F) VAMP7-mCherry continually moves away from the filopodium and we begin to filopodial retraction. We also see an expansion of membrane on the opposite site of the growth cone.

In addition to a filopodial shift, VAMP2-EGFP and VAMP7-mCherry appeared to shift the neuritic membrane to the other tip of the growth cone

marked by an asterisk in Figure A4.   This observation may be a hallmark of continued directional growth for we know that neurite outgrowth and expansion of the plasmalemma occurs by addition of membranes to the tips of the neurite (Bray, 1970; Craig et al., 1995; Dai and Sheetz, 1995).   This is also a mechanism that can be employed during axon turning because turning of a growth cone is a type of directional growth.   In addition, there is evidence for asymmetric membrane fusion to the axonal growth cone upon generation of asymmetric calcium signals (Tojima et al., 2007).   During axon turning, a similar asymmetry in the expansion of the membrane may occur when one side of the growth cone is presented with a guidance cue.   Furthermore, it is plausible that this lopsided membrane delivery, which also includes the movement of functional molecules such as channels and receptors, polarizes the axon to turn in the direction of the attractant.   Here we show for the first time that VAMP7 moves asymmetrically to a single filopodium.   Given that VAMP7 colocalizes with Fzd3 puncta, it may be plausible that VAMP7 vesicles may carry Fzd3 asymmetrically in the growth cone.   However more imaging experiments with Fzd3 fluorescent fusion proteins have to be completed to test this hypothesis.

From time-lapse imaging of VAMP2 and VAMP7 we can help to map the vesicular dynamics in the commissural neuron with respect to its filopodia, lamellipodia and axon shaft.   We know that the growth cone is made up of microtubule and actin networks (Kalil and Dent, 2005) and these cytoskeletal elements were shown to be required for membrane insertion and the movement of vesicles in the growth cone (Buck and Zheng, 2002; Sabo and McAllister,

2003; Zakharenko and Popov, 1998). Also, for future studies by observing the changes in the membrane localization upon stimulation with an attractive cue, we can determine if these vesicles respond in a directional manner. Studies in DRG neurons have shown asymmetric localization of FM dye loaded vesicles when labeled cells were stimulated with NGF on one side of the growth cone (Zakharenko and Popov, 1998, 2000) and vesicles in the commissural neurons could respond similarly when presented with the Wnt guidance cue.

In addition, preliminaries studies showed that commissural filopodial and lamellipodial movements can be visualized by confocal microscopy in the spinal open-book assay (data not shown). Therefore, the imaging studies in spinal open-book assay will help to elucidate the general growth cone behavior of these neurons as they traverse the spinal matrix. During synaptogenesis, dendritic filopodia search for potential targets and are stabilized upon contacting the proper cell adhesion molecules from presynaptic cells (Matteoli et al., 2004). Similarly, for anteriorly turning growth cones, the filopodia on the proximal side of the floor plate may be sampling for Wnt guidance cues, while the distal side of the growth cone may show very little filopodial protrusion. Filopodia in the spinal cord may have very specific patterns of behavior as the growth cone traverses the spinal cord; and their movement may also stem from preferential growth toward attractants.

Acknowledgements

APPENDIX B: FZD3 TRAFFICKING AND ARF6 GTPASE

Wnt proteins are known to serve as anterior-posterior guidance cues in the spinal cord, attracting commissural axons anteriorly toward the Wnt protein gradient. While the mechanism by which this gradient induces the growth cone to turn is unknown, it is tempting to speculate that establishing polarity involves redistribution of Fzd receptor to favor growth towards the Wnt gradient. To understand how commissural axons establish polarity and turn anteriorly in response to Wnt we have been examining the role of the Fzd-PCP pathway in commissural axon guidance and are currently determining how the PCP receptor, Fzd3, is delivered to the growth cone membrane.

Fzd-PCP pathway is a conserved mechanism that polarizes cells in a planar array. PCP molecules become asymmetrically localized along specific tissue axes to provide polarized signaling to an epithelium (Fanto and McNeill, 2004).   For example, in the drosophila wing, PCP core components are distributed asymmetrically along the proximal-distal axis; Fzd is localized distally while the tetra-spanning PCP receptor Vangl is found proximally.   This polarization leads to the growth of an actin rich pre-hair on the distal cell boundary, thereby leading to a global uniform array of fly wing hairs that point distally (Adler, 2002; Shulman et al., 1998; Strutt, 2002).   Similarly, PCP asymmetry has been found in the murine epithelia. Vestibular and auditory hair bundle organization, in particular, the orientation of the kinocilium and stereocilia

in the mouse inner ear are determined by asymmetric spatial distribution Fzd and Vangl (Montcouquiol et al., 2006b; Wang et al., 2006b). However, little is known about the spatial distribution of Fzd and Vangl in the growth cone of a neuron during turning.

The growth cone is a motile structure that senses and responds to the extracellular environment and this feature enables axons to grow to the correct intermediate targets during development, often over great distance. This is in part because the growth cone membrane contains many receptors that may interact with the extracellular matrix and detect small changes in the concentration of guidance cues. A fundamental question in axon guidance is whether or not asymmetric deposition of receptors at the growth cone tip in response to a guidance cue is a crucial intracellular event in turning. To this end, Fzd3 receptor movement has been visualized in the dissociated commissural neurons using time-lapse microscopy (Figure B1).
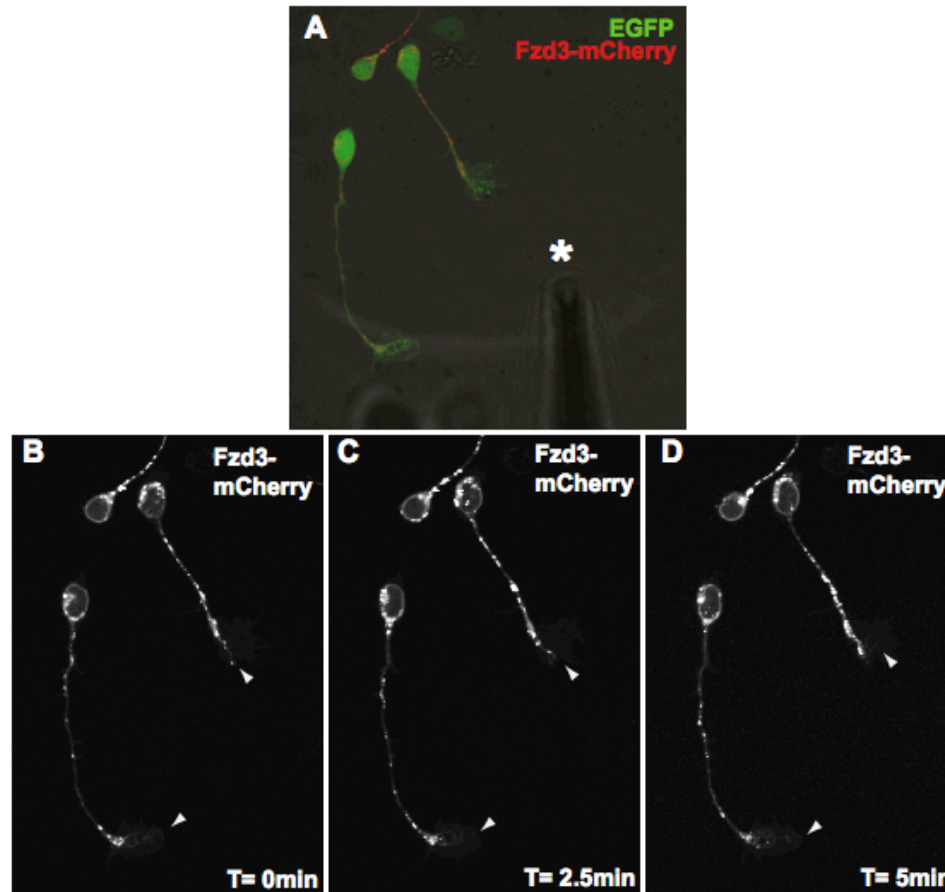
Figure B1   Time-lapse microscopy with commissural neurons expressing Fzd3-mcherry and EGFP
(A) This DIC-fluorescent image merge shows the location of the axons relative to the Wnt source indicated by the asterisk. The DIC image shows the location of the micropipet containing Wnt5a. (B-D) Images were collected every 15 seconds for 15 minutes, these images show the neurons at the indicated time points. Within the first 2.5 minutes, Fzd3-mCherry puncta can be seen directly moving toward the Wnt source. The puncta are indicated by white arrows.

The fluorescent fusion protein, Fzd3-mCherry was tracked in the presence of

Wnt guidance molecules to determine if the receptor is delivered asymmetrically

to the growth cone membrane. Preliminary data suggests that Fzd3 is trafficked

in the direction of the Wnt Ligand. In addition, when longer time-lapse movies

were taken of commissural neurons, we could visualize the growth cone turning

toward the source of the Wnt gradient (Figure B2).
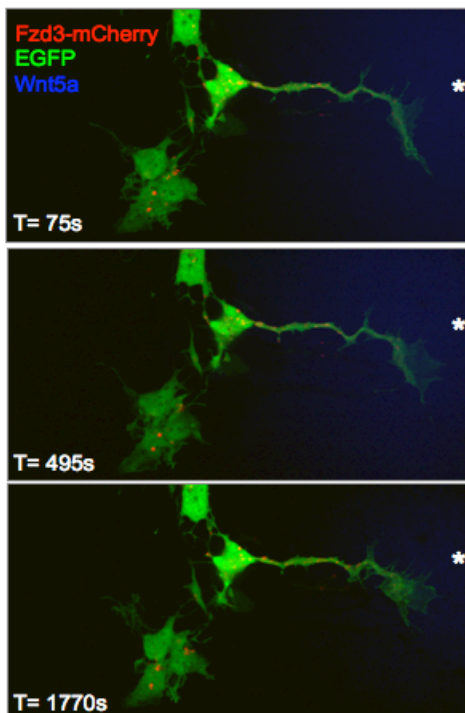
Figure B2 Response of dissociated commissural neurons exposed to Wnt5a gradient via picospritizing
Commissural neurons expressing Fzd3-mCherry and EGFP were subjected to a Wnt gradient and imaged by time-lapse microscopy for 30 minutes. The Wnt gradient is shown in blue, and 2 Hz of 5ug/mL Wnt5a was applied at 10psi for 25ms. Images were collected every 15 seconds.

After 8.25 minutes (495s) of exposure to the Wnt5a source we began to observe

an initial turning of the growth cone. After 29.5 minutes (1770s), the growth cone

had completely shifted toward the Wnt source. These initial experiments show

that Fzd3-mCherry moves in the growth cone toward the direction of ligand and

this appears sufficient to promote turning of the growth cone.

How is Fzd3 trafficked within the growth cone? To determine the mechanism of Fzd3 trafficking to the plasma membrane we chose to look at candidate trafficking proteins to determine if they colocalized with Fzd3 puncta. Small GTPase are molecules that help sort and traffic cargo to different compartments of the cell, among the best characterized are Rab and Arf GTPases. Rab4 and Rab5 are GTPases known to traffic proteins to early endosomes. Rab11 traffics proteins to late and recycling endosomes. Rab8 has been shown to promote cargo delivery to the plasma membrane. Where as Arf6 is a GTPase that has been shown to move cargo in several directions, including from recycling endosomes back to the plasma membrane (Schwartz et al., 2007; Somsel Rodman and Wandinger-Ness, 2000; Stenmark, 2009). We found that Fzd3-mCherry did not colocalize with Rab4-GFP, Rab8-GFP, or Rab11-GFP when cotransfected into HEK293T cells. However, Fzd3-Cherry did colocalize with Arf6-GFP and the SNARE proteins VAMP2 and VAMP7 (Figure B3). (The relationship of VAMP2 and VAMP7 is discussed in further detail in Appendix A)
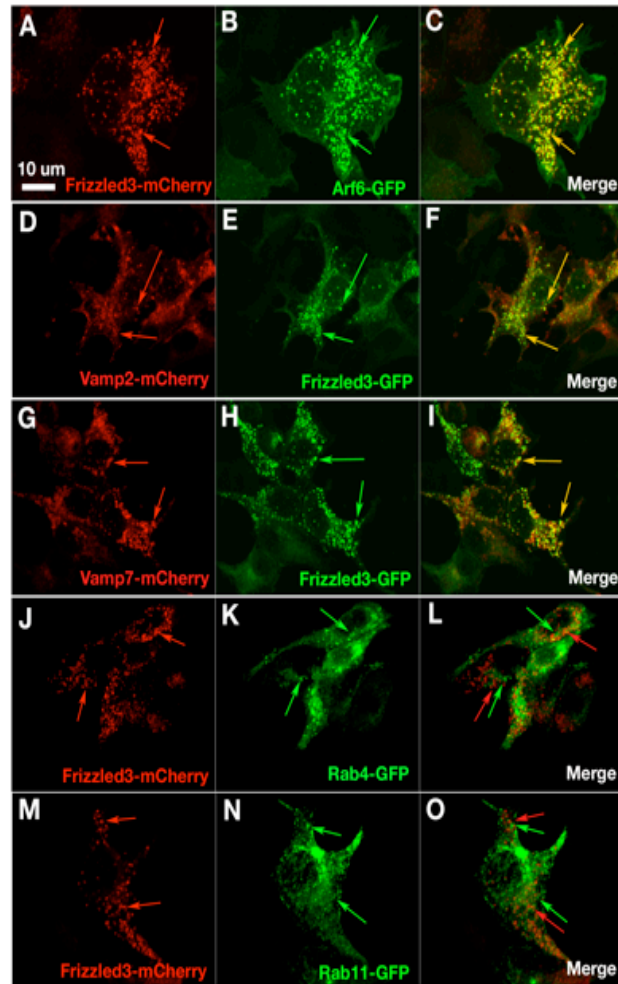
Figure B3 Candidate GTPase screen using co-transfection strategy in HEK cells
The indicated fusion constructs below were cotransfected into HEK293T cells to determine which molecules help traffic Fzd3. We found Fzd3 colocalizes with Arf6, VAMP2 and VAMP7. Red arrows indicate the location of mCherry fusion proteins. Green arrows indicate the location of the GFP fusion proteins. Yellow arrows indicated colocalized mCherry and GFP fusion proteins. (A-C) Fzd3-mCherry and Arf-GFP (D-F) VAMP2-mCherry and Fzd3-GFP (G-I) VAMP7-mCherry and Fzd3-GFP (J-L) Fzd3-mCherry and Rab4-GFP (M-N) Fzd3-mCherry and Rab11-GFP

The candidate screen in HEK293T cells via co-transfection of fusion constructs

indicated ARF6-GFP colocalizes Fzd3-mCherry puncta. Next we sought to

confirm this colocalization in commissural neurons by coelectroporation. They did indeed colocalize in commissural neurons and were both found at the plasma-membrane when over expressed (Figure B4).
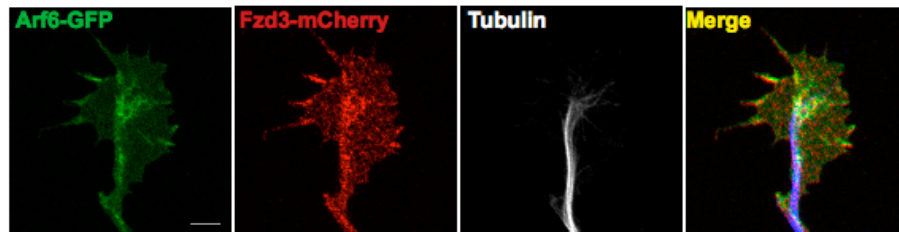
Figure B4 Arf6-GFP and Fzd3-mCherry colocalize in the growth cone
Arf6-GFP and Fzd3-mCherry puncta are found associated together in the central domain and filopodia of rat E13 commissural growth cone.

Arf6 is an ideal candidate for trafficking Fzd3 during the growth cone turning decision. Arf6 is known to be required when immense membrane addition is needed, such as during spermatocyte cytokinesis and during membrane re-spreading of mouse embryonic fibroblast (Balasubramanian et al., 2007; Dyer et al., 2007). In both cases, Arf6 helps recruit endosomal membrane stores in the time of drastic cell shape change. In a similar sense, upon encountering a Wnt guidance cue, Arf6 may help recruit Fzd3 and membrane stores to the growth cone tip to facilitate axon growth and membrane addition.

To test the affect of activating Arf6 in commissural axon growth we used an available inhibitor of Arf6-GAP, QS-11, in our Fzd3 electroporated commissural culture. Arf6-GAP promotes Arf6-GTP hydrolysis to the inactive Arf6–GDP bound form (Donaldson and Honda, 2005). The compound QS-11

has been shown to inhibit Arf6-GAP and increase levels of activated Arf6-GTP

(Zhang et al., 2007a). We electroporated commissural neurons with Fzd3-EGFP

and grew them in the presence of QS-11 and found that the inhibitor markedly

enhance axon elongation of Fzd3 expressing neurites (Figure B5)
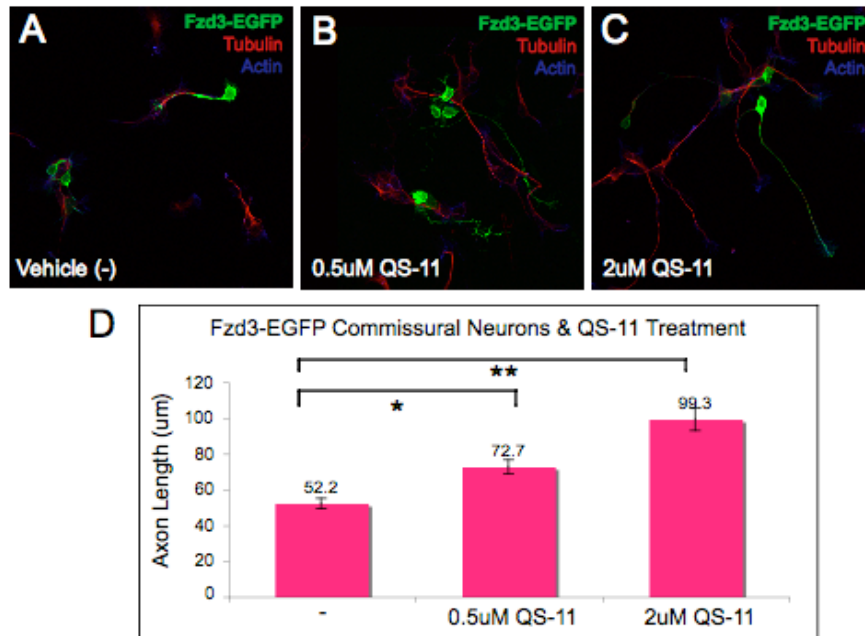
Figure B5 Treatment with QS-11 promotes commissural axon growth
(A-C) Commissural neurons expressing Fzd3-EGFP were incubated with the
following concentration of the Arf6-GAP inhibitor QS-11, 0uM (A), 0.5uM (B) and
2um (C) for 24 hours. They were then fixed and immunostained for EGFP,
tubulin and actin. (D) The axons incubated with QS-11 showed an enhanced
growth in axon length.

In the presence of QS-11 there is a dose-dependent increase in axon length of

Fzd3-EGFP expressing neurites, such that incubation with 2uMQS-11 for 24hrs

resulted in a 200% increase in commissural neurite length (Figure B5D).

Nevertheless, we need to confirm that the presence of QS-11 indeed promoted

the activation of Arf6-GTP in our commissural culture by assaying for the increase levels of this activated form via western blot analysis.

To study if QS-11 affects commissural axons in a more *in vivo* context we cultured our open-book spinal cords in the presence of QS-11. Open-book incubation at lower concentrations of QS-11 (0.5uM, 1uM, 2uM or 10uM) showed no effect on the anterior turning of commissural axons. All DiI injection sites quantified revealed ~80% correct turning, which is equivalent to the DMSO control in rat E14 open-books. However, incubation with the high 50uM concentration of QS-11 revealed DiI injection sites that consistently showed an increase in accurate anterior turning (Figure B5). All of the 17 injection sites quantified turned correctly. In addition, the axons treated with 50uM QS-11 appeared more fasiculated and healthier than the DMSO controls (Figure B6).
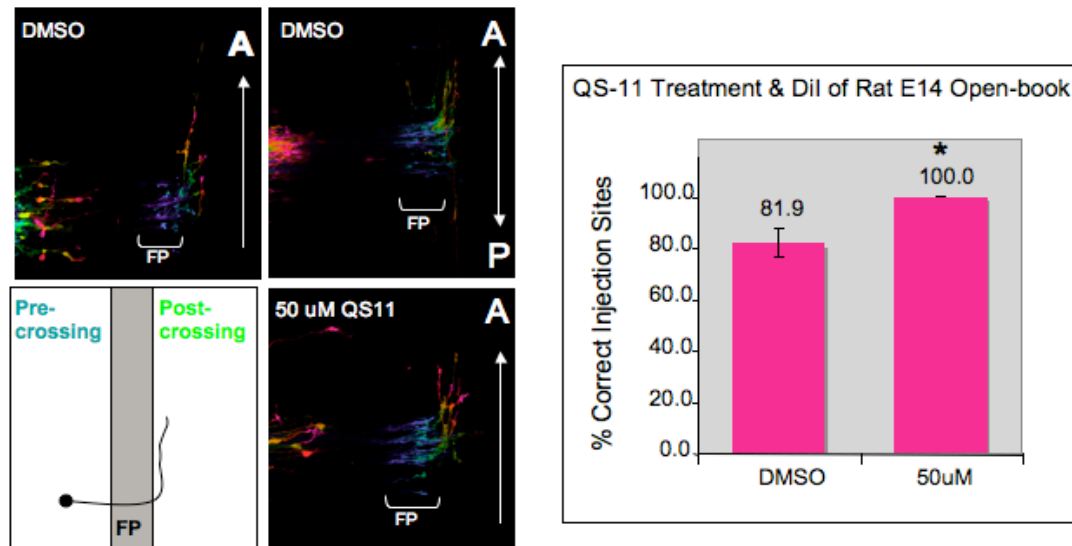
Figure B6 24 hour QS-11 treatment of E13 open-books
The left panel shows a depth coded view of the E14 rat DiI injection sites. The axons treated with 50uM QS-11 appear more thick and fasiculated. Further, the presence of QS-11 corrected the 20% error rate that occurs with the rate ex-vivo explant.

From the evidence on neurite outgrowth and in the open-book assay, QS-11 and by extension Arf6 GTPase, appears to enhance commissural axon outgrowth. Since Arf6 colocalizes with Fzd3 puncta and since an increase in Arf6 appears to enhance the anterior turning of commissural axons (a process that is known to be Wnt-Fzd dependent), we would like to explore the relationship of Fzd3 and Arf6 further in our model system of commissural axon guidance.

We know that GTPases confer directionality to membrane traffic; they act as molecular switches during the traffic events of budding, transport, tethering and fusion (Grosshans et al., 2006; Novick et al., 2006).   Preliminary work presented in this thesis shows that Fzd3 co-localized with Arf6 GTPase but not early or late endosomal GTPases. Arf6 is a small GTPase that regulates post-

endocytic recycling, exocytosis and cytoskeletal reorganization (D'Souza-Schorey and Chavrier, 2006; Prigent et al., 2003), and was shown to be critical in returning lipid rafts to the cell periphery during cell re-spreading after detachment (Balasubramanian et al., 2007). Therefore, it is possible that Arf6 acts as a molecular switch that delivers Fzd3 to the cell membrane during growth cone turning. To test this hypothesis, we need to further image and track the movement of Fzd3-mCherry and Arf6-GFP in commissural neurons during transport to the growth cone. Dominant negative Arf6, Arf6(T27N), can be used to further examine its role effecting shuttling Fzd3 to the plasma membrane. Arf6(T27N) has been shown to block cell spreading by effecting lipid raft traffic (Balasubramanian et al., 2007; Radhakrishna et al., 1999; Song et al., 1998), and it may in a similar manner block Fzd3 delivery to the cell surface. In parallel, it would be of interest to test the functional requirement for Arf6 is commissural axon guidance by down-regulating Arf6 via siRNA to see if this known down effects the Fzd dependent anterior turning decision *in vivo*.

Acknowledgements

APPENDIX C: MATERIALS AND METHODS

In situ hybridization

Mouse E11.5 embryos were fixed overnight at 4C in 4% DEPC treated PFA and i*n situ* hybridization and completed as previously described (Lyuksyutova et al., 2003), using digoxigenin-labeled riboprobes (Roche). All specific probes were obtained by RT-PCR from E11.5 mouse mRNA and subcloned into TOPO II vector (Invitrogen).

DiI axon labeling

To visualize anterior posterior projection of commissural axons DiI labeling was used in the spinal open book preparation. Mouse open-book assay and DiI injections were completed as previously described (Zou et al., 2000); (Lyuksyutova et al., 2003);(Wolf et al., 2008).

Immunohistochemistry

E11.5 mouse embryos of all wildtype, heterozygous, knock out and mutant embryos were fixed in 4% PFA and immunostaining of spinal cord sections were performed as described previously (Lyuksyutova et al., 2003). The following primary antibodies were used: α-TAG-1 (Developmental Hybridoma), α-L1 (Developmental Hybridoma), α-Frizzled3 (Wang et al, J. Neurosci, 2006), α-phospho-JNK (Cell Signaling), α-Vangl2 (Santa Cruz), Dvl2 (Santa Cruz), Pax7

(Developmental Hybridoma), Lhx1/5 (Developmental Hybridoma), α-tubulin (Sigma), DAPI (Sigma), Phalloidin-488 (Invitrogen), α-EGFP (Invitrogen). Confocal images were taken with Zeiss LSM510.

Electroporated commissural culture

Electroporations of rat E13 spinal cords were completed as previously described (Wolf et al., 2008). Neurons were dissociated from these spinal preps and grown as previously described (Augsburger et al., 1999). After 24 hours of growth they were fixed with 2% PFA at 37C for 15 min and immunostained as described (Wolf et al., 2008). The axons lengths were quantified with Zeiss LSM510 software and data were analyzed with an unpaired two-tailed t test for each electroporation condition.

Surface biotinylation and immunoprecipitation

48 hours after transfection with the indicated constructs into HEK293T cells (FuGene, Roche), followed by a bath application of Wnt5a (R&D Systems), surface proteins were subsequently labeled with biotin (Pierce). The cell lysates were collect over a period of 45 minutes on ice in the following lysis buffer: 20mM Tris pH7.6, 150mM NaCl, 1% Triton, 0.1%SDS, 2.5mM EDTA, 2.5mM EGTA, protease Inhibitors (Roche). For the membrane immunoprecipitation, 600ug of protein extracts were incubated and retrieved with strepavidin-coated sepharose beads (Pierce). The following primary antibodies were used for the immunoblot: α-Frizzled3 (Wang et al, J. Neurosci, 2006), α-Vangl2 (Santa Cruz),

α-mCherry (Clonetech), α-JNK (Cell Signaling), α-phospho-JNK (Cell Signaling), α-Flag (Sigma), α-GAPDH (Chemicon)

Animals, mouse lines and breeding

Embryos from E13 stage Sprague Dawley pregnant rats (Charles River) were collected. CD-1 mice (Jackson Laboratories) were staged and collected at mouse E11.5 and E14.5. *Loop-tail* mutant mice (LPT/Le stock, Jackson Laboratories) were provided by A.Wynshaw-Boris (UCSF, San Francisco, Maryland). Celsr3 mutant mice were described previously (Tissir et al., 2005). Fzd3 mutant mice generated by J. Nathans (J.H.U. School of Medicine, Baltimore, Maryland; (Wang et al., 2002); (Lyuksyutova et al., 2003).

REFERENCES

Adler, P.N. (2002). Planar signaling and morphogenesis in Drosophila. Dev Cell 2, 525-535.

Augsburger, A., Schuchardt, A., Hoskins, S., Dodd, J., and Butler, S. (1999). BMPs as mediators of roof plate repulsion of commissural neurons. Neuron 24, 127-141.

Axelrod, J.D., Miller, J.R., Shulman, J.M., Moon, R.T., and Perrimon, N. (1998). Differential recruitment of Dishevelled provides signaling specificity in the planar cell polarity and Wingless signaling pathways. Genes Dev 12, 2610-2622.

Balasubramanian, N., Scott, D.W., Castle, J.D., Casanova, J.E., and Schwartz, M.A. (2007). Arf6 and microtubules in adhesion-dependent trafficking of lipid rafts. Nature cell biology 9, 1381-1391.

Bark, I.C., and Wilson, M.C. (1994). Regulated vesicular fusion in neurons: snapping together the details. Proc Natl Acad Sci U S A 91, 4621-4624.

Ben-Arie, N., McCall, A.E., Berkman, S., Eichele, G., Bellen, H.J., and Zoghbi, H.Y. (1996). Evolutionary conservation of sequence and expression of the bHLH protein Atonal suggests a conserved role in neurogenesis. Hum Mol Genet 5, 1207-1216.

Boutros, M., Paricio, N., Strutt, D.I., and Mlodzik, M. (1998). Dishevelled activates JNK and discriminates between JNK pathways in planar polarity and wingless signaling. Cell 94, 109-118.

Bray, D. (1970). Surface movements during the growth of single explanted neurons. Proc Natl Acad Sci U S A 65, 905-910.

Buck, K.B., and Zheng, J.Q. (2002). Growth cone turning induced by direct local modification of microtubule dynamics. J Neurosci 22, 9358-9367.

Butler, S.J., and Dodd, J. (2003). A role for BMP heterodimers in roof plate-mediated repulsion of commissural axons. Neuron 38, 389-401.

Charron, F., Stein, E., Jeong, J., McMahon, A.P., and Tessier-Lavigne, M. (2003). The morphogen sonic hedgehog is an axonal chemoattractant that collaborates with netrin-1 in midline axon guidance. Cell 113, 11-23.

Chen, W., Ren, X.R., Nelson, C.D., Barak, L.S., Chen, J.K., Beachy, P.A., de Sauvage, F., and Lefkowitz, R.J. (2004). Activity-dependent internalization of smoothened mediated by beta-arrestin 2 and GRK2. Science 306, 2257-2260.

Chen, W., ten Berge, D., Brown, J., Ahn, S., Hu, L.A., Miller, W.E., Caron, M.G., Barak, L.S., Nusse, R., and Lefkowitz, R.J. (2003). Dishevelled 2 recruits beta-arrestin 2 to mediate Wnt5A-stimulated endocytosis of Frizzled 4. Science 301, 1391-1394.

Coco, S., Raposo, G., Martinez, S., Fontaine, J.J., Takamori, S., Zahraoui, A., Jahn, R., Matteoli, M., Louvard, D., and Galli, T. (1999). Subcellular localization of tetanus neurotoxin-insensitive vesicle-associated membrane protein (VAMP)/VAMP7 in neuronal cells: evidence for a novel membrane compartment. J Neurosci 19, 9803-9812.

Craig, A.M., Wyborski, R.J., and Banker, G. (1995). Preferential addition of newly synthesized membrane protein at axonal growth cones. Nature 375, 592-594.

D'Souza-Schorey, C., and Chavrier, P. (2006). ARF proteins: roles in membrane traffic and beyond. Nat Rev Mol Cell Biol 7, 347-358.

Dai, J., and Sheetz, M.P. (1995). Axon membrane flows from the growth cone to the cell body. Cell 83, 693-701.

Dent, E.W., and Gertler, F.B. (2003). Cytoskeletal dynamics and transport in growth cone motility and axon guidance. Neuron 40, 209-227.

Dent, E.W., Kwiatkowski, A.V., Mebane, L.M., Philippar, U., Barzik, M., Rubinson, D.A., Gupton, S., Van Veen, J.E., Furman, C., Zhang, J., et al. (2007). Filopodia are required for cortical neurite initiation. Nature cell biology 9, 1347-1359.

Djiane, A., Yogev, S., and Mlodzik, M. (2005). The apical determinants aPKC and dPatj regulate Frizzled-dependent planar cell polarity in the Drosophila eye. Cell 121, 621-631.

Dodd, J., and Jessell, T.M. (1988). Axon guidance and the patterning of neuronal projections in vertebrates. Science 242, 692-699.

Dodd, J., Morton, S.B., Karagogeos, D., Yamamoto, M., and Jessell, T.M. (1988). Spatial regulation of axonal glycoprotein expression on subsets of embryonic spinal neurons. Neuron 1, 105-116.

Donaldson, J.G., and Honda, A. (2005). Localization and function of Arf family GTPases. Biochem Soc Trans 33, 639-642.

Dyer, N., Rebollo, E., Dominguez, P., Elkhatib, N., Chavrier, P., Daviet, L., Gonzalez, C., and Gonzalez-Gaitan, M. (2007). Spermatocyte cytokinesis requires rapid membrane addition mediated by ARF6 on central spindle recycling endosomes. Development 134, 4437-4447.

Fanto, M., and McNeill, H. (2004). Planar polarity from flies to vertebrates. J Cell Sci 117, 527-533.

Fanto, M., Weber, U., Strutt, D.I., and Mlodzik, M. (2000). Nuclear signaling by Rac and Rho GTPases is required in the establishment of epithelial planar polarity in the Drosophila eye. Curr Biol 10, 979-988.

Fernandez, I., Ubach, J., Dulubova, I., Zhang, X., Sudhof, T.C., and Rizo, J. (1998). Three-dimensional structure of an evolutionarily conserved N-terminal domain of syntaxin 1A. Cell 94, 841-849.

Gandhi, S.P., and Stevens, C.F. (2003). Three modes of synaptic vesicular recycling revealed by single-vesicle imaging. Nature 423, 607-613.

Gerst, J.E. (1999). SNAREs and SNARE regulators in membrane fusion and exocytosis. Cell Mol Life Sci 55, 707-734.

Gordon-Weeks, P.R. (2004). Microtubules and growth cone function. J Neurobiol 58, 70-83.

Gowan, K., Helms, A.W., Hunsaker, T.L., Collisson, T., Ebert, P.J., Odom, R., and Johnson, J.E. (2001). Crossinhibitory activities of Ngn1 and Math1 allow specification of distinct dorsal interneurons. Neuron 31, 219-232.

Grosshans, B.L., Ortiz, D., and Novick, P. (2006). Rabs and their effectors: achieving specificity in membrane traffic. Proc Natl Acad Sci U S A 103, 11821-11827.

Habas, R., Kato, Y., and He, X. (2001). Wnt/Frizzled activation of Rho regulates vertebrate gastrulation and requires a novel Formin homology protein Daam1. Cell 107, 843-854.

Hardin, J., and King, R.S. (2008). The long and the short of Wnt signaling in C. elegans. Curr Opin Genet Dev 18, 362-367.

Helms, A.W., and Johnson, J.E. (1998). Progenitors of dorsal commissural interneurons are defined by MATH1 expression. Development 125, 919-928.

Jaeschke, A., Karasarides, M., Ventura, J.J., Ehrhardt, A., Zhang, C., Flavell, R.A., Shokat, K.M., and Davis, R.J. (2006). JNK2 is a positive regulator of the cJun transcription factor. Molecular cell 23, 899-911.

Jenny, A., Darken, R.S., Wilson, P.A., and Mlodzik, M. (2003). Prickle and Strabismus form a functional complex to generate a correct axis during planar cell polarity signaling. EMBO J 22, 4409-4420.

Kalil, K., and Dent, E.W. (2005). Touch and go: guidance cues signal to the growth cone cytoskeleton. Curr Opin Neurobiol 15, 521-526.

Keino-Masu, K., Masu, M., Hinck, L., Leonardo, E.D., Chan, S.S., Culotti, J.G., and Tessier-Lavigne, M. (1996). Deleted in Colorectal Cancer (DCC) encodes a netrin receptor. Cell 87, 175-185.

Kennedy, T.E., Serafini, T., de la Torre, J.R., and Tessier-Lavigne, M. (1994). Netrins are diffusible chemotropic factors for commissural axons in the embryonic spinal cord. Cell 78, 425-435.

Kibar, Z., Underhill, D.A., Canonne-Hergaux, F., Gauthier, S., Justice, M.J., and Gros, P. (2001a). Identification of a new chemically induced allele (Lp(m1Jus)) at the loop-tail locus: morphology, histology, and genetic mapping. Genomics 72, 331-337.

Kibar, Z., Vogan, K.J., Groulx, N., Justice, M.J., Underhill, D.A., and Gros, P. (2001b). Ltap, a mammalian homolog of Drosophila Strabismus/Van Gogh, is altered in the mouse neural tube mutant Loop-tail. Nat Genet 28, 251-255.

Langenhan, T., Promel, S., Mestek, L., Esmaeili, B., Waller-Evans, H., Hennig, C., Kohara, Y., Avery, L., Vakonakis, I., Schnabel, R., et al. (2009).

Latrophilin signaling links anterior-posterior tissue polarity and oriented cell divisions in the C. elegans embryo. Dev Cell 17, 494-504.

Lee, H., and Adler, P.N. (2002). The function of the frizzled pathway in the Drosophila wing is dependent on inturned and fuzzy. Genetics 160, 1535-1547.

Lee, K.J., Mendelsohn, M., and Jessell, T.M. (1998). Neuronal patterning by BMPs: a requirement for GDF7 in the generation of a discrete class of commissural interneurons in the mouse spinal cord. Genes Dev 12, 3394-3407.

Leung, K.M., van Horck, F.P., Lin, A.C., Allison, R., Standart, N., and Holt, C.E. (2006). Asymmetrical beta-actin mRNA translation in growth cones mediates attractive turning to netrin-1. Nat Neurosci 9, 1247-1256.

Li, L., Yuan, H., Xie, W., Mao, J., Caruso, A.M., McMahon, A., Sussman, D.J., and Wu, D. (1999). Dishevelled proteins lead to two signaling pathways. Regulation of LEF-1 and c-Jun N-terminal kinase in mammalian cells. J Biol Chem 274, 129-134.

Liem, K.F., Jr., Tremml, G., and Jessell, T.M. (1997). A role for the roof plate and its resident TGFbeta-related proteins in neuronal patterning in the dorsal spinal cord. Cell 91, 127-138.

Liem, K.F., Jr., Tremml, G., Roelink, H., and Jessell, T.M. (1995). Dorsal differentiation of neural plate cells induced by BMP-mediated signals from epidermal ectoderm. Cell 82, 969-979.

Lyuksyutova, A.I., Lu, C.C., Milanesio, N., King, L.A., Guo, N., Wang, Y., Nathans, J., Tessier-Lavigne, M., and Zou, Y. (2003). Anterior-posterior guidance of commissural axons by Wnt-frizzled signaling. Science 302, 1984-1988.

Ma, Q., Fode, C., Guillemot, F., and Anderson, D.J. (1999). Neurogenin1 and neurogenin2 control two distinct waves of neurogenesis in developing dorsal root ganglia. Genes Dev 13, 1717-1728.

Martinez-Arca, S., Alberts, P., and Galli, T. (2000a). Clostridial neurotoxin-insensitive vesicular SNAREs in exocytosis and endocytosis. Biol Cell 92, 449-453.

Martinez-Arca, S., Alberts, P., Zahraoui, A., Louvard, D., and Galli, T. (2000b). Role of tetanus neurotoxin insensitive vesicle-associated membrane protein (TI-VAMP) in vesicular transport mediating neurite outgrowth. J Cell Biol 149, 889-900.

Matise, M.P., Lustig, M., Sakurai, T., Grumet, M., and Joyner, A.L. (1999). Ventral midline cells are required for the local control of commissural axon guidance in the mouse spinal cord. Development 126, 3649-3659.

Matteoli, M., Coco, S., Schenk, U., and Verderio, C. (2004). Vesicle turnover in developing neurons: how to build a presynaptic terminal. Trends Cell Biol 14, 133-140.

Montcouquiol, M., Crenshaw, E.B., 3rd, and Kelley, M.W. (2006a). Noncanonical Wnt signaling and neural polarity. Annu Rev Neurosci 29, 363-386.

Montcouquiol, M., Sans, N., Huss, D., Kach, J., Dickman, J.D., Forge, A., Rachel, R.A., Copeland, N.G., Jenkins, N.A., Bogani, D., et al. (2006b). Asymmetric localization of Vangl2 and Fz3 indicate novel mechanisms for planar cell polarity in mammals. J Neurosci 26, 5265-5275.

Moriguchi, T., Kawachi, K., Kamakura, S., Masuyama, N., Yamanaka, H., Matsumoto, K., Kikuchi, A., and Nishida, E. (1999). Distinct domains of mouse dishevelled are responsible for the c-Jun N-terminal kinase/stress-activated protein kinase activation and the axis formation in vertebrates. J Biol Chem 274, 30957-30962.

Narimatsu, M., Bose, R., Pye, M., Zhang, L., Miller, B., Ching, P., Sakuma, R., Luga, V., Roncari, L., Attisano, L., et al. (2009). Regulation of planar cell polarity by Smurf ubiquitin ligases. Cell 137, 295-307.

Novick, P., Medkova, M., Dong, G., Hutagalung, A., Reinisch, K., and Grosshans, B. (2006). Interactions between Rabs, tethers, SNAREs and their regulators in exocytosis. Biochem Soc Trans 34, 683-686.

Osen-Sand, A., Staple, J.K., Naldi, E., Schiavo, G., Rossetto, O., Petitpierre, S., Malgaroli, A., Montecucco, C., and Catsicas, S. (1996). Common and distinct fusion proteins in axonal growth and transmitter release. J Comp Neurol 367, 222-234.

Park, T.J., Gray, R.S., Sato, A., Habas, R., and Wallingford, J.B. (2005). Subcellular localization and signaling properties of dishevelled in developing vertebrate embryos. Curr Biol 15, 1039-1044.

Pfenninger, K.H., and Johnson, M.P. (1983). Membrane biogenesis in the sprouting neuron. I. Selective transfer of newly synthesized phospholipid into the growing neurite. J Cell Biol 97, 1038-1042.

Pitcher, J.A., Freedman, N.J., and Lefkowitz, R.J. (1998). G protein-coupled receptor kinases. Annu Rev Biochem 67, 653-692.

Prigent, M., Dubois, T., Raposo, G., Derrien, V., Tenza, D., Rosse, C., Camonis, J., and Chavrier, P. (2003). ARF6 controls post-endocytic recycling through its downstream exocyst complex effector. J Cell Biol 163, 1111-1121.

Qian, D., Jones, C., Rzadzinska, A., Mark, S., Zhang, X., Steel, K.P., Dai, X., and Chen, P. (2007). Wnt5a functions in planar cell polarity regulation in mice. Dev Biol 306, 121-133.

Radhakrishna, H., Al-Awar, O., Khachikian, Z., and Donaldson, J.G. (1999). ARF6 requirement for Rac ruffling suggests a role for membrane trafficking in cortical actin rearrangements. J Cell Sci 112 (Pt 6), 855-866.

Sabapathy, K., Jochum, W., Hochedlinger, K., Chang, L., Karin, M., and Wagner, E.F. (1999). Defective neural tube morphogenesis and altered apoptosis in the absence of both JNK1 and JNK2. Mech Dev 89, 115-124.

Sabatier, C., Plump, A.S., Le, M., Brose, K., Tamada, A., Murakami, F., Lee, E.Y., and Tessier-Lavigne, M. (2004). The divergent Robo family protein rig-1/Robo3 is a negative regulator of slit responsiveness required for midline crossing by commissural axons. Cell 117, 157-169.

Sabo, S.L., and McAllister, A.K. (2003). Mobility and cycling of synaptic protein-containing vesicles in axonal growth cone filopodia. Nat Neurosci 6, 1264-1269.

Saburi, S., and McNeill, H. (2005). Organising cells into tissues: new roles for cell adhesion molecules in planar cell polarity. Curr Opin Cell Biol 17, 482-488.

Schoch, S., Deak, F., Konigstorfer, A., Mozhayeva, M., Sara, Y., Sudhof, T.C., and Kavalali, E.T. (2001). SNARE function analyzed in synaptobrevin/VAMP knockout mice. Science 294, 1117-1122.

Schwartz, S.L., Cao, C., Pylypenko, O., Rak, A., and Wandinger-Ness, A. (2007). Rab GTPases at a glance. J Cell Sci 120, 3905-3910.

Schweizer, F.E., and Ryan, T.A. (2006). The synaptic vesicle: cycle of exocytosis and endocytosis. Curr Opin Neurobiol 16, 298-304.

Seifert, J.R., and Mlodzik, M. (2007). Frizzled/PCP signalling: a conserved mechanism regulating cell polarity and directed motility. Nat Rev Genet 8, 126-138.

Serafini, T., Kennedy, T.E., Galko, M.J., Mirzayan, C., Jessell, T.M., and Tessier-Lavigne, M. (1994). The netrins define a family of axon outgrowth-promoting proteins homologous to C. elegans UNC-6. Cell 78, 409-424.

Shulman, J.M., Perrimon, N., and Axelrod, J.D. (1998). Frizzled signaling and the developmental control of cell polarity. Trends Genet 14, 452-458.

Simons, M., and Mlodzik, M. (2008). Planar cell polarity signaling: from fly development to human disease. Annu Rev Genet 42, 517-540.

Somsel Rodman, J., and Wandinger-Ness, A. (2000). Rab GTPases coordinate endocytosis. J Cell Sci 113 Pt 2, 183-192.

Song, J., Khachikian, Z., Radhakrishna, H., and Donaldson, J.G. (1998). Localization of endogenous ARF6 to sites of cortical actin rearrangement and involvement of ARF6 in cell spreading. J Cell Sci 111 (Pt 15), 2257-2267.

Stenmark, H. (2009). Rab GTPases as coordinators of vesicle traffic. Nat Rev Mol Cell Biol 10, 513-525.

Strutt, D.I. (2002). The asymmetric subcellular localisation of components of the planar polarity pathway. Semin Cell Dev Biol 13, 225-231.

Strutt, D.I., Weber, U., and Mlodzik, M. (1997). The role of RhoA in tissue polarity and Frizzled signalling. Nature 387, 292-295.

Tissir, F., Bar, I., Jossin, Y., De Backer, O., and Goffinet, A.M. (2005). Protocadherin Celsr3 is crucial in axonal tract development. Nat Neurosci 8, 451-457.

Tissir, F., and Goffinet, A.M. (2006). Expression of planar cell polarity genes during development of the mouse CNS. Eur J Neurosci 23, 597-607.

Tojima, T., Akiyama, H., Itofusa, R., Li, Y., Katayama, H., Miyawaki, A., and Kamiguchi, H. (2007). Attractive axon guidance involves asymmetric membrane transport and exocytosis in the growth cone. Nat Neurosci 10, 58-66.

Torban, E., Kor, C., and Gros, P. (2004a). Van Gogh-like2 (Strabismus) and its role in planar cell polarity and convergent extension in vertebrates. Trends Genet 20, 570-577.

Torban, E., Wang, H.J., Groulx, N., and Gros, P. (2004b). Independent mutations in mouse Vangl2 that cause neural tube defects in looptail mice impair interaction with members of the Dishevelled family. J Biol Chem 279, 52703-52713.

Torban, E., Wang, H.J., Patenaude, A.M., Riccomagno, M., Daniels, E., Epstein, D., and Gros, P. (2007). Tissue, cellular and sub-cellular localization of the Vangl2 protein during embryonic development: effect of the Lp mutation. Gene Expr Patterns 7, 346-354.

Wang, J., Hamblet, N.S., Mark, S., Dickinson, M.E., Brinkman, B.C., Segil, N., Fraser, S.E., Chen, P., Wallingford, J.B., and Wynshaw-Boris, A. (2006a). Dishevelled genes mediate a conserved mammalian PCP pathway to regulate convergent extension during neurulation. Development 133, 1767-1778.

Wang, Y., Guo, N., and Nathans, J. (2006b). The role of Frizzled3 and Frizzled6 in neural tube closure and in the planar polarity of inner-ear sensory hair cells. J Neurosci 26, 2147-2156.

Wang, Y., and Nathans, J. (2007). Tissue/planar cell polarity in vertebrates: new insights and new questions. Development 134, 647-658.

Wang, Y., Thekdi, N., Smallwood, P.M., Macke, J.P., and Nathans, J. (2002). Frizzled-3 is required for the development of major fiber tracts in the rostral CNS. J Neurosci 22, 8563-8573.

Weber, U., Paricio, N., and Mlodzik, M. (2000). Jun mediates Frizzled-induced R3/R4 cell fate distinction and planar polarity determination in the Drosophila eye. Development 127, 3619-3629.

Wilbanks, A.M., Fralish, G.B., Kirby, M.L., Barak, L.S., Li, Y.X., and Caron, M.G. (2004). Beta-arrestin 2 regulates zebrafish development through the hedgehog signaling pathway. Science 306, 2264-2267.

Wilson, S.I., Shafer, B., Lee, K.J., and Dodd, J. (2008). A molecular program for contralateral trajectory: Rig-1 control by LIM homeodomain transcription factors. Neuron 59, 413-424.

Winter, C.G., Wang, B., Ballew, A., Royou, A., Karess, R., Axelrod, J.D., and Luo, L. (2001). Drosophila Rho-associated kinase (Drok) links Frizzled-mediated planar cell polarity signaling to the actin cytoskeleton. Cell 105, 81-91.

Wolf, A.M., Lyuksyutova, A.I., Fenstermaker, A.G., Shafer, B., Lo, C.G., and Zou, Y. (2008). Phosphatidylinositol-3-kinase-atypical protein kinase C signaling is required for Wnt attraction and anterior-posterior axon guidance. J Neurosci 28, 3456-3467.

Wong, H.C., Bourdelas, A., Krauss, A., Lee, H.J., Shao, Y., Wu, D., Mlodzik, M., Shi, D.L., and Zheng, J. (2003). Direct binding of the PDZ domain of Dishevelled to a conserved internal sequence in the C-terminal region of Frizzled. Molecular cell 12, 1251-1260.

Wu, C.C., MacCoss, M.J., Howell, K.E., and Yates, J.R., 3rd (2003). A method for the comprehensive proteomic analysis of membrane proteins. Nat Biotechnol 21, 532-538.

Wu, C.C., and Yates, J.R., 3rd (2003). The application of mass spectrometry to membrane proteomics. Nat Biotechnol 21, 262-267.

Wu, S., Birnbaumer, M., and Guan, Z. (2008). Phosphorylation analysis of G protein-coupled receptor by mass spectrometry: identification of a phosphorylation site in V2 vasopressin receptor. Anal Chem 80, 6034-6037.

Yanfeng, W.A., Tan, C., Fagan, R.J., and Klein, P.S. (2006). Phosphorylation of frizzled-3. J Biol Chem 281, 11603-11609.

Yao, J., Sasaki, Y., Wen, Z., Bassell, G.J., and Zheng, J.Q. (2006). An essential role for beta-actin mRNA localization and translation in Ca2+-dependent growth cone guidance. Nat Neurosci 9, 1265-1273.

Yao, R., Natsume, Y., and Noda, T. (2004). MAGI-3 is involved in the regulation of the JNK signaling pathway as a scaffold protein for frizzled and Ltap. Oncogene 23, 6023-6030.

Yu, A., Rual, J.F., Tamai, K., Harada, Y., Vidal, M., He, X., and Kirchhausen, T. (2007). Association of Dishevelled with the clathrin AP-2 adaptor is required for Frizzled endocytosis and planar cell polarity signaling. Dev Cell 12, 129-141.

Zakharenko, S., and Popov, S. (1998). Dynamics of axonal microtubules regulate the topology of new membrane insertion into the growing neurites. J Cell Biol 143, 1077-1086.

Zakharenko, S., and Popov, S. (2000). Plasma membrane recycling and flow in growing neurites. Neuroscience 97, 185-194.

Zallen, J.A. (2007). Planar polarity and tissue morphogenesis. Cell 129, 1051-1063.

Zhang, Q., Major, M.B., Takanashi, S., Camp, N.D., Nishiya, N., Peters, E.C., Ginsberg, M.H., Jian, X., Randazzo, P.A., Schultz, P.G., et al. (2007a). Small-molecule synergist of the Wnt/beta-catenin signaling pathway. Proc Natl Acad Sci U S A 104, 7444-7448.

Zhang, X., Zhu, J., Yang, G.Y., Wang, Q.J., Qian, L., Chen, Y.M., Chen, F., Tao, Y., Hu, H.S., Wang, T., et al. (2007b). Dishevelled promotes axon differentiation by regulating atypical protein kinase C. Nature cell biology 9, 743-754.

Zou, Y. (2004). Wnt signaling in axon guidance. Trends Neurosci 27, 528-532.

Zou, Y., Stoeckli, E., Chen, H., and Tessier-Lavigne, M. (2000). Squeezing axons out of the gray matter: a role for slit and semaphorin proteins from midline and ventral spinal cord. Cell 102, 363-375.